Analyzing conflicts, crime and violence through complexity

Maykol Rodriguez Prieto

Doctoral Thesis

Submitted to Justus-Liebig-Universität Gießen,

Department of Statistics and Econometrics

Faculty of Economics and Business Studies

On April 21, 2026

1st Supervisor: Prof. Dr. Peter Winker

2nd Supervisor: Prof. Dr. Stefan Peters

Affidavit

I hereby certify that I completed the papers submitted and listed hereafter independently and only with those forms of support mentioned in the relevant paper. When working with the authors listed, I contributed no less than a proportional share of the work. In the analysis that I have conducted and to which I refer in the papers, I have followed the principles of good academic practice, as stated in the Statute of Justus Liebig University Gießen for ensuring good scientific practice.

Maykol Rodriguez Prieto

Gießen, April 21, 2026

Acknowledgments

This thesis is the culmination of a dream that began during the first semesters of my bachelor's degree in mathematics. Since then, step by step, I have built the path that has brought me here. Now I am fully convinced that what is important is not the culmination of that dream itself, but everything it has brought to my life, from the emotions of satisfaction and nervousness to the difficult moments that have taught me valuable lessons, and all the people who have accompanied me over these years.

First, I would like to thank my two advisors, Professor Peter Winker and Professor Stefan Peters. I want to thank Professor Peter Winker for trusting me when he accepted me as his student, allowing me to come to Germany and carry out my research. I also want to thank him for his willingness to read and advise me on each of the projects I developed and for giving me a place in his group. I also want to thank the DAAD for allowing me to carry out my research and fulfill my dream, as well as its entire team for all the help they provided me during these years.

This thesis contains two papers I co-authored with Jorge Marco, to whom I extend my sincere gratitude. He has been a great guide and supports me. Thank you for all the virtual and in-person meetings we held to carry out this research, discussing models, and, as always, the network as the central focus. Thank you for your trust. Que vengan más investigaciones juntos. On the third paper, I want to thank Professor Renan Goetz of Girona University for allowing me to be part of this project.

I want to especially thank Carmen Hersener for greeting me with a smile every morning, for all the conversations we've had during this time, and for her unconditional help. Thanks to my colleagues: Viktoriia Naboka, for her support, the good times, and for always being there for me when I needed her; Albina Latifi, for everything we have shared and those days we studied late into the evenings, encouraging each other; Jana Röder, for the wonderful moments we shared talking about so many things; and Elena Tönjes, who welcomed me when I arrived in Gießen and guided me through those first moments. Thank you all so much for making my stay in Germany so warm and enjoyable.

Finally, I want to thank my family. Anya, for being my companion in Germany since I started this journey; for her unconditional support and for always being there. My parents, my siblings, my niece who, despite the distance, have always been by my side in thought and heart, and my aunt, for our conversations and her support from afar. I also want to thank all my friends in Colombia who, despite the distance, have been very close to me, and all the friends I have made over the years who, in different ways, have been very important in giving me strength and peace. Muchas gracias!

Table of Contents

Chapter 1

1. Introduction

The relationship between conflict, environmental crime, and illicit markets is deep and structural; they reinforce one another and form part of a system that reveals institutional weaknesses, leading to the irreversible destruction of ecosystems, the loss of biodiversity, and serious economic and social repercussions, in addition to violence. Within this system, there are various actors, both direct and indirect. Armed groups involved in conflicts depend on illicit markets and organized crime for financing, while organized crime also benefits from these conflicts by finding opportunities to expand its activities and increase its profits. This thesis examines these interconnections through a complexity theory approach, highlighting how the diverse dynamics analyzed in each chapter are ultimately interrelated and form part of a broader, interconnected system.

Around 40% of conflicts worldwide originate from the control, appropriation, and extraction of natural resources (United Nations Environment Programme, 2009), where the main actors are armed groups that compete for control, often generating violence manifested in deaths, forced displacement, and human rights violations (Collins, 1999; Hoover Green, 2016; Artaza & Guillaumont, 2022). These conflicts usually take place in areas where the presence of the state and institutions is weak or entirely absent, facilitating access to and control over such natural resources. This situation leads to various environmental crimes, as armed groups overexploit and destroy resources due to their need to finance their struggle and maintain control. As a result, they do not follow environmental regulations, acting as short-sighted actors who exploit indiscriminately, causing irreversible damage to ecosystems.

These groups need to commercialize the natural resources, creating connections with other actors who may or may not belong to the same criminal network, and who perform various functions such as transportation and logistics. These criminal networks also use mechanisms such as fraud, corruption (considered one of the main issues in environmental crimes and occur at different levels and in various forms, with governments and large legal companies also being implicated), and violence to achieve their objectives, relying on bribery and threats. Since the resources are extracted illegally, they are transported hidden and concealed within shipments of legally imported goods or through unmonitored, hard-to-access areas, often accompanied by fraud and the corruption of state officials or legal companies that enable their passage through legal routes.

Various studies have shown how transnational criminal networks carry out these activities, operating like multinational corporations of illegality, where violence is also used as a means of enforcing contracts (van Koppen, 2013; Davies, Pettersson & Öberg, 2024). Similarly, organized crime facilitates the return of profits derived from these resources through money laundering, which is then used to finance conflicts (Le Billon, 2005; Levi & Soudijn, 2020).

Besides, conflicts require a high flow of money (Wennmann, 2009), as armed groups and other actors within criminal networks need to maintain control and operational capacity, for example, through the acquisition of weapons and ammunition, as well as the payment and equipping of personnel, transportation, food, and healthcare. In this way, illicit markets enable the transportation, commercialization, and laundering of the capital that is essential for their functioning, making conflicts financially profitable. In addition, armed groups become stronger and more driven by greed, creating a vicious cycle in which greater profits are needed to sustain their operations, which in turn generates more conflict and, consequently, more severe environmental crimes.

The literature shows that armed groups often overexploit natural resources and engage in environmental crimes (Rettberg & Ortiz-Riomalo, 2016; Bhat, 2024; Tosi Rodriguez & Caneppele, 2025). At the same time, the United Nations Office on Drugs and Crime (2020) identifies the illegal trafficking of natural resources as one of the main activities of organized crime. Together, these strands of research highlight a strong connection between conflict dynamics and illicit markets. However, this relationship cannot be generalized, as its functioning depends on specific factors such as the type of natural resource, the geographical context, and the characteristics of the criminal networks involved, including both visible and less visible actors (Kleemans & Christianne, 2008; Middleton & Levi, 2015), such as lawyers, transporters, accountants, and state officials. Likewise, modes of operation, such as routes, transportation methods, and commercialization strategies, can vary significantly. All these dynamics are shaped by their illegal nature, which complicates analysis and obscures how these systems operate.

Another point to highlight is, criminal organizations not only operate outside the law, but often succeed in normalizing illicit practices in different ways. Within the communities where they overexploit resources, this occurs because most of these communities are in regions with high levels of poverty and little to no state presence, allowing armed groups and organized crime to establish norms based on immediate economic gain that run counter to principles of planning, regulation, and conservation.

The study and analysis of conflicts over natural resources, as well as environmental crimes and their relationship with organized crime and its modes of operation, linked to clandestinity and illegality, have been addressed across various fields such as sociology, economics, criminology, political science, investigative journalism, among others. Different approaches have been used, including qualitative and quantitative analysis (Teixeira Aranega, 2025; Lynch & Pires, 2019). However, their opaque nature, combined with the difficulty of obtaining reliable information and data, hinders understanding and limits the development of more accurate analyses to effectively address these phenomena. Considering this, the present study aims to use complexity theory as a tool to achieve a better understanding of conflicts and environmental crimes and their relationship with organized crime. Complexity theory is a scientific approach grounded in chaos theory, which examines the adaptation and evolution of systems through the agents that compose them (Lewin, 1999; Manson, 2001) and their fundamental characteristics, such as nonlinearity, uncertainty, self-organization, and emergent properties (Abel, 2007). These emergent properties arise from interactions among agents but are not observable as a priori (Holland, 1998). The interactions and systems in this study are analyzed using tools such as network theory, agent-based modeling, game theory, among others. The following three chapters that make up this research correspond to three developed articles that apply these approaches within the framework of complexity.

The first paper **"Analyzing Rent Dissipation in Network Conflicts Over Natural Resources"** defines a measure of economic losses through rent dissipation generated by natural resources in the context of armed conflict. This measure is derived from a two-stage game and is tested using different parameters related to the resource and the agents, such as appropriation effort. Positive and negative connections, corresponding to alliances and rivalries among armed groups, are modeled through a signed network. The study presents both analytical and numerical results, showing that power asymmetries among agents lead to high economic losses. Similarly, under conditions of resource abundance, the network structure, that is, the relationships among armed groups, plays a fundamental role. The model is calibrated using the case of the Sudanese gold conflict. This chapter contributes both methodological insights and empirical evidence to inform policies aimed at resolving armed conflicts.

The second paper **“Cocaine Trafficking via Container Ships, Dynamics between Corruption, and Inspections: An Agent-Based Model”** uses an agent-based model (ABM) to simulate cocaine trafficking from ports in South America to ports in Europe. The objective is to simulate the quantity of cocaine trafficked to Europe by testing different parameters, such as container ship size, port inspection capacity, and potential corruption within ports. The model is calibrated using real qualitative data and allows for the exploration of ambiguous aspects of organized crime operations in maritime trafficking, which is currently the most widely used method by perpetrators. The data generated from the simulations were analyzed using Analysis of Variance (ANOVA), revealing that corruption in ports undermines inspection efforts. Similarly, the size of container ships, while important for legitimate trade, also creates opportunities for organized crime to operate. Methodologically, the model exhibits properties of emergence and adaptation.

The third paper **“Enforcement Costs, Coordination and Social Acceptability in Network Interventions”** analyzes targeted interventions in social networks aimed at sustaining cooperation or preventing corruption, which typically require costly enforcement of rules. A theoretical model is developed in which agents not only benefit from cooperation but also exert social pressure on peers who do not cooperate or who engage in corruption. Analytical and numerical results highlight that the effectiveness of interventions by regulators depends not only on central nodes but also on the structure of the network, which leads to different enforcement costs.

The final chapter presents concluding remarks that bring together the main findings of the articles and reflecting on their broader implications.

Chapter 2

Analyzing Rent Dissipation in Network Conflicts Over Natural Resources

The following chapter is based on the paper:	
Title:	Analyzing Rent Dissipation in Network Conflicts Over Natural Resources
Authors:	Maykol Rodriguez Prieto (Contribution 60%)
	Jorge Marco Renau (Contribution 40%)
Status:	Submitted to *Defense and Peace Economics Journal*

Different states of this paper have been presented at:

- 26th Annual Workshop on Economics with Heterogenous Interacting Agents WEHIA. Koper, Slovenia 2023.
- 9th German Network for New Economic Dynamics GENED. Bamberg, Germany 2023.
- BEHAVE summer school on "Agent Based Modelling for social scientist". Brescia, Italy 2023.

Analyzing Rent Dissipation in Network Conflicts Over Natural Resources

Maykol Rodriguez-Prieto[1] and Jorge Marco[2]

[1]Faculty of Economics, Justus Liebig Universitat Gießen, Germany

[2]Department of Economics, University of Girona, Spain

Abstract

This paper develops a two-stage model of conflict over a finite natural resource to analyze how stock abundance, market prices, and network structure affect rent dissipation and the intensity of conflict. In the first stage, agents engage in a networked contest for exclusive control over extraction opportunities, allowing for positive and negative spillovers that represent alliances and rivalries. In the second stage, successful contest agents extract from the common stock subject to possible per-agent extraction caps. The finite stock endogenizes the contested prize, generating two analytically distinct regimes: a stock-constrained regime, in which total prize value increases with stock, and a player-constrained regime, in which it is fixed by the number of agents. The analysis proceeds in two parts. First, taking contest effort as exogenous, closed-form expressions for rent dissipation are derived, with comparative statics for stock, prices, and network effects across regimes. Second, endogenizing contest effort, equilibrium conflict intensity and its sensitivity to the same effects are characterized. Both parts reveal threshold effects and regime shifts: above a critical stock level, further abundance does not affect rent dissipation or conflict intensity, and under endogenous caps, price elasticities can double. The model yields closed-form symmetric equilibria in regular networks and tractable piecewise solutions in more general settings, extending standard contest theory to a resource-constrained environment. The results offer a micro-founded mechanism for non-monotonic resource-conflict relationships and inform policy debates on resource governance.

Keywords: appropriation effort, conflict dynamics, game-theoretic modeling, rent dissipation, resource rents, networks.

JEL classification: C72, D74, Q34.

2.1. Introduction

Conflicts over the control and extraction of natural resources are a persistent feature of both historical and contemporary economies. From disputes over fishing grounds and forestry concessions to struggles over mineral deposits and water rights, agents frequently divert substantial efforts to secure exclusive extraction opportunities. Such conflicts are costly in two ways: directly, by dissipating potential rents through unproductive rivalry; and indirectly, by accelerating depletion of the resource and undermining sustainable use. Understanding how the abundance of the resource, the level of market prices, and the structure of strategic interactions dissipate rents and shape the intensity of these conflicts is central to both positive analysis—explaining observed patterns of contestation—and normative analysis—designing institutions and policies to mitigate wasteful competition.

The analysis of conflict has been dominated by contest-theoretic models, most notably those based on the Tullock contest success function (Tullock, 1980; Skaperdas, 1996), in which agents make effort to increase their probability of capturing a prize of fixed value. This framework has generated influential results on conflict intensity, rent dissipation, and the distribution of payoffs (Hillman and Riley, 1989; Nitzan, 1994). A key limitation of this approach, however, is that the prize is typically specified exogenously, independently of resource abundance or the extraction process itself. As a result, standard contest models abstract from a defining feature of many resource conflicts: the physical and technological constraints that determine how the value of winning is endogenously shaped by the underlying resource stock and the process through which it is exploited.

A related literature expands the previous approach by incorporating network structure into contests, allowing for positive and negative spillovers in appropriation efforts that represent alliances and rivalries, respectively (Hiller, 2017; König, Tessone, and Zenou, 2011; König and Rohner, 2016). These models analyze how network topology shapes equilibrium efforts and payoffs, and to what extent the unique position agents occupy within the network confers advantage or vulnerability in the contest. Yet, here too, the prize is fixed and exogenous. Consequently, the interaction between network structure and the size or divisibility of the contested resource remains unexplored.

This paper addresses this gap in literature by developing a two-stage model in which the value of the contested prize is endogenous, determined jointly by the available resource stock and per-agent extraction limits. In the first stage, agents compete in a networked contest with arbitrary spillovers, representing alliances and rivalries. In the second stage, winners extract from the finite stock subject to quadratic costs and potential caps on per-agent extraction. The finite stock naturally generates two distinct regimes: a stock-unconstrained regime, in which the aggregate prize value rises with stock abundance, and a stock-constrained regime, in which the prize is fixed by the number of contest winners and extraction caps. This structure yields rich comparative statics and threshold effects absent from existing models.

Our central research question is: How do resource stock abundance, market prices, and network structure determine rent dissipation and the intensity of conflict over a finite natural resource?

The contribution of the paper is threefold. First, we introduce a sequential appropriation–extraction framework that endogenizes the contest prize through resource and extraction constraints, thereby linking the physical and technological/knowledge characteristics of the resource to appropriation incentives. Second, we embed this framework in a network contest with arbitrary spillovers, yielding a simple multiplicative network effect that scales conflict intensity and interacts with resource constraints in ways absent from prior models. Third, we derive closed-form comparative statics for stock, price, and network parameters in both unconstrained and constrained regimes, identifying novel, non-monotonic relationships between abundance and conflict intensity, as well as cases where price elasticities are magnified under endogenous caps.

Our approach is theoretical but grounded in empirically relevant characteristics of resource conflicts. The model consists of two sequential stages. In stage one (“appropriation stage”), agents exert effort to secure exclusive control over extraction opportunities; the probability of success is determined by a networked contest success function allowing for bilateral positive and negative spillovers. In stage two (“extraction stage”), winners extract from the finite resource stock. The stock constraint interacts with any per-agent extraction limits to determine the aggregate value of the prize. This approach allows for closed-form symmetric equilibria in regular networks and tractable piecewise solutions for more general network structures, permitting exact analytical comparison between the unconstrained and constrained regimes.

The main results can be summarized as follows. When appropriation effort is taken as exogenous, rent dissipation depends on stock and market prices in the unconstrained regime but is unaffected by stock in the constrained regime. In both cases, network structure scales outcomes multiplicatively. When appropriation effort is endogenous, the intensity of conflict—measured by total effort—leads to similar regime dependence, but with richer interactions between parameters: price elasticities can double under endogenous extraction caps, and the marginal effect of stock abundance vanishes entirely above a critical threshold. Negative spillovers amplify the effect of scarcity on conflict, whereas positive spillovers attenuate it, offering a clear mechanism through which network structure mediates economic shocks.

These findings have broader implications for both theory and policy. Theoretically, they qualify the generality of standard contest predictions by showing how physical constraints can neutralize the effect of abundance on conflict, even in the absence of institutional change. They also integrate network structure into resource-constrained contests, showing that structural imbalances can magnify the responsiveness of conflict to scarcity or price shocks. From a policy perspective, the results imply that interventions targeting network structure—such as promoting cross-faction alliances—can be as important as affecting macro-institutional frameworks in shaping the conflict–resource nexus. They also show that, in unconstrained regimes, resource development in the absence of governance reforms risks increasing both rent dissipation and conflict intensity, whereas in constrained regimes, physical expansion of the resource base may have negligible effects on conflict.

The remainder of the paper is organized as follows. Section 2.2 reviews the relevant literature on contest theory, networked contests, and the economics of natural resources and the resource curse. Section 2.3 presents the two-stage model, defining the contest success function, network structure, and extraction technology, as well as a final definition of rent dissipation, as a metric of economic losses. Section 2.4 characterizes equilibrium behavior and shows comparative statics for stock, prices, the number of agents, and network parameters across regimes through numerical simulations. Section 2.5 calibrates the model to the Sudan conflict for the gold estimating the spillovers. Section 2.6 discusses the implications of the results for existing theory and empirical findings and draws policy implications, focusing on the role of network structure in moderating resource-driven conflict. Section 2.7 concludes with limitations of the analysis and directions for future research.

2.2 Related Literature

The analysis in this paper connects to three strands of economic research: contest theory, networked contests, and natural resource economics, with further links to the resource curse literature. Contest theory provides the core analytical framework for modelling strategic rivalry over valuable prizes. Since the seminal formulation of the Tullock contest success function (Tullock, 1980), subsequent work has characterized equilibrium effort, rent dissipation, and payoff division in settings with symmetric and asymmetric players (Skaperdas, 1996; Hillman and Riley, 1989; Nitzan, 1994; Baye, Kovenock, and de Vries, 1994). Extensions have addressed risk preferences, multiple prizes, and prize-sharing arrangements (Esteban and Ray, 1999; Nitzan and Ueda, 2011). A central theme is the extent of rent dissipation—the proportion of potential surplus consumed by contest effort—which under certain conditions can approach the full value of the prize (Wärneryd, 1998; Congleton et al., 2008). While these models are highly flexible, they almost universally treat the prize as fixed and exogenous, abstracting from its dependence on underlying resource constraints.

A related body of work embeds contests in network structures, introducing bilateral spillovers that capture alliances and rivalries. Bramoullé and Kranton (2007) analyse local public goods in networks, and König, Tessone, and Zenou (2011) and König and Rohner (2016) extend this framework to conflict, deriving equilibrium efforts as functions of network topology. They show how structure determines both the level and distribution of efforts, and how negative spillovers can create persistent antagonisms. However, in these models too, the value of the prize is independent of scarcity, and network effects operate only as multiplicative factors on a fixed contest payoff.

Natural resource economics focuses on the interplay between resource abundance, extraction costs, and rent dissipation under open access. Foundational work by Gordon (1954) and Schaefer (1957) demonstrated how unrestricted access leads to over-extraction and dissipation of rents, while Clark (2010) and others have analyzed optimal management under biological growth, technological change, and dynamic uncertainty. These models capture how scarcity and extraction constraints shape rents, but treat access as exogenously determined, omitting the strategic competition that precedes extraction.

The empirical literature on resource abundance and conflict—central to the resource curse debate—documents that resource-rich economies are prone to rent-seeking, political instability, and in some cases civil war (Collier and Hoeffler, 2004; Sachs and Warner, 1995; Ross, 2012). Explanations emphasize institutional quality (Mehlum, Moene, and Torvik, 2006), rent distribution (Robinson, Torvik, and Verdier, 2006), and the "point-source" nature of resource wealth (van der Ploeg, 2011). Yet recent evidence shows that abundance–conflict relationships are not uniformly monotonic: price or stock booms sometimes leave conflict unchanged (Berman et al., 2017), a finding that existing models struggle to reconcile. In parallel, empirical work on networks in conflict (Christia, 2012; Rohner, Thoenig, and Zilibotti, 2013; Jackson and Nei, 2015) shows that the configuration of alliances and rivalries influences escalation patterns but rarely integrates scarcity into the analysis.

Unlike canonical contest models or standard resource economics, the framework developed here can accommodate real-world situations in which both the value of control and the incentives to compete depend jointly on the physical abundance of a resource and the strategic environment in which competition occurs. For example, the allocation of fishing quotas in West African waters has generated conflict among artisanal and industrial fleets, with the profitability of winning access rights rising with biomass levels but falling once stock scarcity makes extraction technologically costly (Belhabib et al., 2015). In such settings, standard Tullock contests treat the "prize" as fixed, missing the feedback from ecological abundance to contest payoffs. Similarly, disputes over mining concessions in the Democratic Republic of Congo often involve overlapping alliances and rivalries among local militias, foreign corporations, and state actors (Autesserre, 2010), where shifts in global commodity prices alter both the value of concessions and the stability of coalitions. Networked contest models capture some aspects of coalition structure but, without endogenizing prize value, cannot predict the disappearance of resource effects beyond a critical stock. Finally, water allocation conflicts in the Mekong basin illustrate cases where scarcity, extraction technology, and interstate alliances interact: upstream dam construction changes the effective prize size for downstream claimants, while shifting political alignments alter the distribution of effort (Molle et al., 2012).

These examples demonstrate that contests over natural resources often involve a combination of scarcity-dependent prize valuation and network-structured strategic rivalry. By incorporating both elements, the present framework can generate predictions about threshold effects, price sensitivities, and network–scarcity interactions that neither standard contest theory nor conventional resource economics can capture.

2.3. The model

2.3.1. Network structure

The interactions between agents in conflict are modeled by a network g of $n \in \mathbb{N}$ agents. Bilateral relationships are represented by the adjacency matrix $M = \left(m_{ij}\right)_{1 \le i, j \le n}$ associated with the network g. Each pair of agents can exist in one of three states: alliance, enmity, or neutrality, formally defined as follows: $m_{ij} = 1$ indicates that agent i has a positive relationship with agent j (alliance), $m_{ij} = -1$ indicates that agent i has a negative relationship with agent j (enmity), and $m_{ij} = 0$ implies a neutral relationship or no relationship between i and j. By convention, $m_{ii} = 0$ for all agents. Network g is directed if $m_{ij} \neq m_{ji}$. To obtain an undirected network $\bar{g}$, the following transformation is applied: a positive (negative) link between a pair of agents exists in $\bar{g}$ if and only if they reciprocate a positive (negative) relationship. That is, $\bar{m}_{ij} = 1$ if $m_{ij} = m_{ji} = 1$ and $\bar{m}_{ij} = -1$ if $m_{ij} = m_{ji} = -1$. All other configurations are considered neutral, such that $\bar{m}_{ij} = 0$. Let $\bar{m}_{ij}^{+} = 1$ if $\bar{m}_{ij} = 1$, and $\bar{m}_{ij}^{+} = 0$ otherwise; and $\bar{m}_{ij}^{-} = 1$ if $\bar{m}_{ij} = -1$, and $\bar{m}_{ij}^{-} = 0$ otherwise. Figure 1 illustrates all possible network structures among three agents, with positive links (alliances) in green and negative links (enemies) in red, excluding neutral relationships: (1a) All agents are allies, (1b) two allies share a common enemy, (1c) two enmities share a common alliance, and (1d) all agents are enmities. These four network structures are commonly used in conflict analysis literature as they effectively capture agent interaction patterns in conflict contexts (Heider, 1946; Hiller, 2017; König et al., 2017).

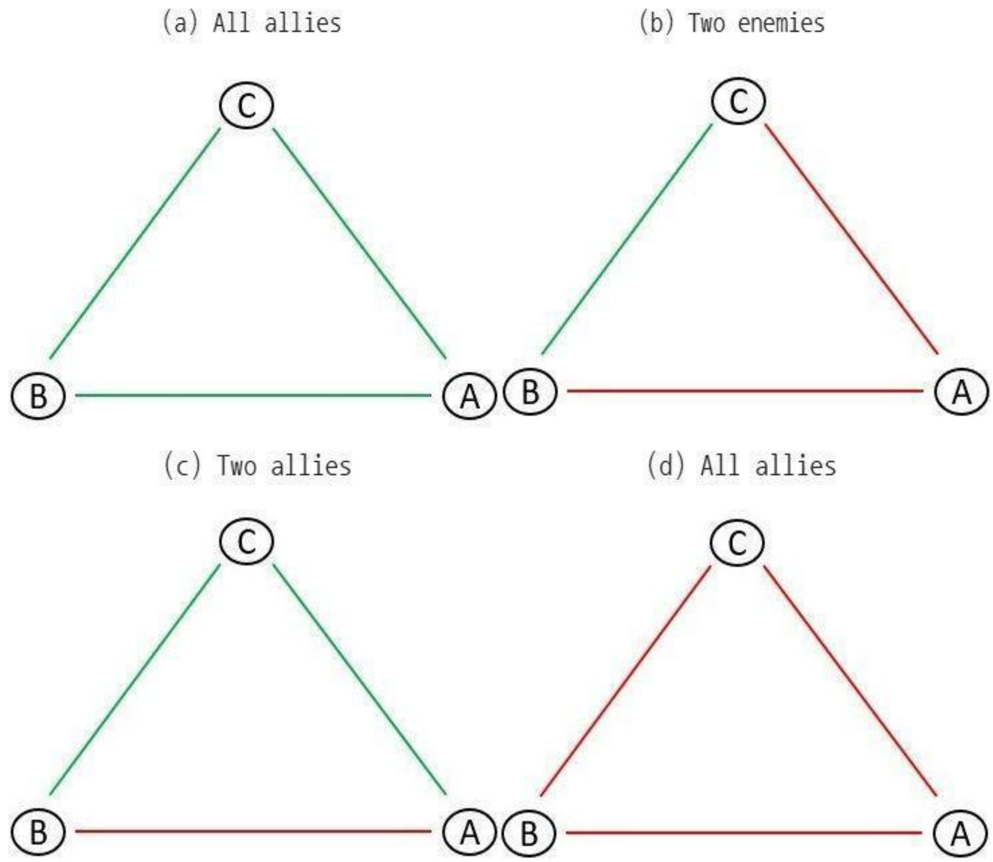

Fig 2.1. Network structures of agents competing for resource rents. Positive interactions (green) indicate allies, and negative interactions (red) indicate enemies. (a) All agents are allies. (b) Allies B and C share a common enemy, A. (c) Enemies A and B share a common alliance; C. (d) All agents are enemies.

2.3.2. Appropriation efforts

Appropriation refers to control over resources, often through force (Anderton and Carter, 2009) and is essential for agents to gain access and use them (Tullock, 1980; Skaperdas, 1996; König et al., 2017). However, their ability to do so is constrained by factors they cannot easily change, such as the size and capacity of their forces in a conflict, which limit how much they can appropriate. For example, consider three agents in conflict over a resource. The first has a large, well-equipped force, the second a smaller but highly trained force, and the third a minimal, disorganized force. The second and third agents are restricted by the size and/or capacity of their forces. Even if they seek to appropriate more resources, their success is limited by their appropriation effort, not by strategic decisions. In the model, appropriation effort is exogenous, defined by fixed constraints rather than agents' choices. This condition is relaxed in Section 3.3.1, where appropriation effort is endogenized as an extension of the model.

Dominance in a conflict is given by the net appropriation effort of agents, $d_i \in \mathbb{R}^+$, which depends on their own appropriation effort, $a_i \in \mathbb{R}^+$, as well as the efforts exerted by their alliances and enmities, such that

$$d_i = a_i + \beta \sum_{j=1}^{n} \bar{m}_{ij}^{+} a_j + \gamma \sum_{j=1}^{n} \bar{m}_{ij}^{-} a_j \,. \tag{1}$$

Parameters $\beta, \gamma \in \mathbb{R}^+$ capture positive and negative spillovers from alliances, $\bar{m}_{ij}^{+} a_j \in \mathbb{R}^+$, and enmities, $\bar{m}_{ij}^{-} a_j \in \mathbb{R}^-$, respectively (König et al., 2017). In equation 1, dominance over resources increases through positive spillovers when allies strengthen control, as in a conflict where they secure key positions or limit enmities from gaining ground. Conversely, negative spillovers reduce dominance when enmities intensify actions, such as disrupting supply lines or challenging control.

Let $d_i^{+} = \max\{0, d_i\}$ denote the positive part of d_i. Equation 1 is simplified to

$$d_i^{+} = \begin{cases} d_i & \text{if } d_i > 0 \\ 0 & \text{if } d_i \leq 0. \end{cases} \tag{2}$$

Equation 2 states that an agent can appropriate and use a resource if and only if their dominance is positive, meaning the sum of their own appropriation effort and positive spillovers exceed those from enmities, $a_i + \beta \sum_{j=1}^{n} \bar{m}_{ij}^{+} a_j > \left| \gamma \sum_{j=1}^{n} \bar{m}_{ij}^{-} a_j \right|$. Otherwise, when $a_i + \beta \sum_{j=1}^{n} \bar{m}_{ij}^{+} a_j \leq \left| \gamma \sum_{j=1}^{n} \bar{m}_{ij}^{-} a_j \right|$, it indicates a lack of capacity to appropriate and use a resource.

2.3.3. The game

2.3.3.1. First stage: Resource appropriation

The $n \in \mathbb{N}$ agents are in conflict over control of a divisible natural resource stock, $S \in \mathbb{R}^{+}$ such as oil reserves or fishery catches. First, each agent i faces an appropriation process, $A_i \in \mathbb{R}^{+}$ defined by

$$A_i = \left(\frac{\left(d_i^{+}\right)^{1-\alpha}}{\sum_{i=1}^{n} \left(d_i^{+}\right)^{1-\alpha}} + \varepsilon_i \left(1-\alpha\right) \right) S. \tag{3}$$

Parameter $\alpha \in \left[0,1\right]$ reflects institutional quality, representing the security of property rights, while function $\varepsilon_i\left(1-\alpha\right): \mathbb{R}^{+} \to \mathbb{R}$ captures the bias in control favoring agent i (Butler and Gates, 2012; Mehlum et al., 2002). Strong institutions and the absence of conflict are represented by $\alpha = 1$, whereas weak institutions and intense conflict correspond to $\alpha = 0$. The specifics of function ε_i and the role of institutions are detailed in section 2.4.

2.3.3.2. Second stage: Resource use

After appropriating the resource, agents optimize extraction through payoff functions that maximize economic gains. Payoffs depend on extraction levels and negative externalities from other agents. With independence of the conflict in place, natural resources face problems of overuse such that each agent i gets economic benefits, $b_i \in \mathbb{R}^{+}$, from resource extraction and economic losses, $c_i \in \mathbb{R}^{+}$, from the negative externalities as a result of the aggregate extractions of all agents. Vector $\boldsymbol{e} = \left(e_i\right)_{1 \le i \le n} \in \mathbb{R}_n^{+}$ represents the extraction profile of all agents, where $\boldsymbol{e}_{-i} = \left(e_j\right)_{1 \le j \ne i \le n-1} \in \mathbb{R}_{n-1}^{+}$. Let denote by $\mathbf{1}$ the n-dimensional vector of ones and the superscript T stand for the transpose operator. With abuse of notation, let $e = \mathbf{1}^T \cdot \boldsymbol{e}$ denote the sum of entries of vector $\boldsymbol{e}$, that is, the aggregate extractions of all agents. The payoff of agent i, $\pi_i \in \mathbb{R}$, that takes account of negative externalities is denoted by

$$\pi_i\left(e_i, \boldsymbol{e}_{-i}\right) = b_i\left(e_i\right) - c_i\left(e_i, e\right). \tag{4}$$

Where $b_i : \mathbb{R} \to \mathbb{R}^+$ is a continuous, twice differentiable, and strictly concave function with $b_i\left(0\right) = 0$, $\frac{\partial b_i}{\partial e_i} > 0$ and $\frac{\partial^2 b_i}{\partial e_i^2} < 0$. Similarly, $c_i : \mathbb{R}^2 \to \mathbb{R}^+$ is a continuous, twice differentiable and increasing function in e_i and e, with $c_i\left(0, e\right) = 0$. Extractions are determined based on appropriation, such that

$$0 \le e_i \le A_i \le S. \tag{5}$$

Based on equations 3, 4, and 5, the following section presents the two extreme case conflict scenarios of the game and their equilibrium outcomes.

2.3.3.3. Setup of the game and timing of actions

The game is played on a network of agents that may include alliances, enmities, or any combination of both. Each agent is endowed with a fixed level of appropriation effort, randomly assigned and constant throughout the game, with total effort held fixed. The resource stock, the extent of spillovers, the intensity of externalities, and the price are fixed within each game, but may vary across repetitions to assess their impact on rent dissipation.

The timing is as follows. In the first stage, agents simultaneously appropriate the resource, with outcomes determined by their effort and their position in the network. In the second stage, agents simultaneously choose resource use, considering their benefits and costs. Individual extraction depends on relative dominance and is negatively affected by the extraction decisions of other agents.

The solution concept is Nash equilibrium. At the end of the game, rent dissipation is measured at equilibrium to capture the inefficiencies arising under different conflict structures. The analysis focuses on two benchmark institutional environments—strong and weak institutions—to capture the maximal variation in rent dissipation. Intermediate cases yield smaller effects.

2.3.4. Conflict scenarios and equilibrium

The lower and upper limits of a conflict are given by $\alpha = 1$ and $\alpha = 0$, respectively. Any other conflict scenario in the game falls within $\alpha \in (0,1)$. The lower limit scenario, $\alpha = 1$, represents very strong institutions and well-established property rights, where conflicts are absent. In this case, the resource can be efficiently allocated, with ε_i reflecting the role of institutions in optimizing resource use and maximizing social welfare. If $\alpha = 1$, equation 3 simplifies to

$$A_i = \left(\frac{1}{n} + \varepsilon_i \left(0 \right) \right) S. \tag{6}$$

Using equations 5 and 6, ε_i is defined as the value that maximizes social welfare, allowing equation 6 to be rewritten as

$$\varepsilon_i \left(0 \right) = \frac{e_i^W}{S} - \frac{1}{n}. \tag{7}$$

Where $e_i^W \in \mathbb{R}^+$ is the extraction level that maximizes social welfare. Next, social welfare and the extraction profile that achieves it are defined. Social welfare, $W \in \mathbb{R}^+$, is individually separable and given by

$$W(\boldsymbol{e}) = \sum_{i=1}^{n} \pi_i \left(e_i, \boldsymbol{e}_{-i} \right) = \sum_{i=1}^{n} b_i \left(e_i \right) - \sum_{i=1}^{n} c_i \left(e_i, e \right). \tag{8}$$

A profile $\mathbf{e}^W := \left(e_i^W \right)_{1 \le i \le n} \in \mathbb{R}_n^+$ is Pareto-efficient if and only if $W(\boldsymbol{e}^W) > W(\boldsymbol{e})$, that is, there is no other profile $\boldsymbol{e}$ that maximizes social welfare. The first-order condition for maximization of social welfare W is

$$\frac{\partial W}{\partial e_i} = \frac{\partial b_i}{\partial e_i} - \sum_{i=1}^{n}\left(\frac{\partial c_i}{\partial e_i} + \frac{\partial c_i}{\partial e}\right) = 0. \tag{9}$$

The solution of equation 9 is denoted by e_i^W, social optimum, such that $\left.\frac{\partial \pi_i}{\partial e_i}\right|_{e_i=e_i^W} = \sum_{i=1}^{n}\left(\frac{\partial c_i}{\partial e_i} + \frac{\partial c_i}{\partial e}\right)$.

Equations 6 and 7 leads to $A_i = e_i^W$, meaning that in equilibrium, appropriation coincides with the extraction level that maximizes social welfare when $\alpha = 1$.

The upper limit scenario, $\alpha = 0$, represents weak institutions and intense conflicts that result in the winner-takes-all outcome. When property rights are insecure, regardless of the reason is crime, civil unrest, drug trafficking, government instability or government's use of eminent domain, the conflict allows the most dominant agents to be more exploitative with resources at the expense of the losers. Using equations 5 and 6, ε_i is defined as the value that maximizes individual profit, allowing equation 6 to be rewritten as

$$\varepsilon_i(1) = 0. \tag{10}$$

If $\alpha = 0$, equations 3, 4 and 5 simplify to

$$0 \le e_i \le \left(\frac{d_i^+}{\sum_{i=1}^{n} d_i^+}\right) S \le e_i^* \le S. \tag{11}$$

Where $e_i^* \in \mathbb{R}^+$ is the extraction level that maximizes individual profit. Focusing on interior solutions, the maximization of agent i's payoff, equation 4, gives the following first-order condition

$$\frac{\partial \pi_i}{\partial e_i} = \frac{\partial b_i}{\partial e_i} - \left(\frac{\partial c_i}{\partial e_i} + \frac{\partial c_i}{\partial e}\frac{\partial e}{\partial e_i}\right) = 0. \tag{12}$$

Given that $\frac{\partial e}{\partial e_i}=1$, it follows that $\frac{\partial \pi_i}{\partial e_i}=\frac{\partial b_i}{\partial e_i}-\left(\frac{\partial c_i}{\partial e_i}+\frac{\partial c_i}{\partial e}\right)=0$. The solution of equation 12 is denoted by $e_i^* \in \mathbb{R}_+$, private optimum, such that $\left.\frac{\partial b_i}{\partial e_i}\right|_{e_i=e_i^*}=\frac{\partial c_i}{\partial e_i}+\frac{\partial c_i}{\partial e}$. Note that the privately optimal extraction profile $\boldsymbol{e}^*=\left(e_i^*\right)_{1\le i\le n}\in\mathbb{R}_n^+$ represents the Nash equilibrium in resource use and therefore it is the expected outcome in the presence of conflict when $\alpha=0$. The profile $\boldsymbol{e}^*$ is a Nash equilibrium if and only if $\pi_i(e_i^*,\boldsymbol{e}_{-i}^*)\ge\pi_i(e_i,\boldsymbol{e}_{-i}^*)$, $\forall i\in\mathbb{N}$, $\forall e_i\in\mathbb{R}_+$. This profile $\boldsymbol{e}^*$ usually leads to the overexploitation of resources. The first-order conditions in equations 9 and 12 and the concavity of b_i (benefits) imply that the expected profile of resource use will be inefficient due to e_i^* is economically dominant, that is, $\pi_i\left(e_i^W,\boldsymbol{e}_{-i}\right)<\pi_i\left(e_i^*,\boldsymbol{e}_{-i}\right)$ and $\sum_{i=1}^{n}\pi_i\left(e_i^W,\boldsymbol{e}_{-i}\right)>\sum_{\substack{i=1\\ e_i\ne e_i^W}}^{n}\pi_i\left(e_i,\boldsymbol{e}_{-i}\right)$, for all agents and $\boldsymbol{e}$. Based on equations 5, 6, 10, and 11, economic inefficiencies are captured by the following inequalities

$$e_i^W<e_i\le e_i^*\le A_i \text{ or } 0\le e_i\le A_i<e_i^W. \tag{13}$$

In a conflict, it can also occur that agents appropriate more resources than they will use, implying that their resource appropriation (first stage) exceeds their immediate extraction capacity or interests (second stage of the game). Such situations lead to economic inefficiencies in the short term if one agent's appropriation of resources prevents others from reaching their optimal resource extractions. Agents may appropriate more resources than they need for strategic and economic reasons, such as: (i) controlling more resources can improve their position in the conflict, allowing them to negotiate or gain an advantage in future interactions, (ii) even if the resources are not needed in the short term, agents may anticipate that their value will increase over time, making appropriation now a future investment, and (iii) agents may appropriate resources to create artificial scarcity, increasing their value and benefiting their economic interests.

2.3.5. Rent dissipation

The rent dissipation (RD) metric quantifies inefficiencies and consequently the economic losses inherent in any conflict scenario. It is defined as

$$RD = 1 - \frac{W(\boldsymbol{e})}{W(\boldsymbol{e}^{W})}. \tag{14}$$

According to equation 14, the minimum RD ($RD = 0$), is reached when both the appropriation and extraction profiles align with the Pareto-efficient profile, which occurs in the presence of strong institutions. In conflict scenarios, the maximum RD ($RD = 1$), can occur in different contexts. For example, when each agent extracts at their maximum profitable interest, intense competition for the resource leads to overexploitation, with total extraction exceeding the socially optimal level. Alternatively, in winner-takes-all scenarios where only one agent extracts and others are excluded, inefficiencies result once again, often resulting in a more concentrated economic loss. In this case, only one agent benefits, while the others gain nothing, creating inefficiency through exclusion. In fact, the numerator of equation 14 captures many suboptimal private equilibria due to the different appropriation efforts that can occur in a conflict.

2.4. Results

This section on the one hand characterizes equilibrium behavior, providing closed-form solutions in the symmetric case and piecewise solutions for mixed constraints, on the other hand shows numerical simulations on the model. The theoretical results of the model identify how the model parameters in the two defined regimes affect rent dissipation. The numerical analysis focuses on three agents, offering insights into the model behavior as network topologies, appropriation effort profiles, stock abundance, and stock prices vary. It then explores how results are influenced by spillovers and an increasing number of agents. (showing that while the main outcomes remain consistent, a higher number of agents leads to a greater value of the outcome variable, RD). Additionally, the parameter appropriation effort is endogenized, therefore the intensity of the conflict is defined, testing implications of parameters into the established regimes.

To build intuition behind the RD metric, consider the following example. There are three economically identical agents whose payoff is given by $\pi_i = 10e_i - 0.5e_i^2 - 0.02e$. According to equations 9 and 11, the private and social optima are given by $e_i^* = 9.8$ and $e_i^W = 8.5$, respectively. The private optimum is economically dominant, $\pi_i^W = 35.9 < \pi_i^* = 48.1$, but does not maximize social welfare, $W(\boldsymbol{e}^W) = 107.7 > W(\boldsymbol{e}^*) = 98.1$. As a result, rent dissipation remains low, $RD = 0.09$, since the marginal cost of the externality is not high enough to significantly reduce extraction at the social optimum. Due to a conflict in which one of the agents is excluded as a result of the appropriation effort profile, rent dissipation increases significantly to $RD = 0.39$. In comparison, under an initial scenario of resource scarcity where extractions are limited by 10 percent, RD decreases to 0.02. In the context of severe scarcity or significant barriers to resource access due to conflict, where extractions are restricted to 65 percent of the efficient level and resource prices have tripled, rent dissipation would be strongly affected, reaching $RD = 0.59$. The following section examines these combined effects to identify tipping points or lines where rent dissipation is highly influenced by the nonlinear effects of appropriation efforts, network structures, stock abundance or scarcity, and prices.

The results highlight the complex interaction between network structure and appropriation effort distribution in shaping RD outcomes. Across all scenarios, competition among agents dictates the dynamics, with RD varying depending on how efforts are distributed. Tipping points emerge where small changes in effort profiles lead to sharp transitions in RD, showing that competitive balance is key to understanding resource appropriation. From an economic perspective, scenarios with mixed efforts and spillovers between agents are particularly valuable. These situations reveal how changes in effort and spillover distribution can lead to significant shifts in RD, amplifying or reducing disparities in resource control and rents, which is crucial for understanding real-world conflicts over shared resources.

2.4.1. Rent Dissipation

In this section, we analyze how key model parameters influence rent dissipation RD. We consider two scenarios: (i) agents face no limits on extraction and can fully extract their appropriated amounts (unrestricted case), and (ii) agents cannot extract the entire appropriated amount (restricted case). For each parameter, we first examine the relationship analytically and then corroborate and extend the findings through numerical simulations. Specifically, we assess the effects of network structure and appropriation effort (Section 2.5.1.2), resource-stock abundance (Section 2.5.1.3), and stock prices (Section 2.5.1.4). Simulations were conducted with three agents, yielding four possible network structures (Fig 2.1). For each structure, we computed all feasible combinations of appropriation efforts across the three agents. Boundary conditions are defined by the maximum effort vectors $x=(100,0,0)$, $x=(0,100,0)$ and $x=(0,0,100)$. In every combination, the price p, resource stock S, and spillovers parameters β and γ were fixed at the base-case values specified in Table 2.1. For the simulations, we focused on the case for which, based on analytical results, the parameter becomes relevant to be tested numerically.

Table 2.1. Description of parameters used in simulations.

Parameter	Description	Symbol	Base case	Source
Rent dissipation	Economic losses of conflict	RD	Outcome variable	Own elaboration
Appropriation effort	Effort group i puts into appropriation	x_i	[0,100]	Tullock (1980)
Signed network	Alliances-enemies network	g	3	Hiller (2017)
Resource	Amount of resource	S	30	Determined by the authors
Price	Price of resource	p	5	Determined by the authors
Positive spillover	Allies' influence on effort	β	0.2	König et al. (2017)
Negative spillover	Enemies' influence on effort	γ	0.4	König et al. (2017)

4.1.1 Overexploitation and externalities

Proposition 2.1. *In the presence of negative externalities, conflict equilibrium features overexploitation relative to the social optimum. Overexploitation is increasing in the number of agents and the resource price and decreasing in the strength of the externality. It is zero in the absence of externalities.*

Proof: See Appendix A.

The intuition behind this result is straightforward. When agents make extraction decisions independently, they consider their own benefits but not the negative effects their actions impose on others. As a result, each agent extracts more than would be optimal from a collective perspective. This gap between individual incentives and the social optimum leads to overexploitation of the resource. The problem becomes more severe as the number of agents increases, since each additional agent imposes further costs on others without internalizing them. Similarly, higher resource prices strengthen incentives to extract, further amplifying total extraction. By contrast, when the negative externalities are stronger, extraction becomes more costly, which moderates agents' behavior and reduces overexploitation. In the absence of externalities, individual and collective incentives are aligned, and the inefficiency disappears. A formal derivation of these results, along with the corresponding comparative statics, is provided in Appendix D.

2.4.1.2 Appropriation effort

Proposition 2.2. *When agents' optimal extraction falls below their appropriation (unrestricted case, $e_i^* < A_i$), the economic losses are not affected by a change in the appropriation. Under restricted case ($e_i^* = A_i$), the effect of appropriation on the economic losses may become positive if appropriation is unbalanced between the different agents***.**

Proof: See Appendix A.

In the unrestricted case, the private optimum fails to optimize the appropriate quantity, so RD depends on a only through e^*. Similarly, e^* is independent of a therefore a change in appropriation does not cause a change in RD, this implies that when agents can extract without constraint, greater appropriation effort does not translate into higher economic losses. However, on the restricted case the private optimum can achieve the appropriate quantity, in this case we analyze the change in the amount appropriated by agent k when the level of appropriation of agent i changes. The effect of appropriation on RD will be positive if the appropriation benefits of the agents are concentrated and not dispersed among the different agents, for example, if one of the agents increases its appropriation effort, it leads to one of the agents obtaining no benefit. The restricted case is explored through numerical simulations to examine how appropriation effort, combined with network effects and spillovers, influences the level of economic losses. The unrestricted case is not analyzed because, without limits on the amount of resources that can be appropriated, agents lack any incentive to increase their appropriation effort to extract more, and consequently the RD remains unaffected.

Fig 2.2 illustrates the joint effects of network topology and appropriation effort profiles on RD. It includes the four network topologies for three agents shown in Figure 1 and overlays all possible appropriation effort profiles satisfying $x_A + x_B + x_C = 100$ on each topology, stock resource and prices are fixed $S = 30$ and $p = 10$ respectively. The appropriation efforts are arranged in ascending order for each agent, considering all possible combinations with the other two. The game outcomes are color-coded: low RD appears in green, high RD in red, and intermediate values in blue. In Figure 2a, where all agents are allies, RD remains low except for extreme cases such as $x = (100, 0, 0)$. For instance, when $x = (40, 30, 30)$, each agent contributes efforts while benefiting from their allies' actions, reinforcing collective control over the resource. Even when one agent slightly increases its effort, such as in $x = (50, 25, 25)$, the positive spillovers prevent a sharp rise in RD, as the cooperative structure mitigates the impact of individual appropriation efforts. In Fig 2.2b, where agent A has two enemies, RD peaks when A dominates appropriation efforts. For example, at $x = (75,15,15)$, A's appropriation intensifies competitive pressures, leading to higher RD. However, a shift towards a more balanced effort profile, such as $x = (60, 20, 20)$, triggers a tipping point. Here, B and C's efforts counteract A's dominance, stabilizing the contest and reducing RD. If appropriation efforts become even more evenly distributed, as in $x = (50, 25, 25)$, the competitive effects weaken further, leading to lower RD despite the presence of negative spillovers. As A loses control over the resource, $x_A < 40$, RD

increases again towards intermediate values. This occurs because B and C appropriate the resource in a more similar manner, generating positive spillovers between them while exerting negative spillovers on A. As a result, the difference in RD between A and its enemies grows. However, this increase is not as pronounced as in the case where A fully dominated the resource. In Fig 2.2c, where agent C has two allies, RD remains low when C dominates resource appropriation. This is due to the positive spillovers benefiting both allies, B and A, equally. For example, when $x=(20,20,60)$, C's appropriation efforts enhance resource control without triggering competitive pressures among the allies. However, this effect is counteracted when one of C's allies accumulates at least 50% of the appropriation effort ($x_A>50$ or $x_B>50$). Since A and B are enemies, positive and negative spillovers offset each other, leading to an increase in RD due to the dominant agent's competitive appropriation. Instead of a single tipping point, as seen in Figure 2b, this scenario presents two tipping lines, starting at $x=(70,30,0)$ and $x=(30,70,0)$, where RD transitions rapidly from low to high. For instance, at $x=(60,30,10)$, the dominance of A over C disrupts the balance, amplifying RD despite the initial presence of positive spillovers. As before, RD remains low when all agents have similar appropriation efforts. In Fig 2.2d, where all agents are enemies, the results follow a pattern similar to Figure 2b but with three tipping points. Transitions from low to high RD occur at $x=(40,30,30)$, $x=(30,40,30)$ and $x=(30,30,40)$. Beyond these points, one agent becomes dominant in the conflict, accumulating rents while generating negative spillovers for the other two, further amplifying differences in rents. For example, at $x=(45,30,25)$, agent A's increasing appropriation efforts lead to a significant rise in RD, as B and C face greater competitive pressure. Similarly, at $x=(30,45,25)$, B's dominance disrupts the balance, intensifying negative spillovers and further increasing RD.

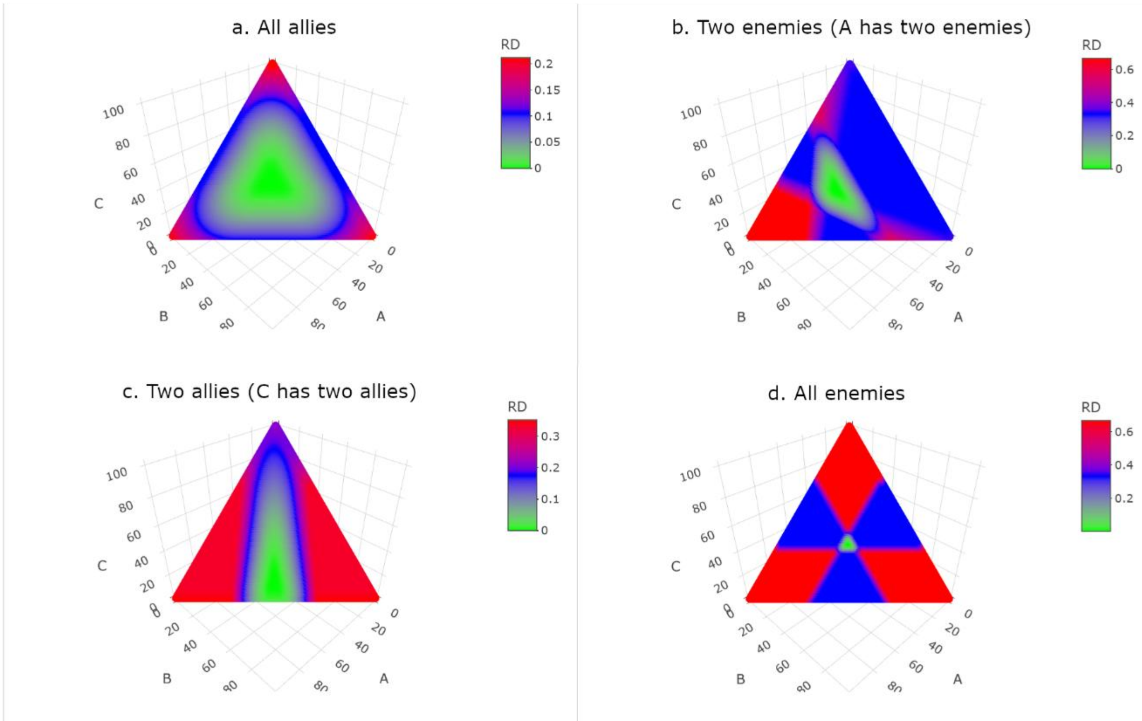

Fig 2.2. *RD* across network structures and appropriation effort profiles: a. All allies; b. A faces two enemies, B and C are allies; c. C has two allies, A and B are enemies; d. All enemies.

2.4.1.3 Stock Effects

Proposition 2.3. *If S is large enough (stock abundance) agents do not have extraction constraints ($e_i^* < A_i$) then, economic losses are not affected in this range. If S is small (stock scarcity), economic losses increase as the extraction accumulates over a small number of agents.*

Proof: See Appendix A. □

Economic losses from resource depletion depend on the size of the stock. When the resource is abundant, agents extract freely without restrictions, and disputes do not arise. However, when the stock becomes limited and conflicts emerge among agents competing for control, economic losses increase as extraction becomes concentrated in the hands of a few, this case is expanded on the numerical simulations, allowing for better intuition of how changes in stock levels lead to changes in RD. In the simulations $S = 30$ and $S = 10$ show the restricted case, while $S = 50$ reflects the restricted case.

The simulation results are presented in Fig 2.3. Across all network structures (Fig 2.1), the mean RD first increases when S rises from 10 to 30 and then decreases as S grows from 30 to 50. This is due to a change in the regime; at $S=30$ and $S=10$, the restricted situation arises, creating disputes between agents, generating economic losses. At $S=50$, there are no stock restrictions, so disputes and economic losses decrease. For example, when all agents are allies, Nash equilibrium , the mean RD is 0.034 at $S=10$, increases to 0.064 at $S=30$, and drops to 0.0051 at $S=50$. In the scenario where all agents are enemies, the mean RD is 0.207 at $S=10$, rises to 0.51 at $S=30$ and then slightly declines to 0.49 at $S=50$.

A closer examination of each network structure (Fig 2.1) shows that the scale and the maximum value of RD vary depending on the structure. When $S=30$ and all agents are allies, the maximum RD reaches 0.25. If there are two allies in conflict, the maximum increases to 0.35. With two enemies or when all agents are enemies, the maximum RD reaches 0.65.

The results also indicate that the combination of resource accumulation through appropriation effort and non-cooperative scenarios leads to higher RD, meaning greater economic losses. For instance, Figure x shows that when one agent (A) faces two enemies, RD rises with A's appropriation effort. Conversely, when agents B and C are as powerful as A, RD remains close to zero because resource extraction is more evenly distributed. In the case where all agents are enemies, RD approaches zero only when all agents exert similar appropriation efforts, preventing the concentration of resources among a few agents.

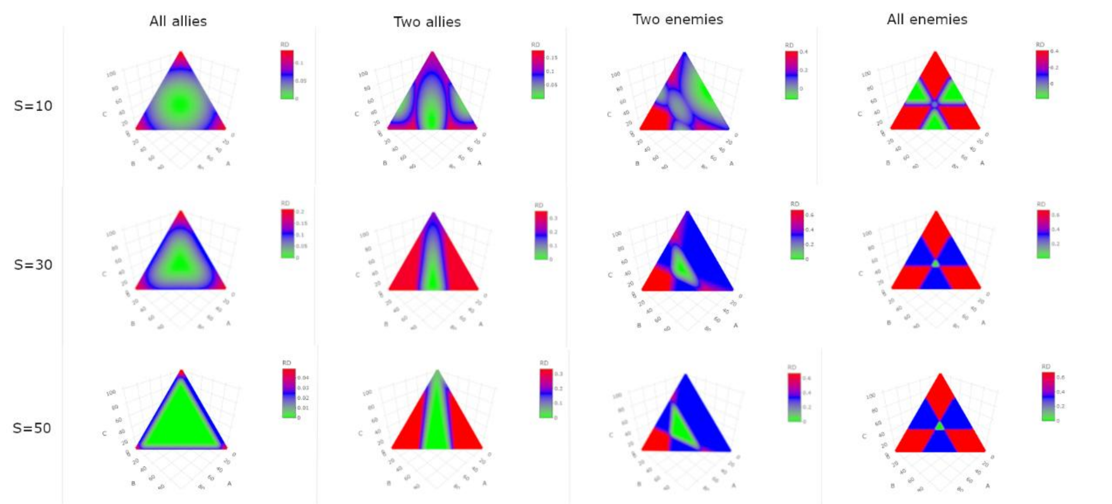

Fig 2.3. *RD* across varying stock (S) values under different appropriation efforts and network structures.

2.4.1.4. Price Effects

Proposition 4. *Under unrestricted case (* $e_i^* < A_i$ *and* $e_i^W < A_i$ *) extraction profiles (private and social) depend on prices. Higher prices raise the benefits under both cooperative and conflict profiles; then economic losses are then less severe when rent over resources are high. On the other hand, under restricted case extractions do not depend on prices, then when agents are more cooperative, economic losses decrease.*

Proof: Appendix A.

When agents face no extraction constraints, both private and social extraction are price dependent. Consequently, rising prices increase profits and reduce economic losses. Higher prices also raise income per unit for all participants, under both cooperation and conflict. Moreover, the relative inefficiency of conflict diminishes as prices rise at low prices, the efficiency gap is large, because conflict wastes considerable value, whereas at high prices the extra profit per unit extracted makes the proportional losses from non-cooperation less significant. Simulation results amplify this effect on different network structures as resource prices rise. Under extraction constraints, the quantity extracted is determined exclusively by appropriation effort, independent of prices; thus, economic losses diminish only as agents increase their level of cooperation.

In these simulations, the price parameter p takes three values: $p=10$ (baseline), $p=20$, and $p=30$, while all other parameters remain at their baseline values (Table 2.1). The model is simulated for each of the four network structures in Fig 2.1, and the results are shown in Fig 2.4. Analyzing the mean RD as prices increase, a clear decreasing trend emerges across all network structures. For instance, when all agents are allies, the mean RD declines from 0.064 at $p=10$ to 0.057 at $p=20$ and further to 0.034 at $p=30$. Similarly, in the scenario where all agents are enemies, the mean RD falls from 0.51 at $p=10$ to 0.38 at $p=20$, and to 0.20 at $p=30$.

Examining the behavior across network structures (Fig 2.1) reveals distinct patterns. In the scenario where all agents are allies (column 1), the green zone expands as prices rise. Profiles that previously exhibited an RD near 0.2 at $p=10$ approach zero when p increases to 30 (e.g., $x=(45,55,0)$). Likewise, the maximum RD decreases from 0.25 to 0.15. When agent C has two allies (column 2), two red zones appear at $p=10$, marked by two tipping lines. These indicate greater appropriation efforts by agents A or B (e.g., $x=(80,20,0)$)). As prices rise, these red areas gradually fade; by $p=30$, they shift from blue to green, signifying a substantial drop in RD. The maximum RD also falls from 0.35 at $p=10$ to 0.20 at $p=30$. For the case in which agent A faces two enemies (column 3), RD remains largely unaffected by price when A exerts greater appropriation effort than B and C, the triangular red region persists even as prices rise. Nevertheless, the maximum RD declines from 0.65 at $p=10$ to 0.40 at $p=30$. In contrast, when A has little power and B and C exert comparable appropriation efforts (e.g., $x=(0,60,40)$), the RD remains close to zero. Finally, in the scenario where all agents are enemies (column 4), areas in which two agents share similar appropriation efforts while the third does not (e.g., $x=(45,55,0)$ or $x=(50,0,50)$) exhibit a sharp decline in RD, from about 0.3 at $p=10$ to nearly 0 at $p=30$. Here too, the maximum RD decreases from 0.65 to 0.40 as prices rise.

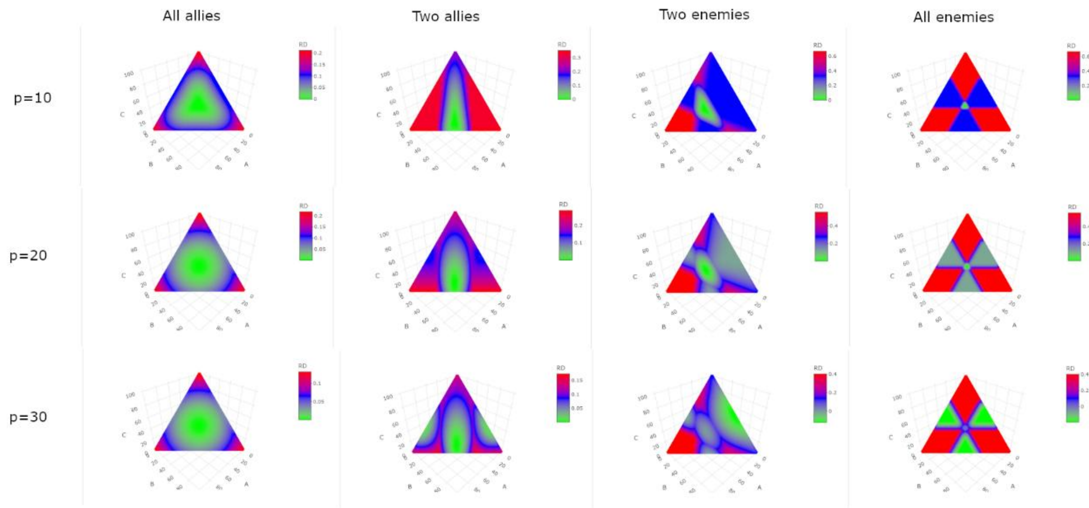

Fig 2.4. RD across varying price (p) values under different appropriation efforts and network structures.

2.4.1.5 Spillovers

We analyze how spillovers affect RD in settings where outcomes are less predictable: two enemies (Fig 2.2b) and two allies (Fig 2.2c). Simulations are conducted with varying values of spillover parameters (β and γ), and four distinct scenarios are considered to understand the effects of these dynamics: (i) Strong negative spillovers ($\beta << \gamma$): Conflict escalates as agents sabotage enemies' extraction sites to weaken their position, maximizing control but drastically increasing RD. Destruction reduces resource access, intensifying competition. (ii) Moderate negative spillovers ($\beta < \gamma$): While conflict remains, occasional agreements or temporary ceasefires allow for limited access, preventing RD from reaching its highest levels. However, tensions persist, and instability can lead to renewed disputes. (iii) Moderate positive spillovers ($\beta > \gamma$): Competition remains, but agents avoid direct destruction of extraction sites, maintaining access to resources. As agents realize that excessive conflict undermines appropriation efforts, RD decreases. (iv) Strong positive spillovers ($\beta >> \gamma$): Investments in access to the resource by one agent provide benefits to their allies. Even if one agent controls most of the resources, the increased access and productivity advantage extends to all allies, resulting in a more evenly distribution of rents among them. Fig 2.5 illustrates the results. In Panel A, agent A faces two enemies. As negative spillovers (γ) grow much larger than positive spillovers (β), the gap in rents between agents widens, causing RD to rise. This indicates that whether agent A has substantial control or reduces it, the level of RD intensifies. Conversely, when positive spillovers (β) dominate, even with agent A maintaining control, the alliance between agents B and C helps to lower RD, as they mutually benefit. Here, despite competition, the enemies avoid excessive destruction and keep access to the resource intact, mitigating RD. In Panel B, group C has two allies. As γ decreases, group C's ability to share resources with agents A and B improves, leading to lower RD across most appropriation effort profiles. Moreover, when β far exceeds γ, RD only increases if one ally, A or B, gains complete control over the resource. This suggests that dominant positive spillovers enable allies to benefit from one another, reducing RD. Yet, when an ally seizes total control, shared benefits are lost, and RD escalates. The interaction between network structure and spillover effects reveals that RD outcomes are influenced not only by the control agents exert over resources but also by how they manage resource access through spillovers within the network. In scenarios with more balanced appropriation efforts and spillover profiles, agents are more effective at managing conflicts, leading to reduced rent disparities. However, in highly competitive situations where one agent dominates resource control, the combination of positive and negative spillovers, along with network effects, can significantly impact resource rent outcomes. Ultimately, a deeper understanding of the joint effects of network structure and spillovers on RD is crucial for designing policies aimed at reducing RD in resource conflicts.

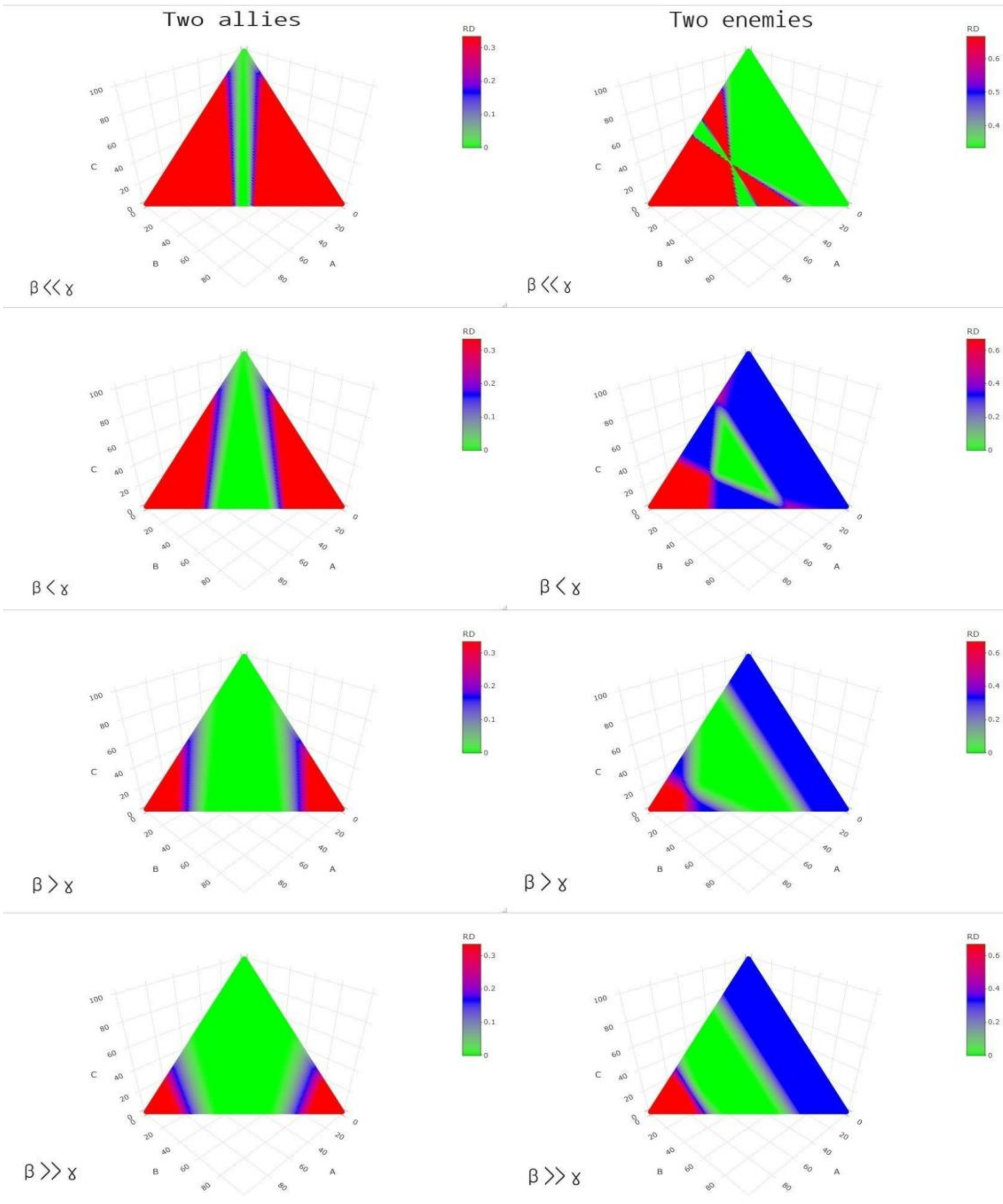

Fig 2.5. Spillover effects on *RD* for different network structures with two allies (Panel A) and two enemies (Panel B) under varying positive (β) and negative (γ) spillover values.

2.4.1.6 Multiple agents

After presenting the results for three agents in Tables 2.2 and 2.3, we expand the analysis to include different numbers of agents: 5, 7, 12, 50, and 100. The previous simulations with three groups showed that price variations lead to higher *RD* values compared to other parameters.

Therefore, we test $p=5$, $p=15$ and $p=30$. Network structure is represented by the ratio connection variable, which indicates whether there are more ally connections than enemy connections (or vice versa). Additionally, the standard deviation ($sd = 1$ and $sd = 10$) reflects whether appropriation efforts among agents are similar or different. A standard deviation of 1 means that groups have similar appropriation efforts. The results in Table 2.2 show instances where cooperation between two allied agents outweighs a link of enmity (i.e., $\beta > \gamma$), Table 2.3. Is the opposite $\beta < \gamma$.

Table 2.2. Results of simulations $\beta < \gamma$

Number of agents	Ratio connection	p=5		p=15		p=30	
		sd=1	sd=10	sd=1	sd=10	sd=1	sd=10
3	pos>neg	0,00	0,002	0,007	0,06	0,03	0,05
	pos<neg	0,0011	0,17	0,092	0,22	0,07	0,18
5	pos>neg	0,14	0,19	0,16	0,22	0,06	0,09
	pos<neg	0,44	0,41	0,39	0,40	0,3	0,27
7	pos>neg	0,19	0,30	0,18	0,26	0,08	0,11
	pos<neg	0,50	0,47	0,47	0,42	0,22	0,22
12	pos>neg	0,49	0,51	0,24	0,26	0,10	0,12
	pos<neg	0,67	0,61	0,49	0,52	0,29	0,26
50	pos>neg	0,83	0,78	0,61	0,50	0,40	0,31
	pos<neg	0,89	0,85	0,72	0,59	0,48	0,37
100	pos>neg	0,90	0,91	0,79	0,74	0,60	0,55
	pos<neg	0,92	0,93	0,82	0,79	0,62	0,62

Pos: more allies than enemies; Neg: more enemies than allies.

Table 2.3. Results of simulations $\beta > \gamma$.

Number of agents	Ratio connection	p=5		p=15		p=30	
		sd=1	sd=10	sd=1	sd=10	sd=1	sd=10
3	pos>neg	0,0	0,007	0,0009	0,01	0,015	0,02
	pos<neg	0,0	0,03	0,02	0,06	0,021	0,05
5	pos>neg	0,005	0,03	0,04	0,07	0,02	0,03
	pos<neg	0,003	0,11	0,11	0,18	0,048	0,08
7	pos>neg	0,01	0,06	0,03	0,06	0,015	0,02
	pos<neg	0,07	0,16	0,07	0,13	0,031	0,05
12	pos>neg	0,08	0,15	0,02	0,04	0,01	0,02
	pos<neg	0,14	0,20	0,04	0,07	0,02	0,02
50	pos>neg	0,02	0,02	0,009	0,010	0,007	0,008
	pos<neg	0,024	0,02	0,01	0,012	0,007	0,008
100	pos>neg	0,015	0,015	0,011	0,011	0,010	0,010
	pos<neg	0,015	0,016	0,011	0,012	0,010	0,010

Pos: more allies than enemies; Neg: more enemies than allies.

According to these results, spillovers exhibit significant sensitivity to an increase in the number of agents, particularly when β is less than γ. As the number of agents grows, the RD increases exponentially, regardless of whether the standard deviation is 1 or 10. A standard deviation of 10 is less impact because no single agent has absolute control. This result also confirms that when the ratio of connections, specifically the number of positive connections in the signed network, is greater, the RD is smaller in magnitude. Similarly, it is evident across all scenarios that an increase in the number of agents and an increase in prices lead to a growth in the RD.

2.4.2 Intensity of the conflict

To keep the algebra tractable and obtain close-form comparative statistics, we introduce three assumptions: (i) Two-stage structure collapsed for tractability. Appropriation a_i is chosen first, which determines what is extracted, that is, winner takes what she appropriates. (ii) All agents' dominance is positive in equilibrium, so the shares are interior. The share is $s_i(a) = \frac{d_i}{\sum_j d_j} = \frac{(H_a)_i}{1^T H_a}$. Extraction equals appropriate share of stock, $e_i = Ss_i(a)$. Therefore, payoff are $\pi_i(a) = pe_i(a) - \frac{1}{2}\varphi a_i^2 = p\left(S\frac{(H_a)_i}{1^T H_a}\right) - \frac{1}{2}\varphi a_i^2$.

Recall that intensity of the conflict is

$$T = \sum_{i=1}^{n} a_i. \tag{15}$$

First order conditions. General equilibrium in vector form $N_i = N_i(a) = (H_a)_i$, $D = D(a) = 1^T H_a = \sum_j (H_a)_j$, then $\pi_i(a) = pS\frac{N_i}{D} - \frac{1}{2}\varphi a_i$.

Differentiating wrt a_i using the quotient rule we can observe that only N_i and D depend on a_i, that is, $\frac{\partial \pi_i}{\partial a_i} = pS\frac{H_{ii}D - N_i(1^T H)_i}{D^2} - \varphi a_i = 0$ and $a_i^* = \frac{pS\left(H_{ii}D - N_i(1^T H)_i\right)}{\varphi D^2}$.

Here $c_i \equiv \left(1^T H\right)_i = \sum_k H_{ki}$ is a constraint, which denotes the ith entry of the row vector $1^T H$.

This is the system of nonlinear equations that pin down a. It is hard to solve in full generality, now we analyze the symmetric solution. Notice that the general case presents nonlinearity through D^2 and no diagonal dominance, so the system resists sequential solution.

To derive a close-form solution for the simplest case, we assume payoff symmetry and no spillovers. We now adopt the simplest symmetrical benchmark that leads to the close-form solution. This implies that (i) no spillovers, $\beta = \gamma = 0$, so $H = I$, and (ii) payoff symmetry, $a_i = a$ then $T = na$.

Under $H = I$, we obtain that, $N_i = a_i = a$, $D = \sum_j a_j = na$ and $1^T H_i = 1$, since column sum of I are 1. Introducing all this into F.O.C, we have that

$$\frac{\partial \pi_i}{\partial a_i} = pS\frac{1 \cdot na - a \cdot 1}{(na)^2} - \varphi a = 0. \tag{16}$$

Then,

$$a^* = \sqrt{\frac{pS(n-1)}{\varphi n^2}}\,;\; T = na == \sqrt{\frac{pS(n-1)}{\varphi}}. \tag{17}$$

In the following sections, we show comparative statistics focusing on exact derivation and elasticity. We analyze it by distinguishing between unrestricted and restricted cases.

2.4.2.1 Stock effects on T

Proposition 2.5. *In the unrestricted case, S is sufficiently large, so the intensity of the conflict T increases with S, but at diminishing rate (specifically, at the square root rate). Doubling S increases T by factor $\sqrt{2}$. In the restricted case, the intensity of the conflict remains constant.*

Proof: See Appendix B.

2.4.2.2 Prices effects on T

Proposition 2.6. *In the unrestricted case, the intensity of the conflict T increases with p but at diminishing rate and on restricted case, once all caps are filled, further increasing price reduce the intensity of the conflict linearly in p (elasticity 1), become both the per-unit value and the cap scale with p.*

Proof: See Appendix B.

The intensity of the conflict is related to the S and p. In the unrestricted case of the amount of resource to be appropriated, it is evident that more resources increase the intensity of the conflict; however, this increase occurs under diminishing returns, indicating that more resources do not drastically change the intensity. In the restricted case, agents have a limit to their appropriation, so the intensity of the conflict does not depend on the stock.

When we analyze prices and their impact on the intensity of the conflict, in the unrestricted case, an increase in prices causes the intensity of the conflict to rise, but as with the stock, further price increases generate progressively smaller increases in intensity. In the restricted case, this can be understood given that agents have a limit to their appropriation; they cannot appropriate more stock. Therefore, higher prices proportionally reduce the intensity of the conflict. Since its elasticity is 1 (linear), if the price rises by 10%, the intensity of the conflict falls by 10%.

The propositions lead to the conclusion that there are two ways to reduce the intensity of the conflict: first, by controlling stock, and second, through prices, which can be understood as an increase in costs. We then see how a regime change, established through the restriction of stock that can be appropriated, reverses the relationship between stock, prices, and conflict. In the restricted case, policies focused on prices should be considered, such as access to international markets. In the unrestricted case, since stock and prices have the same elasticities, conditions of the conflict should be sought that reveal sensitivity between stock and prices, guiding policies that lead to a decrease in the intensity of the conflict.

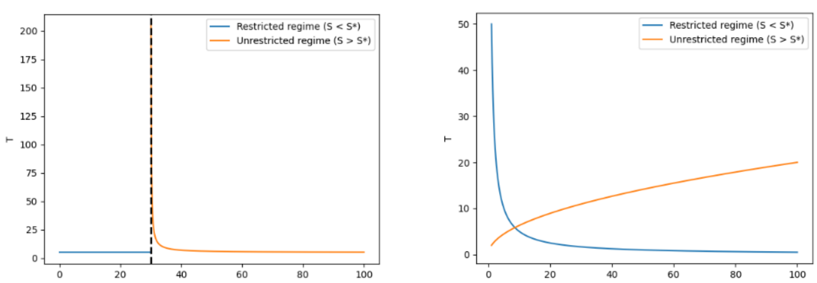

Fig 2.6. Intensity of conflict T before regime change unrestricted vs. Restricted in the amount of resource S that agents can appropriate.

Appendix B shows the effect of spillovers and the number of agents involved in the conflict on the intensity of the conflict.

2.5. Application: Sudan’s gold conflict

We are going to exemplify the rent-dissipation and the intensity of the conflict throughout Sudan’s gold conflict, using different data sources (Soliman & Baldo, 2025; European Union Agency for Asylum [EUAA], 2025; Trading Economics, n.d.). Following South Sudan's secession in 2011, Sudan's oil sector suffered a significant loss of revenue, fueling a boom in gold mining to generate foreign exchange. Gold became central to the Sudanese economy, and its extraction, trade, and export were increasingly controlled by security forces, the military, and paramilitary groups. Consequently, the gold trade has been a major driver of the ongoing armed conflict in Sudan: the struggle to control mines, processing facilities, export routes, and related resources has intensified the war.

Within this conflict, two actors stand out: the Sudanese Armed Forces (SAF), which formally represents the regular army of the Sudanese state. During the transition period following the fall of Omar al-Bashir, the SAF maintained its institutional power. Historically, the SAF has controlled many declared mining sites and extraction zones and has attempted to redirect gold export routes toward Egypt to increase its revenue. The Rapid Support Forces (RSF), originally created as a paramilitary force under the Bashir regime, have grown in economic and military power and compete directly with the SAF. The RSF has used the gold trade as a key source of funding, particularly through export routes to the United Arab Emirates (UAE) and other markets in the region, dominating gold-rich territories and controlling smuggling routes. A third actor [1], the Sudan People’s Liberation Movement–North (SPLM-N), which emerged from the conflict between Sudan and the then-south (now South Sudan), is aligned with or associated with the RSF in certain areas (e.g., South Kordofan/Blue Nile) and exerts territorial control by collaborating with the RSF in the war. In areas where the SPLM-N operates, resource extraction (including gold) is linked to rebel or semi-controlled territory, so the SPLM-N participates indirectly (or directly in some cases) in the exploitation networks and alliances that allow the RSF to extend its economic and military reach. Their alliance with the RSF strengthens the RSF's ability to operate in

[1] There are other non-state armed actors (SPLM-N, tribal militias, traders, Wagner/African Corps). We focus on the SPLM-N because it has had direct clashes with the SAF in the past and has recently been linked to RSF.

southwestern Sudan, enabling them to secure routes, mines, and extraction zones in those regions less controlled by the SAF. The signed network of Sudan conflict is represented in Fig 7.

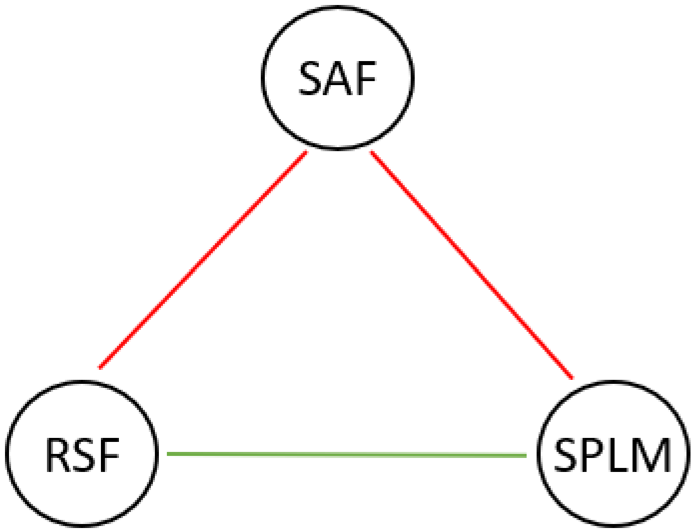

Fig 2.7. Gold Sudan's conflict Signed network. Sudanese Armed Forces (SAF), Rapid Support Forces (RSF) and Sudan People's Liberation Movement–North (SPLM). Connections in red signify a negative relationship, i.e., enemies. In green, it signifies an alliance.

We next describe the necessary parameters to find RD (14) and the intensity of the conflict (15) on the Sudan's conflict.

Stock

According to Soliman and Baldo (2025), Sudan's total gold production before the war in 2022 was around 87 tons, falling by two tons once the war began. Therefore, we can estimate the stock (S) at around 85 tons.

Appropriate portion

For each group, we estimate the portion of total production appropriated A, measured in tons. According to Soliman & Baldo (2025) the RSF controlled 10 tons out of ~85 tons. SAF controls the main producing areas of the River Nile, Northern, and Red Sea states, hence, controlling 64.36 tons in 2024. For the SPLM, we estimate its share based on the proportions controlled by the SAF and RSF. Together, these two groups appropriate 85% of the 64.36 tons. This leaves other armed groups, including the SPLM, with an appropriation range of 0–12%, equivalent to approximately 0–10 tons. Therefore, due to the uncertainty of data we set the SPLM controls around 2 tons, bearing in mind that this does not affect the scale of the quantitative results that we will derive from the analysis.

Appropriation effort

For appropriated effort a, measured in number of combatants, according to EUAA (2025) the RSF, the estimate ranges from 70,000 to around 100,000 combatants, and the SAF's strength was between 120,000 and 200,000 combatants at the start of the war. For the number of combatants of SPLM, there are around 30,000 combatants (Leff & LeBrun, 2014, p. 22).

Appropriation costs

Appropriation costs (φ) measured in US$ represent the cost per combatant. For RSF, the gold production of controlled areas in 2024 to be 10 t of gold, for a value of US$860 million, (Small Arms Survey, 2025; Soliman & Baldo, 2025), of that value, according to other studies on gold and paramilitaries in the region (UNEP, MONUSCO, & OSESG, 2015) 15% goes towards the cost of the combatants; this results in US$129 million and we divide by the number of combatants, which is 70,000. Therefore, the value per combatant is US$1842. For the SAF, according to the website Trending in Economics, an estimated annual military expenditure is US$ 375200000, and the number of combatants is in average 160.000. The result of dividing the expenditure by the number of combatants is US$2345, which would be the expenditure per combatant. For the SPLM, we take as a reference the DR Congo (UNEP, MONUSCO, & OSESG, 2015) where the value per combatant of armed groups similar in size and characteristics is around US$1500.

Total revenue and production costs

According to Soliman & Baldo (2025), SAF produced a total value of US$1.6 billion, corresponding to 27 tons of gold. This results in a total revenue of approximately US$59.3 million per ton (p). Using the production cost (c) of US$1214 per ounce, equivalent to about US$39 million per ton (Abiodun, 2024), SAF's net profit per ton is around US$20.2 million. For the RSF, total revenue was US$860 million for 10 tons of gold, yielding a revenue of US$86 million per ton. Assuming the same cost per ton, the net profit per ton for the RSF is approximately US$47 million. Finally, SPLM generated US$172 million in total revenue for 2 tons, also equivalent to US$86 million per ton, resulting in a net profit per ton of about US$47 million. Table 2.4 summarizes the revenue per ton, cost per ton, net profit per ton, and total profit for each group, as well as appropriation portion, appropriation effort and appropriation costs.

Table 2.4. Parameters to determine RD and intensity of the conflict.

Armed group	p	c	A	a	φ
RSF	US$ 86,000,000	US$ 39,030,977	10 tons	70.000 combatants	US$1842
SAF	US$ 59,259,259	US$ 39,030,977	64,36 tons	160.000 combatants	US$2345
SPLM	US$ 86,000,000	US$ 39,030,977	2 tons	30.000 combatants	US$1500

However, to derive (1) for each agent, it is necessary to estimate the spillover effects. Using equations (1) and (3), and considering agent dominance as defined in equation (1), it is obtained that

$$\begin{cases} d_{RSF} = a_{RSF} + \beta \cdot a_{SPLM} - \gamma \cdot a_{SAF} \\ d_{SAF} = a_{SAF} - \gamma \cdot (a_{RSF} + a_{SLPM}) \\ d_{SPLM} = a_{SPLM} + \beta \cdot a_{RSF} - \gamma \cdot a_{SAF} \end{cases} . \tag{18}$$

Finally, combining all components and applying equation (3), it is obtained that

$$\begin{cases} \dfrac{10}{85} = \left(\dfrac{(70.000) + \beta \cdot (30.000) - \gamma \cdot (160.000)}{(160.000) - \gamma \cdot (100.000) + (30.000) + \beta \cdot (70.000) - \gamma \cdot (120.000)} \right) \\ \dfrac{63}{85} = \left(\dfrac{(160.000) - \gamma \cdot (100.000)}{(70.000) + \beta \cdot (30.000) - \gamma \cdot (120.000) + (30.000) + \beta \cdot (70.000) - \gamma \cdot (120.000)} \right). \\ \dfrac{2}{85} = \left(\dfrac{(30.000) + \beta \cdot (70.000) - \gamma \cdot (120.000)}{(70.000) + \beta \cdot (30.000) - \gamma \cdot (160.000) + (160.000) - \gamma \cdot (100.000)} \right) \end{cases} \quad (19)$$

This system is then converted to

$$\begin{cases} -1850000 \cdot \beta + 11400000 \cdot \gamma - 4050000 = 0 \\ 6300000 \cdot \beta - 6620000 \cdot \gamma - 7300000 = 0 \\ -5890000 \cdot \beta + 9680000 \cdot \gamma - 2090000 = 0 \end{cases} . \quad (20)$$

However, the system is inconsistent due to there are more equations than unknowns. Therefore, we use least square to estimate β and γ. Let, $Ax = b$, such that

$$A = \begin{bmatrix} -1850000 & 11400000 \\ 6300000 & -6620000 \\ -5890000 & 9680000 \end{bmatrix}; \; x = \begin{bmatrix} \beta \\ \gamma \end{bmatrix}; \; b = \begin{bmatrix} 4050000 \\ 7300000 \\ 2090000 \end{bmatrix}. \quad (21)$$

We find x using $x = (A^T A)^{-1} A^T b$. Then $\beta \approx 1.420$ and $\gamma \approx 0.703$.

With all the necessary parameters to find the RD, we obtain that for the gold conflict in Sudan this value is 0.82. This indicates a substantial loss of social welfare attributable to the conflict and the weakening of property rights (82%). In other words, we can think that if the economy could produce 100 (its maximum), due to the conflict only 18 are produced. The remaining 82 points are net losses, such as resources spent on conflict (defense, attack, protection), production that does not take place, destruction or deterioration of assets, disincentives to invest, opportunity costs of not cooperating, and allocation inefficiencies.

Using this value as a baseline, Table 2.5 shows conflict intervention scenarios involving both price increases (p) and decreases in appropriation efforts (a), that is, the number of combatants in the groups. Thus, it is evident that a 25% price increase leads to a 4.37% decrease in RD, a 50% increase results in an 8.32% decrease, and a 75% increase leads to an 11.98% decrease in RD. On the other hand, a 25% decrease in combatants leads to a 5.70% decrease in RD; a 50% reduction results in a 15.47% decrease; and a 75% decrease results in a 35.23% decrease.

Table 2.5. Interventions on RD

Intervention		RD	% change in RD
prices	(+) 25%	0.78	-4.37%
	(+) 50%	0.75	-8.32%
	(+) 75%	0.72	-11.98%
Appropriation effort	(-) 25%	0.77	-5.70%
	(-) 50%	0.69	-15.47%
	(-) 75%	0.53	-35.23%

The example illustrated allows us to identify that reducing appropriation effort by 75%, through policies of arms confiscation or force, is not enough to decrease RD, a fact that would generate more conflict; however, it is a difficult problem to solve, so giving greater consideration to economic instruments as options in conflict resolution is important.

2.6. Discussion and policy implications

The results obtained from the simulation of the two-stage model using the RD allow us to draw several conclusions. First, the relations of cooperation and discord between agents, potentially in competition for a natural resource, play a determining role in shaping the results of the conflict. This phenomenon is captured through signed networks, where positive links represent alliances and negative links represent enmities. Numerous studies, such as those by Löhr et al.

(2021) and Marco and Goetz (2023), emphasize that cooperation, social cohesion, and the flow of information contribute to a more efficient and sustainable use of resources. In the context of an armed conflict, these cooperation networks can be seen as strategic alliances that allow a more rational distribution of the war effort and the extraction of the resource, minimizing economic losses. According to Jackson (2020), the existence of more alliances strengthens community capital, understood as the capacity to sustain cooperative behavior plays a crucial role in maximizing overall social well-being, particularly in managing common goods and fostering collective action within communities. This is reflected in our model, where lower RD values are observed when all network links are positive, indicating lower economic losses compared to conflict-driven scenarios. Therefore, promoting cooperation and dialogue between conflicting parties is essential. Policymakers should implement trust-building and mediation mechanisms to facilitate agreements and alliances among groups competing for resources.

Additionally, the model highlights the significant impact of power asymmetry among agents. In a scenario where all agents are enemies, but one has a significantly higher appropriation force (e.g., superior weaponry), RD peaks, reflecting heightened conflict and greater economic losses. However, under the same network structure, when all agents have equal appropriation power, RD decreases substantially. This phenomenon can be interpreted as a 'deceptive social optimum, where, despite competition, agents implicitly avoid full conflict escalation, resulting in a more stable yet tense dynamic. This behavior aligns with game theory models applied to armed conflicts (Bier et al., 2007; Gries and Haake, 2016; Ho et al., 2022), where actors adjust their strategies based on rational expectations about their adversaries' actions. In balance-of-power situations, mutual deterrence can prevent conflict escalation, whereas significant asymmetry tends to trigger violent confrontations and greater economic losses.

Interventions should aim to level the playing field between conflicting parties. Policies that promote a more equitable distribution of power or resources whether economic, technological, or otherwise can help prevent a dominant actor from monopolizing the benefits and escalating the situation into violent conflict. Measures such as disarmament policies, reduction in military capabilities, and strengthening mechanism for justice and fair resource distribution can contribute to a more balanced and stable environment.

Another relevant aspect of the results is the relationship between resource prices, abundance, and conflict intensity. While the literature is ambiguous regarding the relationship between resource abundance and conflicts over resource appropriation (Collier and Hoeffler, 2004; Dickson et al., 2022; Han and Feng, 2023), studies such as those by Zallé (2023) suggest that the effects of abundance in RD depend on other contextual factors, such as institutional quality. In this sense, armed conflict dynamics can be exacerbated in environments where institutions are weak or corrupt, facilitating the violent appropriation of resources. On the other hand, according to Nillesen and Bulte (2014), increasing resource prices can lead the actors involved to allocate more effort to the conflict, thus increasing RD. In the context of armed conflict, this translates into an escalation of violence as the perceived value of the resource in dispute increases, encouraging greater investment in military or strategic resources. It is essential to develop price control mechanisms or policies that ensure that fluctuations in resource prices do not trigger greater conflict intensity. Programs to stabilize the economy and reduce dependence on a single resource (economic diversification) can mitigate such disputes.

These facts are captured in the developed model and supported by various works based on Tullock's research (Tullock, 1980; Hirshleifer, 1989; Polishchuk and Tonis, 2013) and König et al. (2017), who, in turn, build on Tullock's contest success function. Their work introduces the network as a variable of interest, and it plays a critical role as an exogenous variable in competition, which can ultimately lead to conflict. Furthermore, unlike König et al. (2017), who focus on a dispute over a resource and account for alliances and competitors while disregarding the resource's price, we propose in the second stage of our model that both the quantity of the resource and its price become relevant.

Building on these authors' work, while further refining and expanding the analysis, we propose an integrated, two-stage model that allows us to derive results facilitating the development of more accurate policies. The primary objective of this investigation is to characterize the RD and identify which parameters significantly contribute to its increase. However, to offer effective policies for reducing RD, a more in-depth exploration of the proposed approaches is necessary to enrich the analysis. This could be pursued in future research by, for example, analyzing equilibrium based on directed networks, especially when these are not endogenously determined. Such an analysis would allow us to explore the impact on RD when one group leaves or disappears from the contest (Hiller, 2017), or when links change, such as when enemies become friends or vice versa (Cisneros-Velarde and Bullo, 2020). Moreover, our model performs comparative statics across various parameters, including appropriation effort, network topologies, and resource characteristics (amount and price). Incorporating a dynamic resource into the model would enable a more detailed analysis by allowing us to examine how agents, their relationships, and the tested parameters such as resource quantity and price evolve continuously over time. This research highlights its application to real-world conflicts, as demonstrated in the case of Sudan and gold. The results obtained from calibrating this conflict using the developed model have two implications. The first is methodological, as spillovers are estimated using systems of linear equations, whereas in the literature they are estimated using econometric methods (Konig et al., 2017). The second implication is more policy-oriented, showing that the risk of disaster can be reduced through price adjustments, suggesting that increasing costs could be a strategy worth pursuing.

2.7. Conclusion

This study develops a two-stage model to examine the economic losses generated by competition over a natural resource. Rather than focusing on standard measures of conflict such as fatalities or military capacity, the model captures conflict through its economic consequences. The framework combines two key elements. On the one hand, agents compete to secure control over the resource. On the other hand, they decide how much of the resource to use in order to maximize their gains, taking prices into account. Interactions between agents are shaped by a network of alliances and enmities. The analysis compares two benchmark cases. In the first, agents coordinate and achieve an efficient outcome. In the second, they act in their own interest, leading to inefficient outcomes. The framework can also accommodate intermediate situations, as well as differences in resource availability. The results show that cooperation reduces economic losses, while imbalances in power across agents play a central role in shaping outcomes. When all agents are equally powerful and in conflict, the model converges to a balanced outcome. Changes in prices are found to have a stronger effect on results than changes in resource availability. The model also provides insights for policy, suggesting that measures such as trust-building, mediation, and disarmament can reduce economic losses. It can be extended by allowing dynamic interactions and by letting the network of relationships evolve over time. The framework is illustrated with an application to the gold conflict in Sudan, showing how economic losses can be quantified and how potential interventions can be evaluated.

Appendices

Appendix A (Rent Dissipation).

Model setup

a_i : appropriation effort of agent i

$m_{ij} \in \{-1, 0, 1\}$: signed network (enmity, neutral, alliance)

β, γ : positive and negative spillovers

$d_i = a_i + \sum_j \beta m_{ij}^+ a_{ij} - \sum_j \gamma m_{ij}^- a_{ij}$: dominance

S : total resource stock

A_i : amount appropriated by agent i

e_i : amount extracted by agent i

First stage: Appropriation (resource appropriation)

Case 1. Conflict scenario: resource share is proportioned to dominance

$A_i = \frac{d_i^+}{\sum_j d_j^+} S$, where $d_i^+ = \max\{0, d_i\}$. A_i is endogenous since a_i is fixed and spillovers come from networks effects.

Case 2. Cooperative scenario: each agent gets an efficient allocation, determined by the social planner, $A_i = e_i^w = \arg\max_e \sum_{i=1}^{n} \pi_i(e_i, e)$, this satisfies the social optimum (see second stage) $\frac{\partial b_i}{\partial e_i} = \frac{\partial c_i}{\partial e_i} + \sum_{j \neq i} \frac{\partial c_j}{\partial e_i}$, b_i denotes resource benefits and c_i costs.

Second stage: Extraction (resource use)

Agent i choses $0 \le e_i \le A_i \le S$ to maximize $\pi_i(e_i, e) = b_i(e_i) - c_i(e_i, e)$, with $e = \sum_{i=1}^{n} e_i$. Let us assume $b_i(e_i) = pe_i - \frac{1}{2}\theta e_i^2$ and $c_i(e_i, e) = \delta e_i e$. Where b_i denotes the benefit from resource use and cost c_i the cost associated with own effort and the negative externality.

Rent dissipation

Conflict equilibrium and private optimum

$\pi_i' \equiv \frac{\partial \pi_i}{\partial e_i} = p - \theta_i e_i - \delta e = 0$, therefore, $e_i^* = \frac{p - \delta e}{\theta}$. Summing over all i, for symmetric agents (symmetry payoff) $\pi_i' = p - (\theta + \delta)e_i - \delta \sum_{j \neq i} e_j = 0$. Given symmetry, $\pi_i' = p - (\theta + \delta)e^* - \delta(n-1)e^* = 0$, then $p = e^*\left[\theta + \delta + \delta(n-1)\right] = e^*\left[\theta + \delta n\right]$. $e^* = \frac{p}{\theta + n\delta}$ hence, total extraction is $E^* = ne^* = \frac{np}{\theta + \delta n}$.

Cooperation equilibrium and social optimum

$\pi_i' \equiv \frac{\partial \pi_i}{\partial e_i} = p - \theta_i e_i - 2\delta e = 0$, notice that, for social optimum, $-\delta \sum_{i=1}^{n} e_i e = -\delta 2e \frac{\partial e}{\partial e_i} = -2\delta e \cdot 1 = -2\delta e$. With payoff symmetry, $e = ne_i^w$, $e_i = e_i^\omega = e^\omega$, this gives

$p-\theta e-2\delta(ne^{w})=0$, then $p=e^{w}(\theta+2n\delta)$. Such that, $e^{\omega}=\dfrac{p}{\theta+2n\delta}$, then, total extraction is $E^{\omega}=ne^{\omega}=\dfrac{np}{\theta+2n\delta}$.

Proof Proposition 2.1 (Overexploitation):

Overexploitation is computed as

$O\equiv E^{*}-E^{\omega}=np\left(\dfrac{1}{\theta+n\delta}-\dfrac{1}{\theta+2n\delta}\right)\simeq\dfrac{n^{2}p\delta}{2n^{2}\delta^{2}}\simeq\dfrac{p}{2\delta}$. Note that $O=0$ if $\delta=0$. If $\delta>0$, then increases as n and p increase. However, it decreases if δ is large enough. That is O tends to 0 since agents extract almost nothing when social costs (externalities) exploit.

Rent dissipation is measured as $RD=1-\dfrac{w(e^{*})}{w(e^{\omega})}$. In a symmetric setup, for n agents, we have:

$w(e^{*})=n\left(pe_{i}^{*}-\dfrac{1}{2}\theta(e_{i}^{*})^{2}-\delta e_{i}^{*}e^{*}\right)$ and $w(e^{\omega})=n\left(pe_{i}^{\omega}-\dfrac{1}{2}\theta(e_{i}^{\omega})^{2}-\delta e_{i}^{\omega}e^{\omega}\right)$.

With payoff symmetry, equal appropriation effort ($a_{i}=a$) and symmetric network ($A_{i}=\dfrac{1}{n}S$), we obtain that $e^{\omega}=e_{i}^{\omega}=\dfrac{p}{\theta+2n\delta}$, then $w(e^{\omega})=n\left(pe^{\omega}-\dfrac{1}{2}\theta(e^{\omega})^{2}-n\delta(e^{\omega})^{2}\right)$, which leads to

$w(e^{\omega})=n\dfrac{p^{2}}{\theta+2n\delta}\cdot\dfrac{\frac{1}{2}\theta+n\delta}{\theta+2n\delta}$. On the other hand, $e^{*}=e_{i}^{*}=\dfrac{p}{\theta+n\delta}$, then $w(e^{*})=n\left(pe^{*}-\dfrac{1}{2}\theta(e^{*})^{2}-n\delta(e^{*})^{2}\right)$, therefore, $w(e^{*})=n\dfrac{p^{2}}{\theta+n\delta}$. Rent dissipation is

$$RD = 1 - \frac{\frac{\frac{1}{2}\theta}{(\theta+n\delta)^2}}{\frac{\frac{1}{2}\theta+n\delta}{(\theta+2n\delta)}} = 1 - \frac{\frac{1}{2}\theta\left(\theta+2n\delta\right)^2}{\left(\frac{1}{2}\theta+n\delta\right)\left(\theta+n\delta\right)^2}.$$

Notice that $\delta = 0$ leads to $RD = 0$ (efficient) and $\delta \to \infty$ to $\delta \to \infty$ $RD = 1$ (inefficient); and RD increases non-linearly in δ. Hence, $\frac{\partial RD}{\partial \delta} = \frac{2\theta n^2 \delta}{(n\delta+\theta)^3}$. Remark that, in the limit $\delta \to \infty$, overexploitation $O \equiv E^* - E^\omega = \frac{p}{2\delta} \to 0$, however, the relative loss in social welfare is maximal since $w(e^\omega) >> w(e^*)$ then $RD = 1$. In words, a small excess in extraction in absolute terms can destroy all welfare since payoff is extremely sensitive to externalities.

Proof Proposition 2.2 (Appropriation effort)

In this case, we have that $RD = 1 - \frac{w(e^*(a))}{w(e^\omega)}$, where $w(e^\omega)$ is constant.

Extraction constraint $0 \le e_i \le A_i$, such that, $e_i^* = \min\left\{\frac{p-\delta e}{\theta}, A_i\right\}$; with symmetry or $e_i^* = \min\left\{\frac{p}{\theta+n\delta}, A_i\right\}$. Then, $\frac{\partial RD}{\partial a_i} = -\frac{1}{w(e^\omega)}\frac{\partial w(e^*)}{\partial a_i}$, since $w(e^\omega) = \sum_{i=1}^{n} pe_i^* - \frac{1}{2}\theta(e_i^*)^2 - \delta e_i^* e$, we get $\frac{\partial w(e^*)}{\partial a_i} = \sum_k \left(p - \theta e_k^* - \delta e - \delta e_k^*\right)\frac{\partial e_k^*}{\partial a_i}$.

Case 1. Unrestricted case

Given that $e_i^* < A_i$, then $\frac{\partial RD}{\partial a_i} = 0$. In this case, dominance only affects how much to extract, but not the F.O.C (first order conditions) for private (e_i^*) and social (e_i^ω) optimal extraction.

Case 2. Restricted case

In this case, we have $e_k^* = A_k$, then, $\frac{\partial e_k^*}{\partial a_i} = \frac{\partial A_k}{\partial a_i}$, so, we analyze

$$\frac{\partial A_k}{\partial a_i} = \frac{S}{\left(\sum_j d_j^+\right)^2}\left[\underbrace{\left(\delta_{k_i} + \beta m_{k_i}^+ - \gamma m_{k_i}^-\right)}_{a} - \underbrace{\left(d_{k_i}\sum_k \delta_{ji} + \beta m_{ji}^+ - \gamma m_{ji}^-\right)}_{b}\right],$$

where, $\frac{\partial A_k}{\partial a_i}$ denotes the change in agent k´s quantity A_k when agent i´s appropriation effort a_i changes. $\frac{S}{\left(\sum_j d_j^+\right)^2}$ denotes the overall scaling. When the group´s dominance is large, the impact on A_k is less sensitive to a_i´s variations. a denotes gain effect; or direct effect over d_k^+ (dominance of k). If $i = k$, then 1. In words, it measures how dominance of k changes as a_i changes. b denotes dilation effect. When a_i changes increase total dominance at both the numerator and dominator.

δ_{xi} denotes the Kronecker δ, where is 1 if $i = x$, and 0 otherwise.

Remark that $A_k = \left(\frac{d_n^+}{\sum_j d_j^+}\right)S$, then we use the quotient rule, $\frac{\partial A_k}{\partial a_i} = \left(\frac{\frac{\partial d_k^+}{\partial a_i}\sum_j d_j^+ - d_k^+ \frac{\partial}{\partial a_i}\sum_j d_j^+}{\left(\sum_j d_j^+\right)^2}\right)S.$

The effect of a_i on RD cannot be determined unambiguously. To provide to give the intuition behind of the modeling approach, we provide an example of how to compute last expression for later computation of $\frac{\partial RD}{\partial a_i}$.

Example:

$$n = 3$$
$$a = (60, 20, 20)$$
$$\beta = 0.5$$
$$\gamma = 0.7$$
$$S = 100$$
$$m = \begin{pmatrix} 0 & 1 & -1 \\ 1 & 0 & 1 \\ -1 & 1 & 0 \end{pmatrix}$$

That is 1 and 2 are allies, 1 and 3 enemies, 2-3 are allies.

Initial setup

$$d_1 = 60 + 0.5 \cdot 20 - 0.7 \cdot 20 = 56$$
$$d_2 = 20 + 0.5 \cdot 60 + 0.5 \cdot 20 = 60$$
$$d_1 = 20 + 0.5 \cdot 20 - 0.7 \cdot 60 = -12$$

Then $d^+ = (56, 60, 0)$ and $\sum_j d_j^+ = 116$. $A = \frac{100}{116}(56, 60, 0) = (48.3, 51.7, 0)$

Agent 3 is excluded since $A_3 = 0$, however, she continues to allocate effort into the conflict. The weaker agent 1 gives that and both agents compete for the same resources and therefore agent 1 loses capacity for appropriate resources. At the same time this activity benefit agent 2 since agent 2-3 are allies. Deriving,

$\frac{\partial A_k}{\partial a_i} = \left(\frac{\frac{\partial d_k^+}{\partial a_i} \sum_j d_j^+ - d_k^+ \frac{\partial}{\partial a_i} \sum_j d_j^+}{\left(\sum_j d_j^+ \right)^2} \right) S.$ First, we compute partial derivate

$$p_{j,i} = \frac{\partial d_j^+}{\partial a_i} = \delta_{ji} + \beta m_{ji}^+ - \gamma m_{ji}^- .$$

for each column i, its sum is $S_i = \sum_j p_{j,i}$. In our example

$p = \begin{pmatrix} 1 & 0.5 & -0.7 \\ 0.5 & 1 & 0.5 \\ -0.7 & 0.5 & 1 \end{pmatrix}$, then $S = (0.8, 2, 0.8)$. Now, we use the general expression, $\left[\frac{\partial A_k}{\partial a_i}\right]_{k,i} = \begin{pmatrix} 0.53 & -0.4 & -0.94 \\ 0.07 & -0.03 & 0.07 \\ -0.6 & 0.43 & 0.87 \end{pmatrix}$. It denotes an increase/decrease of A_x for each unit of a_i increased.

Now k denotes who receives the gains and column i who increases effort, a_i . Recall that $\sum_i A_i = 0$ since $\sum_k A_k = S$. As before, $\frac{\partial RD}{\partial a_i} > 0$ when $1 \geq \sum_{i=1}^{n} (k_i^*)^2 > \sum_{i=1}^{n} (k_i^{\omega})^2$. Now, focusing on one interesting case of agent 2.

$$\frac{\partial A_k}{\partial a_2} = \frac{S}{\left(\sum_j d_j\right)^2}\left[\left(\delta_{22} + \beta m_{2,2}^+ - \gamma m_{2,2}^-\right)\sum_j d_j^+ - d_2^+ \sum_j \left(\delta_{j2} + \beta m_{j,2}^+ - \gamma m_{j,2}^-\right)\right].$$

$\sum_j d_j^+ = 116$, $d_2^+ = 60$, $\delta_{22} = 1$, $m_{2,2}^+ = m_{2,2}^- = 0$

Dilution,

$j = 1 : \delta_{12} = 0$, $m_{1,2}^+ = 1$, $m_{1,2}^- = 0 \rightarrow 0 + 0.5 \cdot 1 + 0 = 0.5$

$j = 2 :$ $\delta_{22} = 1$, $m_{2,2}^+ = m_{2,2}^- = 0 \rightarrow 1$

$j = 3 : \delta_{32} = 0$, $m_{3,2}^+ = 1$, $m_{3,2}^- = 0 \rightarrow 0 + 0.5 \cdot 1 + 0 = 0.5$

$$\frac{\partial A_2}{\partial a_2} = \frac{100}{(116)^2}\left(116 - 60 \cdot 2\right) = \frac{-400}{(116)^2} = -0.03$$

On this way, the direct effect from increasing a_2 is high (116), however, the dilution effect is still low here (-120) since agent 2 has two allies and when a_2 increases so does d_1^+ and d_3^+ which to an important increase in total dominance $\left(\sum_j d_j^+\right)$. Since the dominator grows faster than the numerator, A_2 decreases.

Proof Proposition 2.3 (Stock)

We can differentiate between two cases.

Case 1. Unrestricted case (stock abundance)

If S is large enough, then $A_i > e_i^*$ (no constraints). Then the equilibrium extraction is unconstrained, in conflict and $e_i^* = \dfrac{p}{\theta + n\delta}$ (under symmetry). So, increasing S does not affect RD in this range.

Case 2. Restricted case (stock scarcity)

If S is small, then $e_i^s = A_i = k_i S$ (binding constraint) where $k_i = \dfrac{d_i^+}{\sum_j d_j^+}$, and e_i^s denotes extraction under stock scarcity and therefore $e_i^s \leq e_i^*$. This is difficult to predict and requires comparative statistics. Comparative statistics are done.

$RD(S) = 1 - \dfrac{w^*(S)}{w^{\varpi}(S)}$, with $w^*(S) \equiv w(e^*(S))$ and $w^{\varpi}(S) \equiv w(e^{\varpi}(S))$.

$\frac{\partial RD}{\partial S} = -\frac{\partial}{\partial S}\left(\frac{w^*}{w^\omega}\right) = -\left(\frac{w^\omega \frac{\partial w^*}{\partial S} - w^* \frac{\partial w^\omega}{\partial S}}{(w^\omega)^2}\right)$, reorganizing the numerator $w^\omega \frac{\partial w^*}{\partial S} - w^* \frac{\partial w^\omega}{\partial S} > 0$,

then $w^\omega \frac{\partial w^*}{\partial S} > w^* \frac{\partial w^\omega}{\partial S}$, accordingly $\frac{1}{w^*}\frac{\partial w^*}{\partial S} > \frac{1}{w^\omega}\frac{\partial w^\omega}{\partial S}$. Therefore $\frac{\frac{\partial w^*}{\partial S}}{\frac{\partial w^\omega}{\partial S}} > \frac{w^*}{w^\omega}$. $RD < 0$ if the marginal elasticity of w^* with respect to S is larger than w^ω, otherwise $RD > 0$.The sign of RD cannot be determined analytically without ambiguity. However, we can identify situations where $RD > 0$ is more likely to occur, for example in conflict situations.

We have that $e_i^s = k_i S$, $\sum_{i=1}^{n} k_i = 1$, with different vectors for private (k^*) and social (k^ω) optimum. Then the social welfare, with $e = \sum_{i=1}^{n} e_i = S$, can be simplified as follows

$w(S;k) = \sum_{i=1}^{n} pe_i - \frac{1}{2}\theta e_i^2 - \delta e_i e = pS - \frac{1}{2}\theta S^2 \sum_{i=1}^{n} k_i^2 - \delta S^2$, for every vector k. Remark that $\sum_{i=1}^{n} pk_i S = pS$ since $\sum_{i=1}^{n} k_i = 1$ and $\sum_{i=1}^{n} \delta k_i S \cdot S = \delta S^2$. Therefore, $w(S;k) = pS - \frac{1}{2}\theta S^2 \sum_{i=1}^{n} k_i^2 - \delta S^2$

and its derivate $\frac{\partial w}{\partial S}(S;k) = p - \theta S \sum_{i=1}^{n} k_i^2 - 2\delta S$. Applying this result to the private and social vectors where $w^*(S) \equiv w(S;k^*)$ and $w^\omega(S) \equiv w(S;k^\omega)$, it leads to

$$\begin{cases} \frac{\partial w^*}{\partial S} = p - \theta S \sum_{i=1}^{n} (k_i^*)^2 - 2\delta S \\ \frac{\partial w^\omega}{\partial S} = p - \theta S \sum_{i=1}^{n} (k_i^\omega)^2 - 2\delta S \end{cases}.$$

Then, $\frac{\partial RD}{\partial S} = -\left(\frac{w^\omega \left(p - \theta S \sum_{i=1}^{n} (k_i^*)^2 - 2\delta S\right) - w^* \left(p - \theta S \sum_{i=1}^{n} (k_i^\omega)^2 - 2\delta S\right)}{(w^\omega)^2}\right)$.

Reordering terms

$$\frac{\partial RD}{\partial S} = -\frac{(w^{\omega}-w^{*})(p-2\delta S)-\theta S\left(w^{\omega}\sum_{i=1}^{n}(k_i^{*})^2 - w^{*}\sum_{i=1}^{n}(k_i^{\omega})^2\right)}{(w^{\omega})^2}$$

, recall that $w^{\omega} - w^{*} > 0$ and this is reasonable to expect $p - 2\delta S < 0$. Therefore, $\frac{\partial RD}{\partial S} > 0$ if $1 \geq \sum_{i=1}^{n}(k_i^{*})^2 > \sum_{i=1}^{n}(k_i^{\omega})^2$, that is when conflict accumulates extraction over small number of agents. For example, when conflict leads to appropriation $k^{*} = \left(\frac{2}{3}, \frac{1}{3}, \frac{0}{3}\right)$ compared to cooperative case $k^{\omega} = \left(\frac{1}{3}, \frac{1}{3}, \frac{1}{3}\right)$.

Proof Proposition 2.4 (Price)

In this case we have $RD = 1 - \frac{w(e^{*}(p))}{w(e^{\omega}(p))}$.

Case 1. Unrestricted case

Both extraction profiles (private and social) depend on p. We use payoff symmetry. $e_i^{*} = \frac{p}{\theta + n\delta}; e_i^{\omega} = \frac{p}{\theta + 2n\delta}$, then $w(e^{*}) = n\left(\frac{p^2}{\theta + n\delta} - \left(\frac{1}{2}\theta + \delta\right)\left(\frac{p^2}{(\theta + n\delta)^2}\right)\right)$ and $w(e^{\omega}) = n\left(\frac{p^2}{\theta + 2n\delta} - \left(\frac{1}{2}\theta + n\delta\right)\left(\frac{p^2}{(\theta + 2n\delta)^2}\right)\right)$, taking the derivate,

$$\frac{\partial RD}{\partial p} = -\frac{1}{w(e^{\omega})} \cdot \frac{\partial w(e^{*})}{\partial p} + \frac{w(e^{*})}{w(e^{\omega})^2} \cdot \frac{\partial w(e^{\omega})}{\partial p},$$

computing, $\frac{\partial w(e^{*})}{\partial p} = n\left[\frac{2p}{\theta + n\delta} - \left(\frac{1}{2}\theta + \delta\right)\frac{2p}{(\theta + n\delta)^2}\right] = np\frac{\theta}{(\theta + n\delta)^2}$

Similarly, $\frac{\partial w(e^{\omega})}{\partial p} = np\frac{\theta}{(\theta + 2n\delta)^2}$ and therefore

$$\frac{\partial w(e^{\omega})}{\partial p}=-\left(\frac{1}{w(e^{\omega})}\cdot\frac{np\theta}{(\theta+n\delta)^2}\right)+\left(\frac{w(e^{\omega})}{w(e^{\omega})^2}\cdot\frac{np\theta}{(\theta+2n\delta)^2}\right).$$

Apparently, the sign of the last expression cannot be computed analytically without ambiguity. However, reordering the terms, we have that

$$\frac{1}{w(e^{\omega})}\cdot\frac{np\theta}{(\theta+n\delta)^2}>\frac{w(e^{\omega})}{w(e^{\omega})^2}\cdot\frac{np\theta}{(\theta+2n\delta)^2}, \text{ then } w(e^{\omega})>w(e^{*})\left(\frac{\theta+n\delta}{\theta+2n\delta}\right)^2.$$

Recall that $w(e^{\omega})>w(e^{*})$ and that $\left(\frac{\theta+n\delta}{\theta+2n\delta}\right)<1$ such that the last expression holds; which leads to $\frac{\partial RD}{\partial p}<0$. In words, higher prices raise the benefits of extraction under both cooperative and conflict, but the relative inefficiency under conflict. Social losses are then less severe when rents over resources are high.

Case 2. Restricted case

Extractions are fixed by appropriation, then they do not depend on p, such that $e_i^*(p)=A_i$. If $e_i^{\omega}(p)$ is also limited, then $\frac{\partial w^*}{\partial p}=\sum_{i=1}^{n}A_i=S$ and $\frac{\partial w^{\omega}}{\partial p}=\sum_{i=1}^{n}A_i=S$. Introducing this expression in the general equation, it gives $\frac{\partial RD}{\partial p}=\left(-\frac{1}{w^{\omega}}\cdot S\right)+\left(\frac{w^*}{\left(w^{\omega}\right)^2}\cdot S\right)=S\left(\frac{w^*}{(w^{\omega})^2}-\frac{1}{w^{\omega}}\right)$, hence

$\frac{\partial RD}{\partial p}=S\cdot\frac{w^*-w^{\omega}}{\left(w^{\omega}\right)^2}$. Since, $w^{\omega}>w^*$, then $\frac{\partial RD}{\partial p}<0$. However, if both w^{ω} and w^* are linear in p with the same slope in S, because the use of identical quantities, then the ratio $\frac{w^*}{w^{\omega}}$ is independent of p and therefore, $\frac{\partial RD}{\partial p}=0$. Which these situations hold depends on whether the social planner´s allocation also stays the same quotes of A_i or reoptimizes subject to S. Normally, we assume reoptimize from and therefore $\frac{\partial RD}{\partial p} < 0$. Generally, price matters less once quotes are binding.

Extensions

Instead of considering the two extreme cases (unrestricted Vs. restricted), our modelling approach also allows for mixed or partially constrained situations. In any of these cases, instead of summing over n, now take $n = |U| + |B|$, where U represents the unrestricted agents and B the binding, and eliminating the sum over U since $\frac{\partial RD}{\partial S} = \frac{\partial RD}{\partial a} = 0$ for U agents. For prices, this is piecewise. Unconstrained agents (U) increase in p, while Constrained agents (B) stay at A_i. Therefore

$$\frac{\partial w^*}{\partial p} = \sum_{i \in U} \frac{\partial}{\partial p}\left(pe_i^*(p) - \cos ts\right) + \sum_{i \in B} A_i$$

The expression mixes terms that depend on p and constraints. Consequently, $\frac{\partial RD}{\partial p}$ can change sign as p crosses binding thresholds. This produces non-monotone (U-shaped) behavior.

Appendix B (Intensity of the conflict).

Proof proposition 2.5 and 2.6:

In the unrestricted case, let $T = \sum_{i=1}^{n} a_i = na = \sqrt{\frac{pS(n-1)}{\varphi}}$, then, $\frac{\partial T}{\partial S} = \frac{1}{2}\sqrt{\frac{p(n-1)}{S\varphi}} = \frac{1}{2}\frac{T}{S}$. On the other hand, in the restricted case the role of appropriation changes since $\Delta_i = e_i \leq e_i^*$ for all i. Efforts no longer increases the resource, agents cannot extract beyond e_i^*, they only help to secure up to e_i^* units, i.e., “be among the winners” that creates a multi-prize contest for at most M caps of size e_i^*. The binding-cap model is a continuous number of prices such that $\frac{S}{e^*} \geq n$, where $M = n$, that is $M(S,p,n)=\min\left\{n,\dfrac{S}{e_i^*(p)}\right\}$, where M denotes how many agents could be fully satisfy if they win. If S is large, then M stays fixed. Otherwise, M grows with S until it reaches n. Finding the F.O.C, $\pi_i(a)=p\cdot e^* M\dfrac{(H_a)_i}{1^T H_a}-\dfrac{\varphi}{2}a_i^2$. Under symmetry and regular networks, we have that $A=\Delta(H,n)\equiv\dfrac{nH_{ii}-h}{h}>0$, where H_{ii} is the identical diagonal and h the row sum: An special case with no spillovers leads to $\Delta=n-1$. Then, the symmetric interior equilibrium is

$$a^*=\sqrt{\frac{p\cdot e^* MA}{\varphi}}\text{ ; } T=n\cdot a^*=\sqrt{\frac{p\cdot e^*\Delta M}{\varphi}},$$

In this case, we have that $\dfrac{\partial T}{\partial S}=0$. Regarding prices, for simplicity, we employ $e^*=\dfrac{p}{\theta+n\delta}\equiv\dfrac{p}{\varphi}$, where $\varphi=\theta+n\delta$. This leads to $T=\sqrt{\dfrac{p\cdot p\cdot n\cdot\Delta}{\varphi\cdot\varphi}}=p\sqrt{\dfrac{n\Delta}{\varphi\varphi}}$, then $\dfrac{\partial T}{\partial p}=\sqrt{\dfrac{n\Delta}{\varphi\varphi}}=\dfrac{T}{p}$. Therefore, elasticity is $\dfrac{p}{T}\dfrac{\partial T}{\partial p}=1$.

Once all caps are filled, increasing prices increases intensity of the conflict linearity in p (elasticity 1), because both the per-unit value and the cap e^* scale with p. At $p=S\dfrac{p}{\psi}$ the economy switches regimes. That is, T stays continuous but its slope jumps from $\dfrac{1}{2}\dfrac{T}{p}$ (unrestricted) to $\dfrac{T}{p}$ (restricted).

Spillovers effects on T

Unrestricted

In the unrestricted case, in symmetric regular networks, H_a is proportional to $a \cdot 1$, where 1 is a vector of ones. Covertly, if every column sum of H quals the same constant c_i, then $N_i = \left(H_a\right)_i = ca$ and $D = n \cdot c \cdot a$. The c cancels out in the ratio $\frac{N_i}{D}$ and the symmetric solution to the same algebra as the $H = I$ case. So, the close-form solution for T still holds. In words, when symmetry appears, spillovers just scale numerator and denominator equally and drop out of the symmetric expression. However, in asymmetric networks, if spillovers generate heterogeneity in equilibrium (some agents stronger), then the symmetric close-form solution fails, and one must solve the general F.O.C systems in 3.1. On the other hand, in the restricted case, $\Delta = \frac{nH_{ii} - h}{h}$, where h denotes the spillover, $h = \sum_{j=1}^{n} H_{ij}$ and H_{ii} own effect. The intensity of the conflict reads $T = \sqrt{\frac{p \cdot e^* M}{\varphi} \cdot \frac{nH_{ii} - h}{h}}$. Therefore, $\frac{\partial T}{\partial h} = -\frac{T}{2} \cdot \frac{nH_{ii}}{h(nH_{ii} - h)}$ and $\frac{\partial T}{\partial h} > 0$ if $h > 0$.

Restricted

Let $\Delta = \frac{nH_{ii} - h}{h}$, where h denotes the spillovers, $h = \sum_{j=1}^{n} H_{ij}$ and H_{ii} own effect. The intensity of the conflict reads $T = \sqrt{\frac{pe^* M}{\varphi} \cdot \frac{nH_{ii} - h}{h}}$. Then, $\frac{\partial T}{\partial h} = -\frac{T}{2} \cdot \frac{nH_{ii}}{h\left(nH_{ii} - h\right)}$ and $\frac{\partial T}{\partial h} > 0$ if $h > 0$.

That is, when positive spillovers dominate over negative ones. Notice that $nH_{ii} - h > 0$ needs to hold for a positive equilibrium. This means that own efforts enforce primitive dominance more than it enforces enmities, or more than enmities´ efforts enforces agents´ dominance. If $nH_{ii} - h < 0$, the incentive to invest effort disappear because enmities ´spillovers offset own effects.

Size effects on T

Let $T=\sqrt{\dfrac{pS(n-1)}{\varphi}}$, then $\dfrac{\partial T}{\partial n}=\dfrac{1}{2}\sqrt{\dfrac{pS}{\varphi}}\cdot\dfrac{1}{\sqrt{n-1}}=\dfrac{1}{2}\dfrac{T}{(n-1)}$, therefore $\dfrac{\partial T}{\partial n}>0$.

With linear shares, marginal gain from extra effort falls because the share is a fraction of the total; quadratic cost leads to interior equilibrium where marginal benefit equals marginal cost, producing sublinear effects.

Chapter 3

Cocaine Trafficking via Container Ships, Dynamics between Corruption, and Inspections: An Agent-Based Model

The following chapter is based on the paper:	
Title:	Cocaine Trafficking via Container Ships, Dynamics between Corruption, and Inspections: An Agent-Based Model
Authors:	Maykol Rodriguez Prieto (Contribution 100%)
Status:	Submitted to *Trends in Organized Crime*

Different states of this paper have been presented at:

- 19th Annual Social Simulation Conference. Cracow, Poland 2024.
- MARESC 2025: European Workshop on Maritime Systems Resilience and Security. Rostock, Germany 2025.
- 25th Annual Conference of the European Society of Criminology.
- 3rd Conference of the Network for Drug Studies in Latin America (REDESDAL). Bogotá, Colombia.

Cocaine Trafficking via Container Ships, Dynamics between Corruption, and Inspections: An Agent-Based Model

Maykol Rodriguez-Prieto

Faculty of Economics, Justus Liebig Universität Gießen, Germany

Abstract

Drug trafficking represents one of the world's largest illicit markets, and the cocaine trade has experienced significant growth in recent decades. Notably, cocaine trafficking to Europe has increased considerably, with traffickers predominantly exploiting the global container shipping industry to transport their cargo. Consequently, ports are key points in this dynamic. This study utilizes an agent-based model to simulate the trafficking of cocaine from South America to Europe using container ships. The model assesses the impact of container ship size, inspection capacity, and corruption levels at both ports of departure and arrival on the annual volume of cocaine trafficked (measured in tons). The resulting data are analyzed using ANOVA, which identifies the most significant model parameters, followed by Tukey's test to examine variations across parameter levels. The findings reveal nonlinear interactions between inspection capacity and corruption, and the quantity of cocaine trafficked. Similarly, evidence shows that corruption at both ports is the most significant factor undermining law enforcement initiatives and facilitating cocaine trafficking.

Keywords: Maritime trafficking, Cocaine, Ports, Law-enforcement, Corruption, Agent-Based Modelling.

3.1 Introduction

Drug trafficking is one of the main activities of transnational organized crime, emerging as one of the largest industries worldwide. Daily, kilos of various types of drugs are transported across international borders by air, land, and sea (Kelly et al., 2005; Jenner, 2013). Although drug trafficking is part of the broader drug trade supply chain, comprising cultivation, production, trafficking, distribution, and consumption, Jenner (2013) notes that trafficking is the only stage that is transnational in nature, involving the movement of drugs from the country of production to the country of consumption. A substantial increase in drug trafficking during the 1960s led to a corresponding rise in drug consumption in both the United States and Europe. This growth was further fueled by globalization, advancements in communication, transportation, and information technologies, as well as the reduction of trade barriers. These factors allowed the drug industry to expand rapidly, eventually becoming one of the largest and most influential industries in the world (Jenner, 2013). This increase has become a global issue with devastating effects. In addition to rising consumption and public health concerns, it has contributed to elevated crime and violence rates, including homicides and displacement. Moreover, drug trafficking poses significant environmental threats, as traffickers continue to expand operations, often contributing to illegal deforestation.

The cocaine market has experienced a major boom in recent years, driven by factors like increased coca cultivation, higher global demand, new markets, and strong economic incentives. While the U.S. has traditionally been the center of the cocaine trade, recent shifts have led traffickers to focus more on Europe. One key reason is that Colombian traffickers, who once controlled the routes to the U.S., have been replaced by Mexican cartels. These cartels now dominate the U.S. market, forcing Colombian groups to shift their operations to Europe (United Nations Office on Drugs and Crime [UNODC], 2011).

According to the United Nations Office on Drugs and Crime (UNODC, 2024), Europe has become an increasingly attractive market for drug traffickers. Between 2011 and 2023, cocaine consumption in Western, Central, and South-Eastern Europe surged by 80%. In 2021 alone, authorities recorded 407 drug-related incidents in European waters, resulting in the seizure of

576,411 kilograms of narcotics. Cocaine was the second most seized drug, accounting for 28% of the total, equivalent to 163,077 kilograms.

A key reason for this shift is the higher market prices for cocaine in Europe. For example, while a kilogram of cocaine sells for around USD 28,000 in the United States, it can go for USD 40,000 in France and Spain, and as much as USD 240,000 in Estonia. Additionally, Europe has less severe legal penalties for possession and consumption. For instance, the European Union spends only USD 3–4 billion per year on supply reduction efforts, compared to the USD 17.4 billion spent by the United States. As a result, European border security forces can only intercept 10–12% of the total cocaine entering the continent (Center for Strategic and International Studies [CSIS], 2023).

In the early 1980s, Colombian drug cartels used light aircraft to smuggle cocaine into the United States. For Europe, they initially relied on people traveling on commercial flights for small amounts and fishing boats for larger quantities. These boats were intercepted at sea by speedboats, which then transported the drugs to the coast, as described in an investigative report by InSight Crime in 2021.

Today, the situation has changed dramatically. Maritime trafficking accounted for 89% of cocaine seizures in 2021 (United Nations Office on Drugs and Crime [UNODC], 2023). Over the past decade, the primary method for smuggling large quantities of cocaine from South America to Europe has been through containers, exploiting the vast and legitimate global container trade. Data from the National Center for Research and Analysis against Maritime Drug Trafficking (Centro Nacional de Investigación y Análisis contra Narcotráfico Marítimo, Armada de Colombia, 2021) indicates that in 2021, container-based smuggling was the most common method in Europe, with 151 incidents—representing 26% of total cases—and 151,139 kilograms of narcotics seized. This underscores the critical role of seaports as hubs for both legal and illegal activities. Ports are frequently cited in connection with organized crime, as noted by Sergi (2020) and Eski (2019). They serve as key entry and exit points for drugs, other illicit goods, and smuggled individuals, and are particularly challenging to monitor and secure. According to Europol, over 90 million containers arrive at European ports each year, offering ideal concealment for illicit operations.

As researchers such as Nordstrom (2007) and Sergi (2020) have noted, the rise of container shipping has transformed both legal and illegal commerce. Today, maritime transport accounts for approximately 80% of global trade volume (United Nations Conference on Trade and Development [UNCTAD], 2024). In Europe, this trend has accelerated since the 1950s, following the standardization of the twenty-foot equivalent unit (TEU) shipping container[2]. This innovation made maritime trade faster, more cost-effective, and more secure, thereby driving globalization and supporting the development of major logistics hubs such as the ports of Rotterdam, Hamburg, and Antwerp (Levinson, 2016). In 2023, maritime transport represented 47.7 % of the total value of goods exchanged between the European Union and non-EU countries, according to data from Eurostat in 2024, underscoring Europe's strong reliance on seaborne trade. Essential commodities—including oil, gas, raw materials, food, and manufactured goods—are predominantly transported to Europe by sea, according to information released by the European Commission in 2024. Data shared by the maritime research platform PortEconomics in 2024 indicate that the top 15 EU ports collectively handled approximately 76.77 million TEUs, reflecting a 5.9 % year-on-year increase.

Traffickers exploit the vast scale of legal maritime trade to smuggle illicit goods into Europe, often concealing drugs within legitimate cargo. With over 80% of global trade transported by sea, the volume of containers arriving at European ports is immense, yet only 2% to 10% of these are physically inspected (Zaidi, 2007). This limited inspection capacity creates a substantial loophole for criminal networks. Further exacerbating the issue is widespread corruption[3]: traffickers often rely on bribery and collusion to access ports, retrieve illicit shipments, and operate with impunity. Organized crime has deeply infiltrated key ports in both South America and Europe, involving not only port workers but also high-ranking officials such as Coast Guard officers who may accept bribes to overlook smuggling operations (Sergi, 2020; Zaitch, 2002; Antonopoulos, 2008; Eski & Bujit, 2016; Kostakos & Antonopoulos, 2010). Ports, while serving as gateways for international trade and essential nodes within the global supply chain, also represent critical points of vulnerability (Pettit & Beresford, 2009; Liu et al., 2018). They are

[2]Standardization of the 20-foot equivalent unit (TEU) container ensures uniform size and design for efficient global transport of goods.
[3] While corruption is widespread and takes many forms, this analysis centers on traffickers' use of bribery and threats to move shipments.

complex systems where diverse public and private actors interact continuously to ensure the efficient and secure functioning of maritime commerce (Macário, 2014).

An Agent-Based Model (ABM) (Rykiel, 1996; Epstein, 1999) is presented in this research to contribute to the understanding and gain a clearer picture of containerized cocaine trafficking from South America to Europe, focusing on the importance of both departure and arrival ports by analyzing two key factors: inspection capacity and corruption. Specifically, it explores how these factors influence the flow of cocaine through containerized shipments from departure ports located in or near major cocaine-producing regions to arrival ports, primarily in Europe, where the substance is distributed for consumption. The model also seeks to test how an increase in the size of container ships, a significant trend in recent decades benefits legal maritime trade while also enabling traffickers to exploit this growth.

Agent-Based Modeling approaches in the study of crime have great potential, as they enhance understanding, generate new insights, and facilitate the formalization of theories. Agents following relatively simple behavioral rules can produce complex and unexpected outcomes due to their dynamic interactions (Gilbert & Troitzsch, 2005; Groff et al., 2019). Several models focus on specific types of crime (e.g., burglary, robbery, drug trafficking), aiming to simulate criminal behaviors and movements within their environment while testing strategies for crime reduction (Malleson et al., n.d.; Weisburd et al., 2017). Drug trafficking is one of the main activities of organized crime, which operates through a network structure. Some studies have used ABMs to examine this phenomenon, focusing on the resilience, adaptability, and evolution of criminal networks (Magliocca et al., 2022; Manzi & Calderoni, 2024).

The developed model focuses on a particular stage in the supply chain employed by organized crime: the transportation of cocaine from production and processing sites to consumption markets. This transfer is mainly carried out via maritime routes. In the study of maritime security and blue crimes, some investigations use ABM, particularly in the analysis of piracy (Vaněk et al., 2013; Sibley, 2016). These studies have provided valuable insights; however, while both piracy and drug trafficking are considered blue crimes, they belong to different categories, piracy is classified as a crime against mobility, whereas drug trafficking is part of criminal flows (Bueger & Edmunds, 2020).

3.2 Model description

The ABM is designed following the ODD (Overview, Design concepts, Details) protocol Grimm et al. (2010) and is implemented through *NetLogo 6.3.0* Wilensky (1999).

3.2.1 Purpose

The purpose of this ABM is to predict the amount of cocaine trafficked in one year through container ships departing from ports in producer countries and arriving at ports in consumer countries. The model considers factors such as the size of container ships and specific port characteristics, including law enforcement capacity, meaning the ability of ports to inspect containers and levels of corruption, which influence whether cocaine-laden ships can depart or arrive undetected. At each time step, traffickers adapt their loading strategies by monitoring recent seizures: they avoid using ports where inspections have resulted in higher confiscation rates.

3.2.2 Entities, state variables and scales

The model considers three key entities: drug traffickers, container ships, and ports of departure and arrival. Drug traffickers identify potential container ships and load cargo at the ports of departure. The container ships, which vary in size, follow predetermined routes that are known to the traffickers as they travel from the departure port to the arrival port. The ports, both departure and arrival are responsible for inspecting the vessels. The main variables per agent type are given in Table 3.1. Corruption allows the departure and arrival of loaded container ships that have that have been identified in inspection stage. Each time step traffickers adapt their loading behavior by identifying ports where there have been the most seizures, they subsequently avoid loading container ships that depart from or arrive at those ports.

Table 3.1. Main variables per agent type.

Agent type	Variable	Description	Values	Temporal
Trafficker	amount_cocaine_t	Amount of cocaine loaded onto container ships	0.1-1.0 tons	Each iteration
	power_load	Capacity to load container ships	[0.1,1]	Each iteration
Container ship	initiation	Departure port where container ship sets sail	Agent	Each iteration
	destination	Arrival port where container ship sets sail	Agent	Each iteration
	boat_size	Size of container ship	[5000 (S), 10000 (M), 15000 (B)]	Each iteration
	weighting_infected	Parameter of being infected	[0, 1]	Each iteration
	infected?	Determine if container ship is loaded by a trafficker	True/False	Each iteration
	amount_cocaine_b	Amount of cocaine that is loaded	[0.1, 50] tons	Each iteration
	potential-boat?	Container ship identified by traffickers available to be load.	True/False	Each iteration
Departure port	law-enforcement	Inspection capacity	[0, 1]	Each iteration
	departure-corruption	Corruption measure	[0, 1]	Each iteration
	departure_port_seizure	Amount of container ship seized	Integer	Each iteration
Arrival port	law-enforcement	Inspection capacity	[0, 1]	Each iteration

	arrival-corruption	Corruption measure	[0, 1]	Each iteration
	arrival_port_seizure	Amount of container ship seized	Integer	Each iteration

3.2.3 Basic principles, process overview and scheduling

The ABM is designed to simulate the trafficking and seizure of cocaine transported via container ships from South America to Europe, with ports functioning as fundamental agents within the system. In the model, traffickers load cocaine onto container ships at departure ports, each trader can load only one container ship (a container ship can hold thousands of containers depending on its size measured in TEU) and can load this between 0.1 and 1 ton. These ships are then subjected to inspection at departure ports and depending on the levels of law enforcement and corruption either be intercepted or allowed to proceed. Upon arrival at European ports, the ships are again inspected under similar conditions. The successful trafficking of cocaine depends on whether inspections are ineffective or circumvented through corruption.

The model is based on several key assumptions. While inspired by real maritime container transport, it is not georeferenced; the ports represented are generic and do not correspond to actual locations in South America or Europe. The number of departure and arrival ports is fixed at 10. It is estimated that between 1,500 and 2,000 container ships travel annually from South America to Europe, with an average of 80 to 85 container ships departing every 18 days. Each time step in the model represents an 18-day period, which reflects the average duration of a transatlantic voyage between South America and Europe—a journey that typically ranges from 12 to 25 days, depending on maritime and logistical conditions. The general structure of the model is illustrated in Fig 3.1, and its operation is described as follows:

1. Loading and departure:
    - At each time step (18 days), cocaine traffickers attempt to load container ships with cocaine (measured in tons).
    - Each container ship has predetermined departure and arrival ports, and traffickers have this knowledge.

   - This information influences traffickers' decisions regarding which container ships to use—if either the departure or arrival port has recently been involved in multiple seizures, they may choose to avoid that container ship. Upon departure, the ship may be subject to inspection, depending on the law enforcement capacity of the port.
2. Inspection at Departure Ports:
   - If a container ship is not carrying cocaine, it continues its journey unimpeded.
   - If a container ship transports cocaine, if it is inspected and the inspection capacity is strong, the cocaine must be confiscated.
   - However, if corruption is present, the cocaine may evade seizure, allowing the container ship to proceed with its illicit cargo.
   - A container ship can only depart for Europe with cocaine if either the inspection is ineffective or corruption prevents confiscation.
   - If corruption is minimal or absent, container ship is intercepted, and the cocaine should be confiscated.
3. Journey and Arrival:
   - If a loaded container ship is not intercepted at the departure port, it continues its journey to Europe.
   - Upon arrival, it may again be subject to inspection, depending on the enforcement capacity at the destination port.
   - Weak inspections allow cocaine trafficking to succeed. Strong enforcement should lead to seizure.
   - However, as at departure ports, corruption at arrival ports can enable trafficking despite inspections.
   - When corruption is absent, all detected cocaine shipments are seized.

The total amount of successfully trafficked cocaine due to weak inspections and/or corruption is measured over one year. In the model, this corresponds to 21 steps. Once this period is completed, the simulation stops.

Model verification was carried out to ensure the correct behavior of agents using print statements and systematic parameter manipulation (Sibley, 2016). Extreme cases were also tested

(Rykiel, 1996), including scenarios with zero law enforcement at both departure and arrival ports, as well as scenarios with maximum enforcement. Similarly, cases with zero and maximum corruption levels were examined. Additionally, monitors were implemented to track the number of seizures, and visual indicators were used, such as changing the color of a port after more than five seizure events to reflect heightened risk. In response, traffickers adapted their behavior by choosing not to load container ships departing from or arriving at those ports.

On the other hand, the amount of cocaine that a container ship could carry, as well as the volume traffickers were able to transport, was estimated using qualitative information drawn from reports by organizations such as the (Centro Internacional de Investigación y Análisis contra el Narcotráfico Marítimo [CIMCON], 2020) and the (United Nations Office on Drugs and Crime [UNODC], 2023), as well as from media sources. For instance, one key reference point is the 151 tons of cocaine seized in Europe in 2021 from containers alone. Additionally, estimates of port inspection capacity (law-enforcement) ranging between 2% and 10% were also considered to calibrate the model parameters.

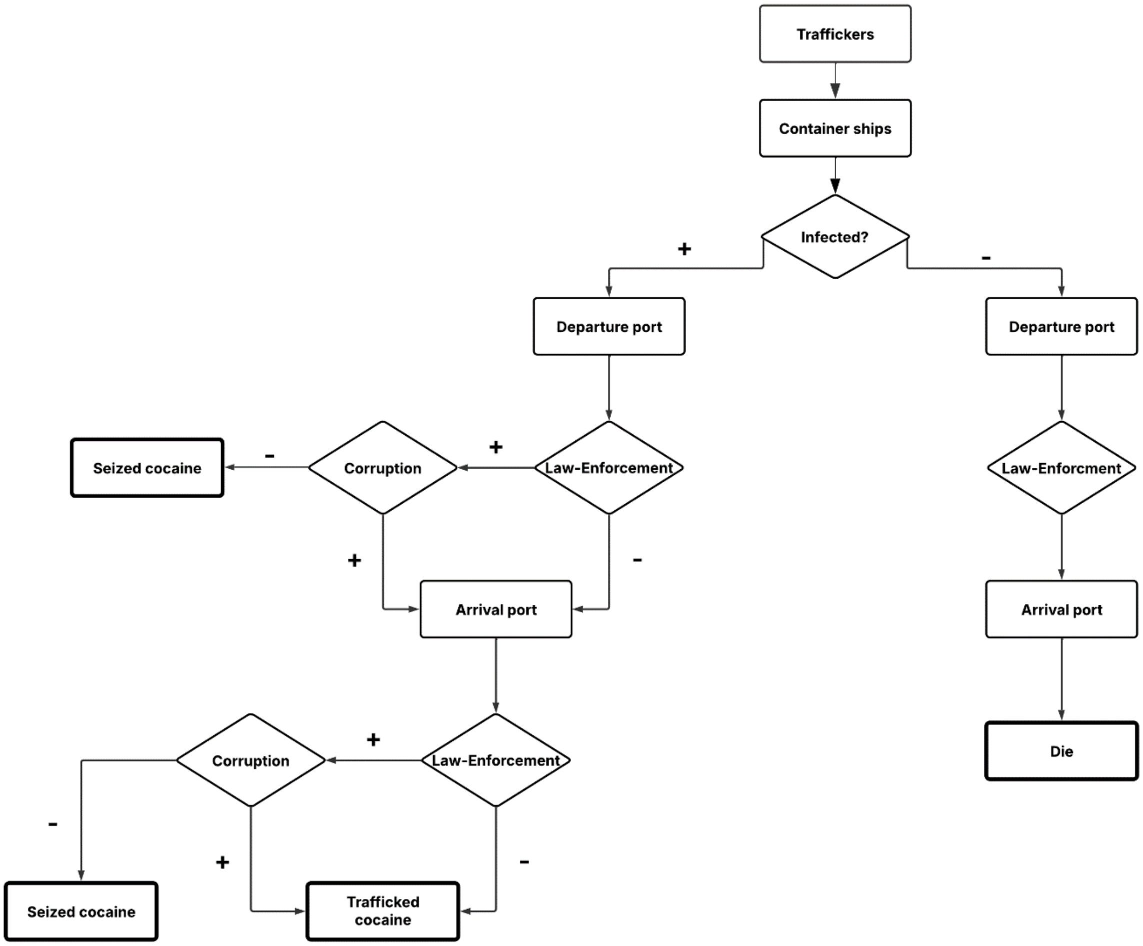

Fig 3.1. Diagram of maritime cocaine trafficking via containers. Traffickers load container ships departing from ports of departure and, depending on the capacity of law enforcement, are inspected. Whether inspection is poor or corrupt, the container ships arrive at ports of arrival, where they are inspected according to the capacity of law enforcement. Whether inspection is poor or corrupt, cocaine is trafficked. If inspection capacity is good at either the ports of departure or arrival, the cocaine is seized

3.2.4 Design concepts

Emergence

The model evaluates how inspection capacity and corruption at ports interact to influence the quantity of cocaine trafficked. This relationship is nonlinear, as small changes in law enforcement or corruption at either departure or arrival ports can lead to disproportionate variations in trafficking outcomes. The emergent property observed is that the combined effects of these parameters generate patterns in drug trafficking that are not directly predictable from individual port conditions alone.

Adaptation

Traffickers adapt their strategies based on previous inspections. If a port has had frequent seizures, traffickers are less likely to load container ships departing from or arriving at that location. This adaptive behavior shifts trafficking routes over time, concentrating activity in ports with lower law-enforcement.

Sensing

Traffickers assess the corruption level and enforcement capacity at each port before deciding whether to load a container ship. If they detect a high probability of seizure, they may opt to avoid that port. Similarly, port authorities inspect ships to determine whether cocaine is present, but the effectiveness of these inspections depends on enforcement capabilities and corruption levels.

Stochasticity

Stochasticity is incorporated into multiple aspects of the model to introduce variability in trafficking dynamics. First, each trafficker is randomly assigned a quantity of cocaine and a loading capacity for container ships. Second, traffickers randomly select container ships for loading, as long as these meet predefined criteria. Additionally, the size of the container ships, within small, medium and large, is randomly determined. Finally, the inspection capacity and corruption levels at both departure and arrival ports vary randomly, affecting the likelihood of successful trafficking or seizure. These stochastic elements ensure that each simulation run produces different outcomes, reflecting the inherent uncertainty in real-world drug trafficking operations.

Observation

The collection and analysis of simulated data generated by running multiple instances of the model with different parameter combinations. The primary objective is to track the total amount of cocaine trafficked and seized, as well as the effects of inspection capacity and corruption levels. Data is gathered throughout the simulation, and after completion, statistical analysis and visualizations are applied to identify patterns, trends, and the influence of parameter interactions.

Initialization

The model includes 8 parameters that need to be set at initialization. These parameters are shown in Table 3.2. These parameters do not change from the start of the simulation process until it ends. The parameter *Number_traffickers* is set to 50. Similarly, *Min_size_boat* and *Max_size_boat* are set to 80 and 85, respectively, in order to ensure that the average number of container ships generated by the simulation is approximately 1,750 by the end of the run. This value aligns with real-world estimates of the annual number of container ships traveling from South America to Europe.

Table 3.2. Parameters of the model

Parameters	**Description**	**Value**
Number_traffickers	The number of drug traffickers.	[0,100]
Min_number_boats	The minimum number of container ships.	[0,120]
Max_number_boats	The maximum number of container ships.	[0,120]
Size_boats	The minimum size of container ships.	{5000,10000,15000}
Law_enforcement_departure	The inspection capacity at departure ports.	[0, 1.0]
Law_enforcement_arrival	The inspection capacity at arrival ports.	[0, 1.0]
Corruption_value_departure	The level of corruption at the departure ports	[0, 1.0]
Corruption_value_arrival	The level of corruption at the arrival ports	[0, 1.0]

Input data

The model represents maritime cocaine trafficking that is not calibrated to a particular real-life port, therefore no specific input data is used.

Simulation experiments

In this experiment, five parameters were varied according to a 3×5×5×7×7 factorial design, as shown in Table 3.3. Each parameter combination was replicated 20 times, resulting in a total of 73,500 simulation runs. The response variable is the amount of cocaine trafficked, measured in tons. The objective of the experiment is to assess how individual parameters and their interactions influence the flow of cocaine, identifying the conditions that lead to both higher and lower levels of trafficking.

Table 3.3. Tested parameters

Parameter	Setting values
Size_boats	5000, 10000, 15000
Law_enforcement_departure	0.1 0.3, 0.5, 0.7, 1.0
Law_enforcement_arrival	0.1 0.3, 0.5, 0.7, 1.0
Corruption_value_departure	0, 0.1, 0.2, 0.5, 0.7, 0.9, 1.0
Corruption_value_arrival	0, 0.1, 0.2, 0.5, 0.7, 0.9, 1.0

3.4 Results

3.4.1 Sensitivity Analysis

Sensitivity analysis is conducted using the Morris method (Morris, 1991) to globally identify the parameters with the greatest impact on the model's output, specifically the quantity of cocaine trafficked. This analysis considers two metrics, μ^* and σ, which measure the magnitude of a variable's effect and the variability of its impact, respectively. A high μ^* value indicates that the variable has a significant influence on the model output, while a high σ value suggests non-linearity or strong interactions with other variables. The results of the method present the sensitivity analysis for each parameter, highlighting *size boats* ($\mu^* = 174.36$) *Corruption value departure* ($\mu^* = 168.36$) and *Corruption value arrival* ($\mu^* = 168.50$) as the most influential parameters, based on their high μ^* values. These parameters exert the strongest overall influence on the model's outcome. Additionally, *Corruption value departure* and *Law enforcement arrival* exhibit the highest σ values, suggesting that their effects on the outcome are highly context-dependent and sensitive to interactions with other variables.

3.4.2 Analysis of variance ANOVA

To analyze the significance of the data produced in the simulations, an Analysis of Variance (ANOVA) was conducted to test the effect of each parameter on the outcome variable (trafficked cocaine), based on prior approaches (Sthle & Wold, 1989; Armstrong, Eperjesi, & Gilmartin, 2002; Kleijnen, 2005). In the initial analysis, only interactions between inspection capacity (law enforcement) and corruption levels, up to the fourth order, were tested. However, only second-order interactions were found to be significant. Additionally, higher-order interactions are difficult to interpret (Sibley, 2016; Yandell, 1997).

The results indicate the size of container ships is highly significant factor in determining the amount of cocaine trafficked. The F-statistic for the size of container ships (*Size boats*) is 1248.87 ($p < 0.001$). Regarding the port inspection parameters, *Law enforcement departure* ($F = 2388.45$, $p < 0.001$) and *Law enforcement arrival* ($F = 2100.18$, $p < 0.001$) have a significant impact on cocaine trafficking. For the corruption parameters, we have *Corruption value departure* ($F = 17893.08$, $p < 0.001$) and *Corruption value arrival* ($F = 15742.84$, $p < 0.001$).

Among significant second-order interactions are:

- *Law enforcement departure* and *Corruption value departure* ($F = 971.42$, $p < 0,001$):
  Fig 3.2. Highlights that when law enforcement at ports of departure is low, resulting in limited inspection capacity, cocaine trafficking remains high-ranging between 350 and 400 tons per year-regardless of the presence of corruption. However, as law enforcement efforts increase, corruption becomes a significant factor, undermining inspection capacity to some extent and allowing similar quantities of cocaine to continue being trafficked. Only in the case where corruption is zero is it evident that high inspection capacity reduces cocaine trafficking.

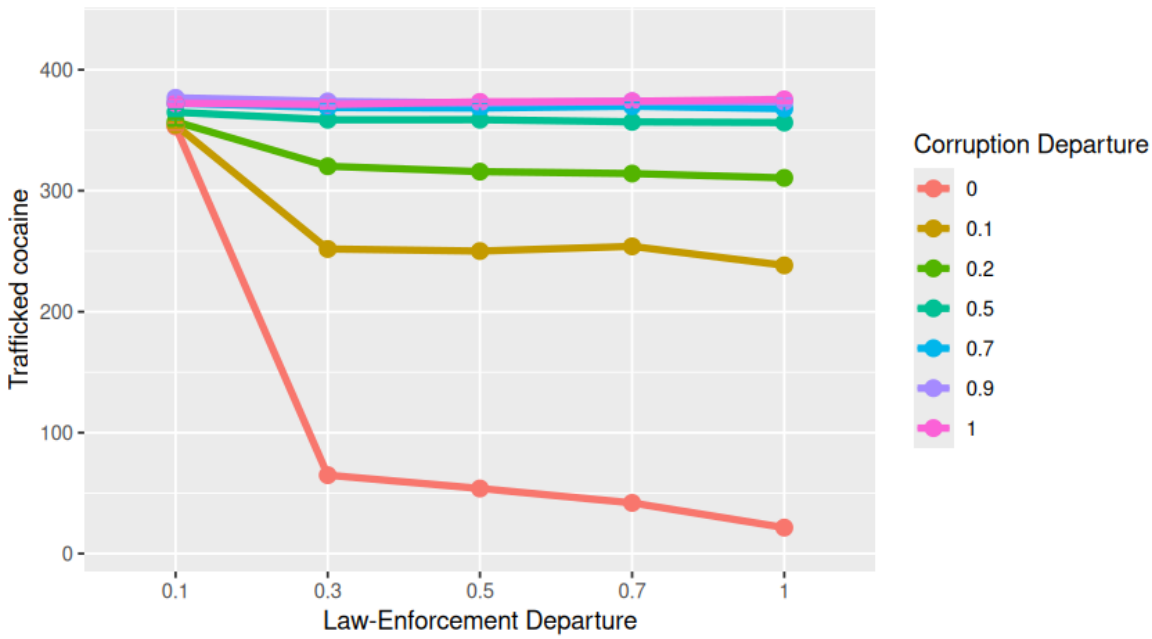

Fig 3.2. Trafficked cocaine by departure law-enforcement and departure corruption

- *Law enforcement arrival* and *Corruption value arrival* ($F = 788.03$, $p < 0.001$):
  As in the previous case, high levels of corruption at ports of arrival enable cocaine trafficking to remain high within a single year, even as law enforcement increases. Fig 3.3. Details the interaction between inspection capacity and corruption at ports of arrival. As observed at ports of departure, only the absence of corruption allows law enforcement to be effective, leading to a reduction in the amount of cocaine trafficked.

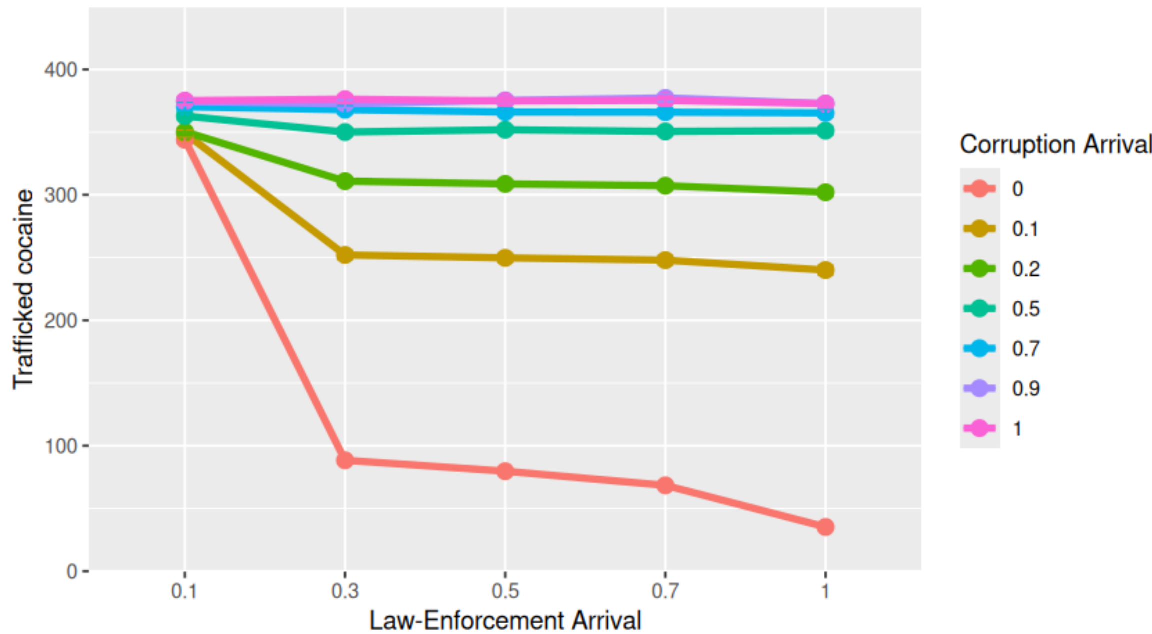

Fig 3.3. Trafficked cocaine by arrival law-enforcement and arrival corruption

- *Corruption value departure* and *Corruption value arrival* (F = 368.37, $p < 0.001$):

  Fig 3.4. Reveals that even minimal corruption in ports, whether at departure or arrival significantly increases the volume of cocaine trafficking. For instance, when corruption is present in 10% of departure ports (with no corruption at arrival ports), 95 tons of cocaine are trafficked. However, if corruption in departure ports rises to 20%, the trafficked amount surges to 220 tons, a staggering 131.5% increase. This demonstrates how small increments in corruption can disproportionately amplify drug flows.

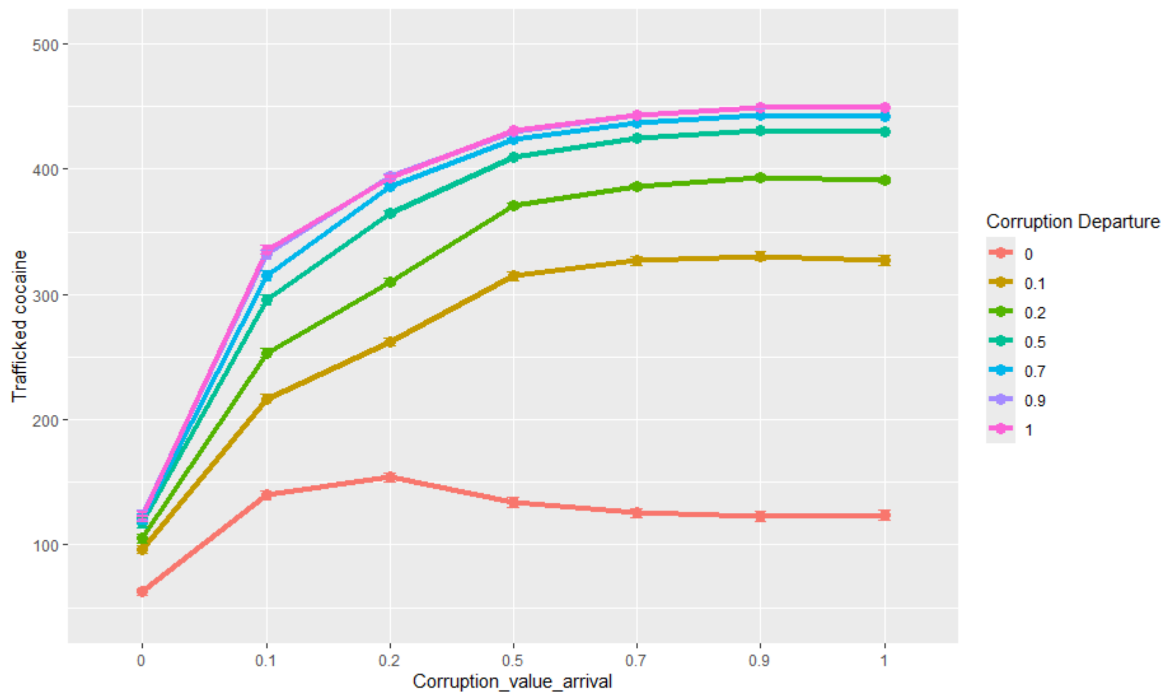

Fig 3.4. Trafficked cocaine by departure corruption and arrival corruption.

3.4.3 Tukey test

The Tukey test, also known as Tukey's Honest Significant Difference (HSD) test, is a post-hoc analysis based on the studentized range statistic (Yandell, 1997; Ravichandran & Padmanaban, 2023). It is conducted after identifying significant variables in the ANOVA and aims to compare all possible pairs of levels of the explanatory variables to determine statistically significant differences. The following results correspond to the data generated by ABM.

- *Container ships size (Size boats):* The results indicate that increasing container ship size from 5,000 to 10,000 TEU leads to an increase of 25.52 tons of cocaine trafficked. A further increase from 10,000 to 15,000 TEU results in an additional 6.35 tons. Both differences are statistically significant.
- *Law enforcement:* Regarding law enforcement at both ports of departure and arrival, an increase in inspection capacity from 0.1 to 0.3 is associated with a reduction in cocaine trafficking of 63.06 tons at ports of departure and 58.20 tons at ports of arrival. However, increases from 0.3 to 0.5 and from 0.5 to 0.7 do not yield statistically significant changes. In contrast, a further increase from 0.7 to 1.0 in law enforcement capacity results in a decrease of 5.87 tons at ports of departure and 7.63 tons at ports of arrival.

- *Corruption:* Regarding corruption at both ports of departure and arrival, our analysis shows that increases in corruption levels are associated with higher volumes. Specifically, an increase in corruption from 0 to 0.1 is linked to an additional 162.67 tons at ports of departure and 144.65 tons of arrival. Similarly, an increase from 0.1 to 0.5 corresponds to an increase of 89.39 and 85.47 tons, respectively; from 0.5 to 0.7, the increase is 10.33 and 13.78 tons; and from 0.7 to 0.9, 4.68 and 7.36 tons. All these differences are statistically significant. However, the change from 0.9 to 1 does not result in a significant difference.

3.5 Discussion

In this paper I develop and analyze an ABM to describe the maritime trafficking of cocaine through containers from ports of producing countries (South America) to ports of arrival (Europe). This study aims to understand and analyze the amount of cocaine that can be trafficked in relation to the inspection capacity and levels of corruption present at ports of departure and arrival. Specifically, it seeks to answer the research question: How do inspection capacity and corruption at maritime ports influence the volume of cocaine trafficked? By exploring this question, the study contributes to a deeper understanding of the complex system of maritime cocaine trafficking and highlights the critical role of ports. Over time, this process has evolved, becoming more sophisticated and increasingly reliant on explicit violence. This is evident in cartel warfare in both producing and destination countries (e.g., the Netherlands, Belgium), where acts of territorial control have been documented. Additionally, hidden forms of violence are also present, such as the infiltration of criminal gangs into ports.

Furthermore, this research seeks to bridge the information gap in the study of cocaine trafficking dynamics. Due to its illegal nature, reliable data and detailed insights into its operations are scarce, making this study a valuable contribution to a deeper understanding of the phenomenon. It is important to emphasize that multiple factors beyond maritime and port control have contributed to the growth and evolution of maritime cocaine trafficking.

First, coca leaf production in Colombia, Peru, and Bolivia has steadily increased over the past decade. Simultaneously, Mexican cartels have consolidated control over trafficking routes to the United States, displacing other networks such as those based in Colombia, Italy, and the

Balkans toward the European market. This geographic reorganization, combined with persistent socioeconomic inequalities in Latin America, has entrenched drug trafficking as a viable livelihood in regions with limited access to formal employment opportunities.

Second, rising global demand has further intensified trafficking. According to (UNODC, 2023), an estimated 22 million people used cocaine in 2021, representing a 13.4% increase compared to 2018. At the same time, trafficking networks have become more fragmented and specialized. While the supply chain was once dominated by a few powerful actors, it now consists of smaller, more agile organizations, each managing a specific segment of the trafficking process. This shift has led to increasingly sophisticated and diversified operations, with growing criminal presence at both departure and arrival ports, including many that had not previously shown significant trafficking activity.

Third, recent investigations have highlighted the growing use of non-traditional South American ports, such as those in Chile, Argentina, and Uruguay (Sampó & Troncoso, 2023). This diversification of routes complicates enforcement efforts and underscores the need for targeted interventions based on identifiable and manageable risk factors. Despite this, the model focuses specifically on variables that are more controllable or that reflect systemic vulnerabilities within legal trade routes, such as container ship size, port inspection capacity, and levels of corruption.

The first result concerns the size of container ships. When law enforcement effectiveness is set at 0.1 and corruption at 0.2, the model shows that cocaine trafficking increases by 2.13% when container ships have a capacity of 10,000 TEUs, and by 2.43% when capacity rises to 15,000 TEUs. This result is significant. Over recent decades, container vessels have grown substantially in both size and technological complexity. In the 1980s, typical ship capacities were around 4,600 TEUs, while by the early 2000s, vessels such as the Anna Maersk could carry up to 9,000 TEUs. Today, some ships exceed 20,000 TEUs. In the Latin American context, however, most container ships fall within the 5,000 to 15,000 TEU range.

This trend toward larger vessels presents multiple challenges. First, increased capacity means a higher number of containers to manage and potentially inspect, placing significant pressure on port authorities, who must also avoid operational delays. This widens the gap between inspection demand and actual capacity, which traffickers can exploit. Second, the physical structure of larger ships can limit access to certain container areas particularly upper layers complicating effective inspection procedures and creating further enforcement blind spots.

The second key variable in the model is port inspection capacity. While this is quantified in the simulation, it encompasses a complex set of processes involving cooperation among multiple actors both official and unofficial operating within the port. Inspection capacity can be broadly defined as the combination of operational procedures, technological infrastructure, and human resources used to examine incoming cargo, ensure regulatory compliance, and prevent illicit activities such as smuggling and drug trafficking. Given the high volume of daily container arrivals, inspection rates remain relatively low, creating an opportunity structure conducive to cocaine trafficking.

According to model results, increases in inspection capacity impact traffic reduction.

This highlights the importance of strengthening inspection systems to disrupt traffic flows. One proposed strategy involves the adoption of advanced inspection technologies, such as X-ray scanners and dual-energy imaging systems. However, these technologies are prohibitively expensive and require substantial investment in infrastructure, ongoing maintenance, and trained personnel resources that are often lacking in many countries.

According to a January 2025 news dispatch from Agence France-Presse, the Port of Rotterdam—Europe’s largest seaport and a long-standing entry point for cocaine—has reduced drug seizures through a combination of technological innovation, enhanced public-private cooperation, and targeted container screening based on indicators such as cargo origin, content, and route irregularities. However, this has also revealed the adaptability of criminal organizations, which have responded by redirecting shipments to smaller or less-secured ports where inspection protocols are weaker (Bernard, 2009), as reported by an investigative piece from InSight Crime in 2023.

Fourth, corruption emerged as a critical variable in the model, reinforcing Europol’s assertion that it is the primary enabler of criminal infiltration in ports and logistics chains (Europol, Port of Antwerp-Bruges, Port of Hamburg, & Port of Rotterdam, 2023). Criminal networks leverage tools such as social media, bribery, and coercion to compromise individuals involved in port operations. Once compromised, these insiders provide criminal groups with direct and often unrestricted access to port infrastructure, cargo management systems, and security protocols.

Simulation results indicate that even small increases in corruption levels can significantly boost cocaine trafficking, effectively undermining inspection efforts and weakening enforcement capacity. Moreover, port-related corruption is increasingly associated with violence. According to the same Europol report, violence is frequently used to intimidate and secure compliance from compromised port workers and external facilitators (Europol, Port of Antwerp-Bruges, Port of Hamburg, & Port of Rotterdam, 2023). It is also deployed to assert dominance among rival criminal factions operating within port environments and to resolve internal disputes within trafficking networks.

To address these dynamics, the European Commission[45] proposes a comprehensive set of policy measures aimed at reducing the influence of organized crime and corruption in seaports. These include strengthening intelligence-sharing mechanisms between local, national, and private-sector actors; establishing specialized anti-corruption units within port authorities; and adapting anti-mafia frameworks to the maritime context. However, addressing corruption in ports requires a deeper understanding of the structural and contextual conditions that sustain it.

While this study focuses on quantifiable and systemic vulnerabilities within the trade and inspection framework, the broader sociopolitical and institutional dimensions of corruption fall outside its scope and remain a critical area for future research. While the model offers valuable insights into how corruption influences trafficking dynamics, it is important to acknowledge certain limitations. In particular, due to the lack of detailed empirical data, the simulation relies on stylized representations of port inspection processes and corruption mechanisms. These abstractions, though necessary for operationalizing the model, may oversimplify the complex institutional, social, and procedural dynamics that shape enforcement outcomes. As such, the

[4] This follows up on the EU Roadmap to fight Drug Trafficking and Organised Crime and is in line with President von der Leyen's commitment to take action in 2024 to fight drugs smuggling and criminal infiltration into European ports.

[5] https://ec.europa.eu/commission/presscorner/api/files/document/print/pl/ip_24_344/IP_24_344_EN.pdf

results should be interpreted as indicative rather than predictive, and as a starting point for deeper, data-informed explorations of port vulnerability.

Similarly, the study can be extended by incorporating a detailed characterization of both departure and arrival ports, considering attributes such as geographic location, port size, infrastructure, cargo volume, and inspection capacity. To effectively integrate this spatial and operational data, Geographic Information Systems (GIS) can be employed (Crooks et al., 2018). GIS allows for the visualization and analysis of spatial relationships between ports, trade routes, and regional vulnerabilities, providing a valuable layer of contextual insight. By incorporating GIS, agent-based models (ABM) can simulate how variations in port characteristics and geographic configurations influence trafficking strategies, enforcement outcomes, and systemic vulnerabilities. This spatial integration would enable more precise, location-sensitive analyses and facilitate the identification of high-risk corridors or nodes within maritime trade networks, ultimately supporting more targeted, evidence-based policy interventions.

3.6 Conclusions

In summary, the developed agent-based model simulates the cocaine trafficking process from departure ports in South America to European ports via container ships, the most used method by traffickers.

The results reinforce the notion that organized crime systematically leverages the scale and complexity of legal maritime trade to conceal illicit shipments. Two main vulnerabilities in port systems are identified: first, limited inspection capacity, with less than 10% of the more than 90 million containers arriving annually at European ports being inspected; and second, widespread corruption, which allows traffickers to infiltrate port operations, bribe key personnel, and manipulate container handling.

Furthermore, the results underscore the model’s nonlinear dynamics as an emergent property. Small increases in inspection capacity can lead to disproportionately large reductions in cocaine trafficking. Conversely, even minimal increases in corruption levels result in sharp rises in trafficked cocaine demonstrating the outsized impact of this variable. Notably, the simulations show that corruption can entirely undermine inspection efforts: when corruption is present, improvements in inspection capacity have no significant effect on reducing cocaine flows. Another key finding is the relationship between container ship capacity and trafficking volume. As ship sizes increase, so does the amount of cocaine trafficked, illustrating how traffickers exploit the logistical scale and structural complexity of larger vessels to evade detection. This research clarified the issue of cocaine trafficking via container ships by using synthetic data informed by insights from qualitative studies and reports, paving the way for future investigations into the specific dynamics that can enhance security policies and strategies.

Chapter 4

Enforcement Costs, Coordination and Social Acceptability in Network Interventions

The following chapter is based on the paper:	
Title:	Enforcement Costs, Coordination and Social Acceptability in Network Interventions
Authors:	Maykol Rodriguez Prieto (Contribution 40%)
	Jorge Marco Renau (Contribution 30%)
	Renan Götz (Contribution 30%)
Status:	Working paper

Different states of this paper have been presented at:

- 1st Seminar on Economics, Institutions and History: Violence, Social Conflicts and the Economy. Girona, Spain 2026.

Enforcement Costs, Coordination and Social Acceptability in Network Interventions

Maykol Rodriguez-Prieto[1], Jorge Marco[2] and Renan Goetz[2]

[1]Faculty of Economics, Justus Liebig Universität Gießen, Germany

[2]Department of Economics, University of Girona, Spain

Abstract

We study network interventions when cooperation depends on informal enforcement operating at local scales. We develop an analytical framework in which agents benefit from cooperative behavior but also incur costs from sustaining it through interactions with others. These costs depend on network structure and capture how coordination and social pressure affect the effectiveness of interventions. Unlike standard approaches that prioritize highly connected individuals, we show that the most effective targets depend on how cooperation is sustained within social networks. Well-connected individuals can generate broad impact but often face greater enforcement costs, while individuals in tightly connected groups can support cooperation more effectively but with more limited reach. This creates a trade-off between the spread of interventions and the ability to maintain cooperative behavior. We further show that the distribution of connections in the network plays a key role in shaping intervention outcomes, as it determines how enforcement responsibilities are shared across agents. Our results highlight that effective policy design must account for the multi-scale nature of network interactions. Interventions that maximize diffusion need not be optimal under limited budgets when cooperation must be actively sustained, implying that targeting strategies must balance reach with enforcement costs.

Keywords: Clustering; Cooperation; Enforcement costs; Network interventions; Targeting.

JEL classification: C72; D85; O12.

4.1. Introduction

Cooperative behavior often spreads not directly through formal enforcement, such as fines or subsidies, but through informal enforcement, such as peer-to-peer channels. In development programs, microfinance loans are more likely to be repaid when group members monitor each other. In health, vaccinations or sanitation practices often diffuse through friends and relatives rather than through official campaigns. In communities that share natural resources such as forests or fisheries, peers pressure one another to prevent overexploitation. In all these cases, the success of an intervention depends not only on who is targeted but also on how cooperation is sustained within social networks of trust and enforcement.

This creates a practical challenge for regulators and policymakers, who must decide which agents to target to maximize overall social impact under budget constraints. Existing research highlights the importance of network structure in this decision. A key insight is that interventions aimed at central agents—those with many or influential connections, often termed hubs—tend to generate the largest social multipliers, as behavior cascades through the social network. This benchmark view has been supported empirically; for example, targeting central villagers in microfinance programs in India accelerated take-up, and similar effects have been documented in agriculture, health, and technology adoption.

Yet this benchmark, rooted in diffusion models of global propagation, overlooks two important considerations of sustained cooperation by social norms. First, cooperation rarely emerges without incurring social costs. Sustaining it often requires agents to exert costly pressure on their peers, whether through reminders, sanctions, or social exclusion. Moreover, these enforcement costs are heterogeneous, as hubs often face higher costs, either because they must pressure more peers or because their peers expect them to enforce norms more actively. Second, in highly clustered local neighborhoods, an agent’s peers are often interconnected. In such contexts, enforcement can reduce costs, as multiple peers coordinate pressure on the same agent; however, this redundancy limits the overall social impact of individual enforcement, creating a tradeoff between efficiency and sustaining cooperation within the social network. Both heterogeneous enforcement costs and clustering-induced redundancy are important when formal and informal enforcement interplay for sustaining cooperation but are largely absent from standard targeting models.

The distinction between diffusion and norm enforcement is important for cooperation. In diffusion models, social multipliers spread widely across the social network, and eigenvector centrality offers a precise guide for budget allocation by capturing influence across long network paths. By contrast, in norm-enforcement contexts, the relevant interactions are local. Peer pressure is exerted primarily within an agent's local neighborhood, often termed circle of trust or reference network, and social multipliers decay quickly across the social network. Two agents may have the same eigenvector score but different enforcement responsibilities if one is embedded in a tightly clustered neighborhood and the other in a sparse neighborhood. In such cases, degree (number of connections) and clustering (the redundancy of those connections), not eigenvectors, determine better who bears costs and who can sustain cooperation most effectively.

This paper aims to fill this gap. The central question in this paper is: How should a planner allocate interventions across networks of interactions when enforcement costs are endogenous, nonlinear, and shaped by local network structure? To answer, we develop an analytical framework where each agent's utility includes both the benefits of cooperation and the costs of enforcing cooperation among peers. Enforcement depends on degree and clustering and may exhibit concave or convex curvature. Concave costs mean that additional peers increase their effort at a decreasing rate, for example, when monitoring peers becomes easier as one gains more experience with repeated enforcement. Convex costs mean that each extra peer increases their effort disproportionately, as might happen if social expectations escalate with each additional peer.

Our contributions are threefold. First, we show that the curvature of enforcement costs determines whether interventions should prioritize hubs or the periphery. With concave costs, less-redundant hubs are preferred, as their high connectivity produces increasing marginal returns. With convex costs, more-redundant peripheral agents are favored, as coordination limits disproportionately high enforcement costs. Second, we show that clustering directly reduces marginal effectiveness by creating redundancies. Third, we analyze how degree variance shapes expected interventions. Together, these results refine the policy prescriptions of existing targeting models. We illustrate the framework using stylized networks to show how the planner's choice changes with local network structure.

The implications extend beyond microfinance to public health campaigns, education, and local commons management. Across these settings, policymakers must decide whether to concentrate resources on leaders or spread them across the periphery. Our results show that the right strategy depends not just on network centrality but also on the shape of enforcement costs and the redundancy of local neighborhoods, both of which are observable in practice.

The rest of the paper is organized as follows. Section 2 reviews the literature on network interventions, cooperation, and enforcement. Section 3 and 4 presents the model and the game, respectively. Section 5 derives the main results and illustrates them in stylized networks. Section 6 discusses policy implications and extensions. Section 7 concludes.

4.2. Related literature

The theoretical literature on network targeting builds from models of strategic complements, or substitutes, and linear-quadratic interaction games where interventions at a subset of agents propagate through the network. A foundational contribution is Ballester et al. (2006) key player approach, which identifies agents whose removal or support most affects overall social outcomes. A recent benchmark is provided by Galeotti et al. (2020), who develop a framework based on spectral decompositions and centrality metrics to characterize optimal targeting in such settings. In their framework, a planner typically concentrates resources on a small set of hubs because they generate the largest social multipliers. The formal characterization and policy prescriptions in this literature emphasize eigenvector-type measures and singular-value decompositions of the interaction matrix as the objects that determine optimality (Bonacich, 1987; Jackson, 2008). Recent advances extend these methods to large populations through graphon or mean-field approaches (Parise & Ozdaglar, 2023), to structural interventions targeting connections rather than agents (Sun et al., 2021), and to interventions under uncertainty or informational frictions (Shin, 2024). These contributions provide accurate predictions for global propagation under linear effects and symmetric spillovers but abstract from the heterogeneity in costs or redundancy generated by clustering at the local level.

A substantial empirical strand asks whether the theoretical predictions perform well in the field. Detailed characterization of social network structures in development and health contexts has repeatedly shown that targeting hubs produces large diffusion gains. Banerjee et al. (2013) document that diffusion centrality identifies effective seeds for microfinance adoption in Indian villages. Beaman et al. (2018) find that targeting central farmers increases the adoption of new agricultural technologies. In health settings, Kim et al. (2015) show that central actors were able to spread behavioral changes effectively in a randomized controlled trial. Other studies emphasize similar mechanisms in technology adoption (Breza et al., 2018) and labor markets (Calvó-Armengol & Jackson, 2007). These empirical contributions validate the central role of network position in many practical settings, but they typically do not model or estimate the endogenous costs of sustaining cooperation, nor the role of local redundancy and social acceptability in limiting marginal reach.

A related empirical strand emphasizes social pressure and norm enforcement as informal mechanisms that sustain cooperative behavior and determine the costs of interventions. Laboratory experiments by Fehr and Gächter (2000) demonstrate that costly enforcement increases contributions in public goods games (Bramoullé & Kranton, 2007) but imposes substantial efforts on norm enforcers. Field studies of group lending highlight the role of social collateral (Jackson et al., 2012), where sanctions among peers enforce repayment (Besley & Coate, 1995). Anderson et al. (2009) document enforcement costs in informal savings groups, while Ostrom (1990) argues that sanctioning institutions are central to governing commons. Chandrasekhar et al. (2020) show that clustering amplifies redundant enforcement in social networks, lowering efficiency. Goetz and Marco (2024) show that clustering lowers enforcement costs, as peers can coordinate actions against those who deviate from the norm. These findings indicate that enforcement costs vary systematically across agents and local network structure, a dimension largely absent from standard targeting models.

The literature emphasizes that interventions are multilevel and that local network structure, i.e., clustering and degree heterogeneity, matters in practice (Golub & Sadler, 2017; Jackson, 2008). Spectral approaches are effective in diffusion models of global propagation for identifying key agents when payoffs and social multipliers are linear and symmetric. Yet they abstract from enforcement cost structures and from redundancies captured by clustering, which are central when cooperation is sustained through peer pressure and multipliers are concentrated locally. Our model therefore emphasizes degree and clustering rather than eigenvector centrality. In spectral models, global measures capture propagation because higher-order paths shape payoffs and objectives. By contrast, our specification derives enforcement costs and benefits primarily from local interactions: the marginal effect of targeting an agent depends on their degree and the redundancy of their peers, and any spillovers remain local, represented by a symmetric matrix with modest off-diagonal mass. When payoffs and costs are local and separable, optimality conditions depend on local network features rather than global eigenvectors. Accordingly, targeting rules based on degree adjusted for clustering may provide effective policy guidance under endogenous enforcement costs. Our model allows enforcement costs to be convex or concave. This extension leads to new comparative statics. Given that enforcement contains a degree-based nonlinear component, Jensen's inequality implies that increasing the variance of the degree distribution reduces average intervention levels when costs are concave but increases it when costs are convex. Intuitively, when enforcement costs are concave, concentrating connections in a few agents lowers total interventions, since the cost of the average degree exceeds the average individual cost. When costs are convex, highly connected agents increase aggregate interventions, since the average individual cost exceeds the cost of the average degree. For a planner allocating a fixed budget, higher degree variance has opposite effects depending on cost curvature, and this distinction is difficult for existing spectral models to capture.

In summary, this paper connects three pieces of literature: target interventions, cooperation in networks, and informal enforcement. By introducing endogenous, nonlinear enforcement costs and by deriving policy implications for when to target less-redundant hubs versus more-redundant peripheral agents, we refine the benchmark view of these literatures.

4.3. The model

The model consists of three key elements: the social network that structures local interactions within the community, the enforcement mechanisms that shape incentives for cooperation, and individual decision-making based on utility differences and resource extraction. Together, these elements capture how local interactions, social pressure, and policy interventions influence whether agents follow sustainable or exploitative strategies. We describe each component and its role in determining cooperation.

4.3.1. Social networks

The interaction among $n > 1$ agents within a community is characterized by a social network $G = (N, L)$, with $N = \{1, ..., n\}$ denoting the set of agents and L the set of links that are the unordered pairs of elements from N. The elements in L consist of the values of the indicatrix link function $l : N \times N \to \{0,1\}$ such that $l_{ij} \equiv l(i, j) = 1$ if $(i, j) \in L$ and $l_{ij} = 0$ otherwise. The model focuses on undirect networks so that $l_{ij} = 1 \Leftrightarrow l_{ji} = 1$[6]. For each agent i, $G(i)$ denotes their set of peers (neighborhood) and $k_i = \sum_{j \in N(i)} l_{ij} \in \{1, \cdots, n-1\}$ its size (degree). The cohesiveness of agent i ′s neighborhood is given by $\tau_i = \frac{m_i}{\left(k_i\left(k_i - 1\right)/2\right)} \in [0,1]$, where the nominator $m_i = \left|\{l_{uv} : u, v \in G(i), l_{uv} = 1\}\right|$ measures the current number of links within the neighborhood and the denominator $\left(k_i\left(k_i - 1\right)/2\right)$ measures the maximal number of links within the neighborhood.

4.3.2. Social norms, payoffs and profile of actions

The community adopts an action profile $\mathbf{a} = \left(a_i\right)_{1 \le i \le n} \in \mathbb{R}_+^n$. Each agent benefits from their action but contributes to a public bad, $A \in \mathbb{R}_+$. Payoff $\pi_i(a_i, A) : \mathbb{R}_+^2 \to \mathbb{R}_+$ is a continuous, twice-differentiable function that increases in a_i and decreases in A. A social dilemma emerges because the action a_i^P maximizes private benefits but does not align with the action a_i^W that maximizes social welfare. The social dilemma is defined by $\pi_i\left(a_i^P, A\right) > \pi_i\left(a_i^W, A\right)$ and $\sum_{\substack{i=1 \\ a_i \neq a_i^W}}^{n} \pi_i\left(a_i, A\right) < \sum_{i=1}^{n} \pi_i\left(a_i^W, A\right)$, for all i and A. The social dilemma can be resolved if the action a_i^W evolves into an accepted cooperative social norm (Young 2015, Nyborg et al. 2016). This requires each agent to be aware of the norm, able to comply with it, and acknowledge its contribution to societal welfare (Sen 1979, Bicchieri 2006, Bicchieri et al. 2021). Agents are identified by their adherence to the norm, facing a binary choice: taking action $a_i = 1$ (cooperator,

---

[6] Moreover, agents are not linked to themselves and there is no more than one link between agents.

C) aligns with the norm and results in a_i^W, while taking action $a_i = 0$ (deviator, D) deviates and results in a_i^P. The action profile is $\mathbf{a} \in \{0,1\}^n$ and the public bad $A = n - \sum_{i=1}^{n} a_i$ ranges from $A^W = 0$ to $A^P = n$.

4.3.3. Informal and formal enforcement

This section presents two mechanisms that address the social dilemma. Informal enforcement relies on social pressure and coordination among compliant peers to sustain cooperation through local interactions. Formal enforcement operates through fines imposed on defectors or subsidies granted to compliers, reducing the short-term gains from defection. Both mechanisms align individual incentives with the collective interest without requiring full coordination across agents.

4.3.3.1. Informal enforcement

Social pressure is the influence exerted by an agent's peers to promote cooperation. It operates within neighborhoods, where agents respond to the behavior of those with whom they share trust and repeated interactions (Manski 1993, Bicchieri 2016, Duernecker and Vega-Redondo 2017, Nyborg 2018), while agents outside this neighborhood have negligible impact on decision-making (Banfield 1958, Platteu 2000). Mechanisms of social pressure include ostracism, verbal reprimands, or reputational consequences that increase the individual cost of defection. In common-pool resource settings, such as fisheries, an overexploiting fisher may be excluded from collective activities or informal trade networks, reducing short-term gains. The strength of social pressure depends on the number of norm-enforcing ties in the agent's neighborhood (Goetz and Marco 2025). Direct and indirect norm-enforcing ties are defined next.

Definition 4.1 [Direct norm-enforcing ties]. *Direct norm-enforcing ties are the links among an agent and their norm-compliant peers, capturing the degree of adherence to the social norm within the agent's neighborhood. Their total number equals the number of compliers in the agent's neighborhood.*

Direct norm-enforcing ties are computed by

$$k_i^C = \left|G^C(i)\right| = \sum_{j \in N(i)} a_j, \tag{5}$$

Where $G^C(i) \subseteq G(i)$. The tightness of direct norm-enforcing ties within the neighborhood is

$$c_i = \frac{k_i^C}{k_i} \in [0,1], \tag{6}$$

and measures the proportion of agent i's dyads that involve norm-complying peers.

Definition 4.2 [Indirect norm-enforcing ties]. *Indirect norm-enforcing ties are the links among an agent's norm-compliant peers, capturing their collective capacity to coordinate social pressure when the agent deviates from the social norm. The total number of indirect norm-enforcing ties corresponds to the number of links connecting compliant peers within the agent's neighborhood.*

Indirect norm-enforcing ties are computed as

$$m_i^C = \left|\left\{l_{uv} : u, v \in G^C(i), l_{uv} = 1\right\}\right|. \tag{7}$$

The tightness of indirect norm-enforcing ties within the neighborhood is

$$\tau_i^C = \frac{m_i^C}{\bar{m}_i} \in [0,1], \tag{8}$$

where $\bar{m}_i = \left(k_i\left(k_i - 1\right)/2\right)$. Equation (8) measures the total number of triads involving agent i and two compliers with respect to the maximum number of triads within agent i's neighborhood. It is assumed that compliers that are linked always coordinate social pressure.

See Fig 4.1 for an illustration. Both agent i's (Panel A) and j's (Panel B) neighborhoods, $G(i)$ and $G(j)$ respectively, have identical $k_i = k_j = 5$ dyads, $k_i^C = k_j^C = 3$ direct norm-enforcing ties, and $m_i^C = 1 > m_j^C = 0$ triads. However, they differ in the number of indirect norm-enforcing ties, $m_i^C = 1 > m_j^C = 0$, since, in $G(j)$, agent j's peers interact in a way such that norm-complying peers are not linked.

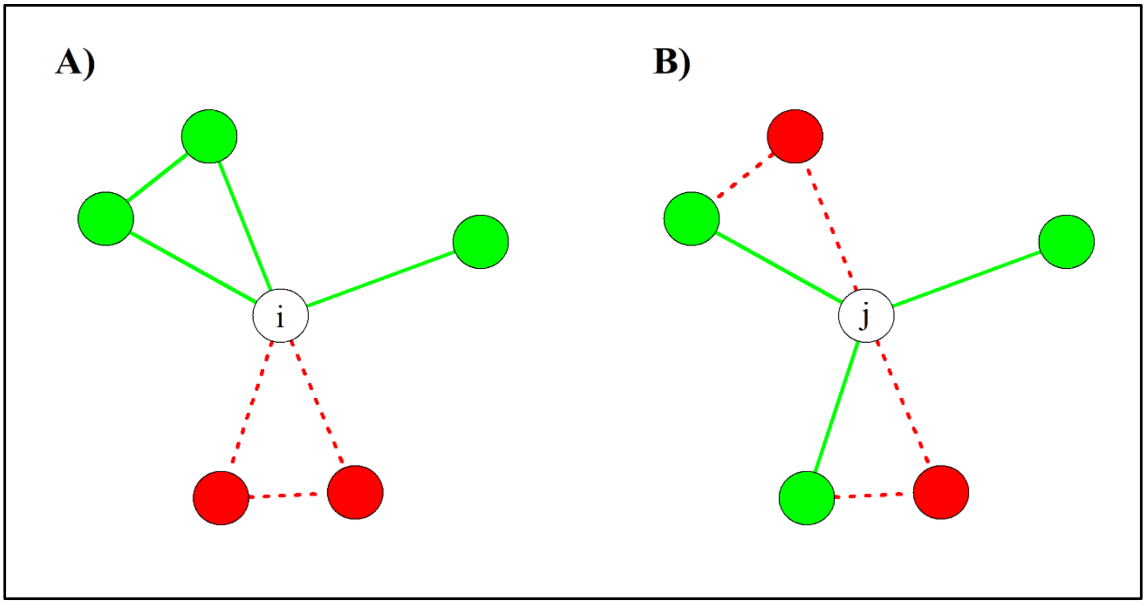

Fig 4.1. Norm-enforcing ties as an extension of social ties and cohesiveness. Green and red circles represent agent i's (j's) peers who are compliers and defectors, respectively. Norm-enforcing ties are represented by continuous green lines, whereas the rest of the social ties are represented by discontinuous red lines. In panel A, agent i has three direct norm-enforcing ties and one indirect norm-enforcing tie. In panel B, agent j has three direct norm-enforcing ties and no indirect norm-enforcing ties.

Social pressure is directly related to the payoff difference between defectors and compliers. The defector's extra benefits, $\pi_i^D - \pi_i^C$, impose higher costs on compliers, and social pressure is interpreted as a response to these losses (Fehr et al. 2002, Dohmen et al. 2009, Mani et al. 2013, FeldmanHall et al. 2018).

Definition 4.3 [Reciprocity]. *Reciprocity is the propensity of agents to respond to the actions of others by sanctioning defection in proportion to payoff differences, thereby maintaining fairness within their neighborhood.*

Based on norm-enforcing ties and reciprocity the strength of social pressure on agent i is defined by

$$\omega_i^C \equiv (1-a_i)\,\omega_i^C(c_i,\tau_i^C)\left(\pi_i^D - \pi_i^C\right). \tag{9}$$

Equation (9) implies that social pressure flows exclusively from compliers to defectors. The social pressure function $\omega_i : \mathbb{R}_+^2 \to \mathbb{R}_+$ is continuous, twice differentiable, and increasing function in c_i and τ_i^C, with $\omega_i(0,0) = 0$. Social pressure is only effective if defectors perceive it as meaningful and proportionate (Bicchieri and Muldoon 2014), such that $\omega_i(1,1) \in (1, \Upsilon]$ with $\Upsilon \ll \infty$.

A social pressure function is defined to capture the effect of compliers on the agent within the neighborhood

$$\omega_i(c_i, \tau_i^C) = \delta_0 c_i + \delta_1 \tau_i^C . \tag{10}$$

Where $\delta_0 + \delta_1 = \Upsilon \geq 1$ captures the influence capacity of direct and indirect norm-enforcing ties to social pressure. Intuitively, $\delta_0 > \delta_1$ occurs when social pressure comes mainly from the compliant peers directly connected to the agent. In this case, each neighbor monitors the agent and exerts pressure simply by being compliant themselves. For instance, in a fishing community, when peers adhere to sustainable practices, such as limiting their catch below an allowed quota, an agent experiences social pressure to conform merely by being observed. Each neighbor contributes independently, so no coordination is needed. Direct ties dominate because the agent responds to the monitoring and behavior of individual compliant peers. In contrast, $\delta_1 > \delta_0$ occurs when social pressure depends more on how compliant peers interact with each other. Here, peers monitor the agent collectively through their coordinated behavior. For example, if peers coordinate sharing fishing spots or alternate access to common equipment, the agent faces pressure generated by the neighborhood's joint enforcement rather than by any individual neighbor. Indirect ties dominate because the coordinated monitoring among compliant peers amplifies social pressure beyond the sum of individual effects. Social pressure reflects the balance between the influence of individual peers and the coordination among them.

Assumption 4.1 [Perfect monitoring]. *All agents have complete and immediate information about their peers' actions, allowing social pressure to be applied without delay.*

In cases of imperfect monitoring, a coordination mechanism is required to ensure consistent responses to agents who take opposite actions. However, since such mechanisms do not offer further insights into the emergence of cooperation, they are excluded from the current analysis.[7]

Exerting pressure may entail costs for agents. These costs may appear as a result of two informal enforcement mechanisms: monitoring peers' actions and ostracizing those who deviate. Standard models of social norms typically abstract from such enforcement costs, however, incorporating them offers a more realistic approximation of how cooperative norms operate in practice (Fehr and Gächter 2000, Calvó-Armengol and Jackson 2010) Ignoring these costs tends to exaggerate the effectiveness and stability of norm enforcement, as it implicitly assumes that agents can discipline peers without using resources or facing risks of social retaliation. By contrast, taking account of pressuring costs captures the tradeoffs agents face when sustaining cooperation.

Let $\upsilon_i^C \in \mathbb{R}_+$ denote the costs for a cooperator to pressure noncooperating peers, formally given by

$$\upsilon_i^C \equiv \upsilon_i^C \left(1-c_i, k_i\right). \tag{11}$$

The function $\upsilon_i^C : \mathbb{R}_+^2 \to \mathbb{R}_+$ is continuous and twice differentiable, with υ_i^C decreasing in c_i. This function increases in k_i, with $\upsilon_i^C\left(1, k_i\right) \geq \upsilon_i^C\left(1-c_i, k_i\right)$.

A pressuring cost function is defined to capture the effect of exerting pressure to agent's peers

$$\upsilon_i^C = \alpha\left(1-c_i\right) k_i^{\beta}. \tag{12}$$

As group size increases, the costs of monitoring and ostracizing peers increase, requiring more efforts to enforce norms and counteract contrary actions.

With respect to the costs of exerting pressure the following assumption is made.

[7] Although imperfect monitoring is expected to weaken the effectiveness of social pressure, its implications can still be studied indirectly within the present modelling framework by modifying the pressure and pressuring cost functions.

Assumption 4.2 [Exerting costly social pressure]. *Agents pressure peers who act differently from them, accepting personal costs for doing so, and refrain from free riding on other pressuring agents of the same type.*

Cooperative norms rely on agents' intrinsic motivation to enforce them, despite the costs (Fehr and Gintis 2007).[8]

4.3.3.2. Formal enforcement

Formal enforcement refers to policy instruments, such as fines imposed on defectors or subsidies granted to compliers, that directly reduce the extra benefits gained by defectors. These measures are designed to reduce the social losses caused by defection and operate in proportion to utility differences. They are denoted by

$$\theta_i \in \mathbb{R}_+. \tag{13}$$

Formal enforcement is externally imposed through policies and operates instantaneously, whereas informal enforcement emerges endogenously from repeated interactions among peers and depends on the structure and dynamics of these interactions to sustain cooperation.

4.3.4. Utility and decision-making

The agent's utility is given by

$$u_i^{\{C,D\}} = \pi_i\left(a_i, A\right) - \left(1 - a_i\right)\omega_i{}^C - a_i \upsilon_i{}^C. \tag{14}$$

In (14), the first term represents the payoff structure of the social dilemma, with $\pi_i\left(0, A\right) > \pi_i\left(1, A\right)$ for all A. The second term reflects utility losses from social pressure, while the third term accounts for the associated pressuring costs. As such, utility from cooperation is given by $u_i^C = \pi_i\left(1, A\right) - \upsilon_i^C$ and from noncooperation by $u_i^D = \pi_i\left(0, A\right) - \omega_i^C$. The decision to cooperate is represented as a choice rule that depends on the utility difference between u_i^D

[8] If agents lack intrinsic motivation to exert peer pressure, they may free ride on other pressuring agents' efforts, creating an additional social dilemma that falls outside the scope of this study. Even though agents may pressure other agents of the same type to enforce peer pressure (a meta-norm; (Axelrod 1986)), this model focuses on cooperation and omits the second-order public good problem. Therefore, the influence of intrinsic motivation on costs is excluded, assuming all agents are willing to bear the costs of exerting peer pressure.

and u_i^C. While agents may regard cooperation as socially desirable at the level of the broader network, their behavioral choices are based only on observations of their immediate peers' actions and the link structure of their neighborhood. This localized decision-making process captures bounded rationality in a meaningful way: agents operate with partial information and do not possess, let alone process complete knowledge of the network structure and all agents' choices (Frick et al. 2022). Incomplete knowledge and the limited information processing capacity of the agents suggest that an optimal response in the presence of a large number of agents, each occupying a distinct position within the social network, would likely exceed the limits of rational decision-making. Moreover, the interdependence of decisions implies that each agent's choice influences and is influenced by the behavior of all other agents. This mutual dependence generates even more complexity, introducing additional uncertainty in both anticipating others' actions and assessing the potential outcomes of one's own decisions.

As a consequence of bounded rationality and the complexity of interdependent decision-making, agents are unable to make perfectly rational choices that establish fixed behavioral rules. Instead, agents adapt their behavior over time, adjusting to the observed actions of peers and evolving contextual factors (Brock and Hommes 1997, Wallace and Young 2015). Because agents are aware of their limited processing and informational capacity, they know that their ex-ante choice of the highest utility does not guarantee ex-post optimality. However, agents can assess the robustness of their choice. This makes probabilistic choice/reasoning, favoring the action with the more robust advantage, an internally coherent response to bounded rationality rather than an arbitrary departure from standard optimization. Probabilistic reasoning has been employed in games based on random utility, Bayesian learning, quantal response models or rational inattention models (Mertens 2002). It is articulated by the SoftMax (logit-type) choice rule (Blume 1993, McKelvey and Palfrey 1995, Fudenberg and Levine 1998, Moffatt 2020) given by

$$p_i^C = \frac{1}{1+e^{\left(u_i^D - u_i^C\right)}}, \text{ and } \; p_i^D = 1 - p_i^C . \tag{15}$$

We interpret the utility difference $u_i^D - u_i^C$ as the net utility differential between the two options. As the difference in the net utility differential increases (decrease), the probability of agents acting cooperatively p_i^C decreases (increases).

4.4. The game

We develop a game to analyze the evolution of cooperation in social networks. In the game, agents simultaneously learn and adjust their actions over time, gradually converging toward an equilibrium.

4.4.1. Initialization

At the start of the game, $t=0$, initial conditions are established, setting the baseline for agents' interactions and behavior.

- *Social networks*. A large social network G is generated.[9] The structure of the network remains fixed throughout the game.
- *Cooperative norm*. A social planner defines the action that maximizes social welfare. The cooperative norm, $a_i = 1$, is common knowledge and lies within the feasible action set of all agents.

At time $t=1$, the action profile of agents, $\mathbf{a}(t=1) \in \{0,1\}^n$, determines the initial level of cooperation. Initial actions are randomly distributed across agents.

- *Level of cooperation*. At time $t \in \{0,1,\cdots,T\}$ the number of agents that behave cooperatively is given by $C(t) = \sum_{i=1}^{n} a_i(t)$ and the number agents that behave non-cooperatively is given by, $D(t) = n - C(t)$.
- The social network structure remains fixed within each run of the game and systematically varied across runs to assess their influence on cooperation.

4.4.2. Timing of actions

- *Step 1*. At each time step $2 \le t < T$, agent i cooperates with probability $p_i^C(t)$. All agents make their decision simultaneously based on the observed actions of their peers at time

[9] The network formation model developed by Jackson and Rogers (2007) allows us to generate networks that reflect realistic patterns of social interaction. By combining random and strategic link formation, it produces networks with empirically observed characteristics, such as heavy-tailed degree distributions and clustering, making it particularly well-suited for studying cooperative dynamics in large-scale social contexts.

$t-1$. Individual actions are independent of each agent's past actions, such that $a_i^C(t) \perp a_i^C(\tau)_{\tau < t}$.

- *Step 2*. The game ends when $t = T$, with $T \gg 2$ being finite but large.

4.4.3. Evolution of cooperation

At any two consecutive time periods, t and $t+1$, the agents' actions follows a sequence of n independent[10], but non-identically distributed random variables, modeled as a Poisson binomial distribution of Bernoulli trials, $\mathbf{a} \in \{0,1\}^n$. At $t+1$, the expected level and variance of cooperation[11] are given by

$$\begin{aligned} \mathrm{E}\left[C\left(t+1\right)\right] &:= \sum_{i=1}^{n} p_i^C\left(t\right) \\ Var\left(C\left(t+1\right)\right) &:= \sum_{i=1}^{n} p_i^C\left(t\right)\left(1-p_i^C\left(t\right)\right). \end{aligned} \tag{16}$$

Equation (16) shows that when all agents are indifferent with respect to their choice, the expected number of cooperators is $\mathrm{E}\left[C\left(t+1\right)\right] = n/2$ and the variance of cooperators attains its maximum value, $Var\left(C\left(t+1\right)\right) = n/4$. In this case, the evolution of cooperators follows a binomial distribution of actions, reflecting the highest possible uncertainty regarding individual behavior.

4.4.4. Equilibrium

The evolution of cooperation may converge to multiple equilibria, including the full cooperation and full noncooperation outcome (Nyborg and Rege 2003, Bicchieri 2006).

Definition 4 [Equilibrium]. An equilibrium of the game is attained when $\mathrm{E}\left[C\left(t\right)\right] = \mathrm{E}\left[C\left(\xi\right)\right]$, for any $0 \le t < \xi \le T$.

---

[10] An agent's actions at time influence other agents' actions at time, however, the probability of an agent to cooperate at times and are independent because all agents take decisions simultaneously.

[11] The computation of other statistical properties of the Poisson binomial distribution, such as its probability density function, becomes increasingly complex as the number of trials grows, often requiring approximations using the Poisson or normal distribution.

The game has two boundary equilibria: full cooperation and full noncooperation equilibria. The full noncooperation equilibrium arises when all agents act solely to maximize their private benefits. This corresponds to the Nash equilibrium where $\mathrm{E}\left[C(t)\right]=\mathrm{E}\left[C(\xi)\right]=0$ and $Var\left(C(t)\right)=Var\left(C(\xi)\right)=0$. In contrast, the full cooperation equilibrium is attained when all agents prioritize maximizing social welfare. This corresponds to the first-best solution of the game or Pareto-efficient outcome where $\mathrm{E}\left[C(t)\right]=\mathrm{E}\left[C(\xi)\right]=n$ and $Var\left(C(t)\right)=Var\left(C(\tau)\right)=0$. Any interior equilibrium constitutes a second-best solution to the game, being bounded from below by the privately optimal outcome and from above by the socially optimal (welfare-maximizing) outcome.

4.5. Preliminary results

For all cases, define the vector $\theta=\left(\theta_1,...,\theta_n\right)\in\mathbb{R}_+^n$ such that total budget is defined as $B=\sum_{i=1}^{n}\theta_i$. The intervention for any agent i at time t is θ_i such that $\theta_i=u_i^D-u_i^C$ and therefore $p_i^C=\frac{1}{2}$. Consequently, $\mathrm{E}\left[C(t+1)\right]=\frac{n}{2}$.

We now analyze the following three cases for three different networks with different densities (Fig. 4.2), star graph, whose density is close to 0, a graph with density close to 0,5 and the complete graph with density equal to 1. Total budget is measured to different compliance levels, it means the amount of agents into the network cooperate, in other words, when $C=0$ no one of agents is complier, and $C=1$ all agents are compliers.

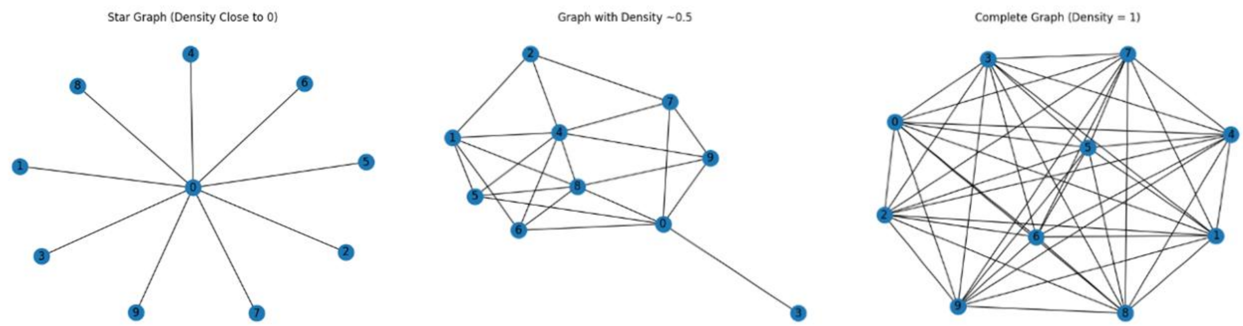

Fig 4.2. Network densities. Star Graph (density ~ 0). Graph with middle density (~ 0.5). Complete Graph (density ~ 1).

Case 1. Compute total budget B when $\delta_1 = 0$ (see equation 10) and $\alpha = 0$ (see equation 12), that is, when there is no influence of indirect norm-enforcing ties and exerting pressure to peers is costless. In Case 1 (Fig 4.3), the results show that the highest budget is reached at the lowest level of compliance for all network densities, this is due to a greater direct influence of peers, which generates a higher cost when there is no cooperation, Additionally, a low-density network implies fewer connections between agents. Given that $\delta_1 = 0$, only $\delta_0 > 0$ contributes to the dynamics, meaning that pressure arises exclusively from connected pairs. As a result, even with fewer links, the associated costs are relatively high, leading to a higher overall budget. As the compliance level increases, the budget decreases across all cases. However, from the early stages of this increase, the budget associated with the star graph (i.e., a network with density close to 0) remains higher than in the other two graphs. For instance, at a compliance level of 0.2, the total budget for the star graph is approximately 600, whereas for the medium-density (0.5) and complete (density ~ 1) graphs, the budget is around 300 and 350, respectively.

As the value of C continues to increase, the total budget declines in all network structures. Nevertheless, the star graph consistently exhibits a higher budget compared to the other configurations. It is also observed that for values of C greater than 0.6, the budget approaches zero in all cases, a fact that for the star graph is not the case for the following cases 2 and 3.

Case 2. Compute total budget B when $\delta_1 > 0$ and $\alpha = 0$. A more collective approach to supervision involves not just one neighbor monitoring the community, but the entire community. Results in Fig 4.3 (Case 2) show that the total budget decreases as compliance levels C increase;

however, unlike in Case 1, this decline follows a linear pattern, for the star graph, since the budget only approaches zero when the compliance level reaches 1, i.e., when all agents cooperate. In contrast, for the medium-density and complete graphs, the results are similar to those observed in Case 1. These findings suggest that low-density structures, such as the star graph, require a larger budget due to the limited connectivity among agents, and therefore collective social pressure is not evident as in the graphs with greater density.

Case 3. Compute total budget B when $\delta_1 > 0$ and $\alpha > 0$, at different values of β (see equation 12, this parameter graduates the curvature of the pressuring cost function from concave to convex cases). In this case, use for illustration the star network: targeting hubs vs targeting peripheral agents. Results are shown in Fig 4.3. Case 3, $\beta = 2$ is fixed. Unlike Cases 1 and 2, Case 3 shows a significantly higher budget at low levels of compliance. This is primarily due to the additional costs associated with exerting pressure on defectors υ_i^C, that is activated when $\alpha > 0$, which becomes substantially greater in the absence of cooperation. However, for low compliance levels, the star graph exhibits a comparatively lower budget, this occurs because only the central nodes maintain connections, and thus only they incur supervision costs. In contrast, higher-density graphs involve a larger number of supervised connections, leading to increased overall costs.

As compliance C increases, the budget in medium and high-density graphs rapidly approach zero, beginning around $C \approx 0,4$. This behavior is not observed in the star graph, where the budget only approaches linearly zero when C reaches 1. This suggests that in networks with hubs i.e., agents with a high degree of connectivity, as in the star graph, the supervision costs associated with these central nodes can become disproportionately large.

Analyzing and relating costs to network topology, it is important to note that when network density is approximately zero, hubs are present (star graph), while higher density leads to greater homogeneity and, consequently, more redundancy. Furthermore, when costs are concave, intervention in hubs is advantageous because their high connectivity produces increasing marginal returns, meaning greater pressure that leads to increased cooperation. On the other hand, when costs are more convex, intervention in more peripheral nodes is preferable, as coordination limits implementation costs.

Applying these two assumptions to the results obtained, we observe the following in Fig 4.3. Case 1 shows concave costs, where all three curves initially decline, indicating that for low levels of C, cooperation is achieved without requiring a high budget. Therefore, intervening in central nodes would be beneficial. In case 2, a similar result to that of case 1 is observed; however, the curve representing a density close to zero does not show such a pronounced decrease. This implies that, for these graphs, more nodes need to be targeted, and therefore, focusing on central nodes would be more costly. Case 3 is the closest to representing convex costs. The initial decline is steeper for all three graphs compared to the other cases, especially for the graph with a density close to zero. This suggests that targeting only hubs is not very efficient, so it is advisable to focus on peripheral nodes.

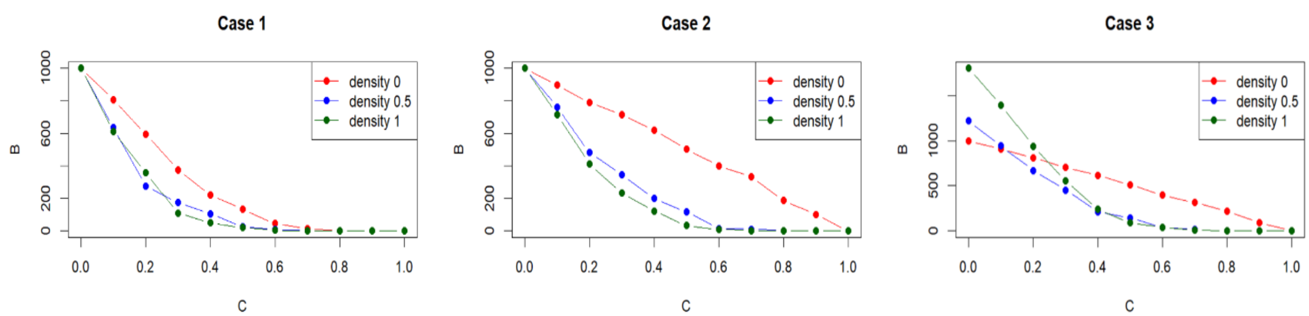

Fig 4.3. Total budget based on different compiler levels for different network densities. Based on equations 10 and 12: Case 1 $\delta_1 > 0$ and $\alpha = 0$. Case 2 $\delta_1 > 0$ and $\alpha = 0$ and Case 3 $\delta_1 > 0$ and $\alpha > 0$.

Case 4. Analyze how expected total budget B changes as network structure (degree variance) changes. In this case, use for illustration complete, random and scale-free networks. Use Jensen's inequality for deriving analytical results. Consider only the cases when $\delta_1 = 0$ and $\alpha > 0$. The results are presented in Fig 3. The expected total budget is θ. It can be observed that as the compliance level increases, θ decreases. Specifically, when the compliance level p is 0.1, θ is close to 1000; as the level increases to 0.7, θ drops to around 100; and when full cooperation is achieved ($p = 1$), the expected θ approaches zero.

Furthermore, examining the relationship between θ and degree variance reveals important patterns. In scale-free networks characterized by hubs presence (it is reflected by higher $p\_network$ values in Fig 4.4.) the degree variance tends to be low due to the coexistence of nodes with both very high and very low degrees. However, the effect of degree variance on the expected θ depends on the level of compliance. In cases of low and medium compliance, the high degree variance, typical of non-scale-free networks, leads to higher values of θ. For example, when $p = 0.2$, degree variance of 125 corresponds to an expected θ of approximately 750, whereas a variance of 300 corresponds to an expected θ of about 900. In this context, the average θ across all cooperation levels is around 400. In contrast, at higher levels of compliance (e.g., $p = 0.8$) θ becomes relatively insensitive to changes in degree variance, remaining approximately constant across different network configurations.
This reinforces the fact that for network structures with a greater presence of hubs and low density, a larger budget is needed to achieve greater cooperation compared to denser networks and/or those with greater variance.

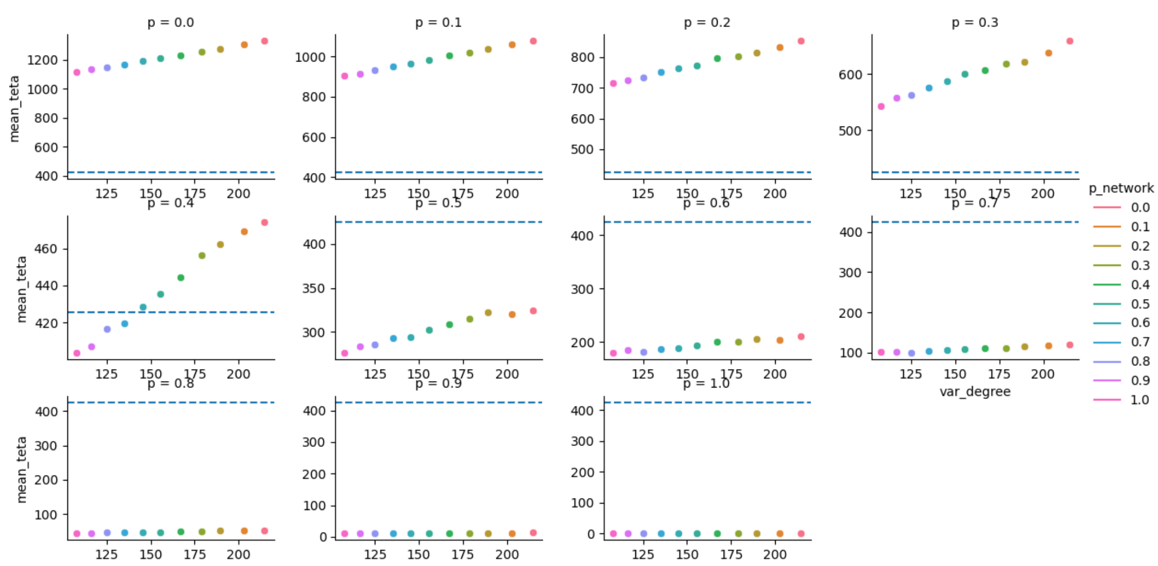

Fig 4.4. Expected θ and variance of degree for different complier levels and network formation.

4.6. Discussion of the results

Cooperative behavior, such as peer monitoring and trust, plays a fundamental role in maximizing social impact through interventions by regulators and policymakers. Cooperative behavior can be understood through a social network, where agents are connected by ties of friendship, family, or shared common resources. In this context, regulators must decide which agents to target to maximize socioeconomic impact, subject to a budget constraint.

If we take the example of a fishery, where the goal is to optimize and improve resource management, the government or an institution promotes an intervention in which tools are subsidized to monitor and maintain internal control through technology that enables the recording of fishing activities. One option would be to subsidize each fisher individually so that each adopts the technology and records their data separately. Another option would be to target community leaders, who would then be responsible for recording information for each fisher; in this case, peers or connections monitor one another.

Although the existing literature on diffusion models suggests targeting central nodes, this work shows that this approach must be analyzed more carefully and highlights the importance of network structure, considering characteristics such as the degree of each agent and how agents are clustered (redundancy). In the example, the fishery can be described as a network where peers monitor each other (if they are connected) in terms of rule compliance and accurate reporting of catches. This monitoring entails a cost depending on how many peers must be supervised; therefore, central nodes face higher enforcement costs. At the same time, depending on how agents in the fishery are connected (i.e., the number of links among them), the density of the network is defined. The more connections there are between nodes, the denser the network becomes, which reduces the burden on central nodes and lowers individual enforcement costs.

The theoretical model developed both analytically and numerically defines, for each agent, a utility function that depends on cooperation and the costs associated with their peers cooperating. Interpreting the results of the model and illustrating them through the fishery example, subsidies for internal monitoring show how enforcement costs can exhibit different curvature patterns depending on network structure (degree and redundancy) and the level of compliance. Based on the results in Figure 2, Case 1, where there is no influence of indirect norm-enforcing ties and exerting pressure on peers is costless—shows concave costs. This suggests targeting central nodes regardless of network density. In a fishery with these characteristics, training a leader could have a greater effect, influencing many fishers at low marginal cost.

In Case 2, where joint monitoring exists, if the fishery viewed as a social network is dense, enforcement costs are like those in Case 1. Therefore, it is optimal to target nodes with higher degree to manage the subsidy. However, if the network has low density (approximately zero), targeting only central nodes may be costly.

In Case 3, due to the additional costs associated with exerting pressure on non-compliant agents, the results show that costs are convex for both low- and high-density network structures. This implies that targeting central nodes becomes costly because each additional agent to supervise disproportionately increases the monitoring burden. This effect is more pronounced in low-density networks. However, as shown in Figure 2, Case 3, for densities of 0.5 and 1, the cost curves are more concave. This is because agents can monitor whether their peers are correctly using the technology and accurately reporting catches, which reduces individual costs. Therefore, a broader intervention targeting peripheral nodes would be more effective.

The analysis of the model highlights that interventions by regulators or institutions—through policies and/or subsidies aimed at maximizing socioeconomic impact—must consider the multiscale nature of network interactions. In this analysis, we examine network structures such as centrality, redundancy, and density. We also emphasize the role of peer monitoring costs, an aspect that the targeting literature has largely overlooked. The model incorporates these costs through parameters capturing both direct and indirect peer influence, as well as the additional costs associated with exerting pressure on defectors. Simulations and theoretical results show that enforcement costs are non-trivial, implying that strategies based solely on maximizing the reach of interventions are not necessarily optimal under budget constraints. Therefore, interventions must balance potential diffusion by adjusting targeting strategies according to the structure and characteristics of the network.

An important avenue for future research is the application of this framework to contexts of corruption and anti-corruption enforcement. In such settings, cooperative behavior can be interpreted as compliance with rules and norms, while defectors correspond to agents engaging in corrupt practices. Individuals are embedded in social and professional networks where monitoring, reporting, and sanctioning often rely on informal mechanisms such as peer pressure, reputation, and trust. In this context, our framework suggests that the effectiveness of anti-corruption interventions, such as audits, transparency tools, or whistleblowing incentives, depends not only on targeting influential individuals, but also on how enforcement responsibilities and social pressure are distributed across the network. Highly connected actors, such as public officials or organizational leaders, may have the potential to influence many others, but they also face higher costs and risks when enforcing compliance. Conversely, tighter and more redundant local networks may be more effective at sustaining honest behavior through mutual monitoring, even if their overall reach is limited. This perspective highlights that anti-corruption policies should account for the network structure of interactions and the costs of informal enforcement, rather than relying solely on strategies that maximize visibility or diffusion.

There are several aspects that this document does not address, but which are important for strengthening regulators' decision-making when implementing interventions. First, scenarios with imperfect information must be considered. This study assumes that the regulator has partial knowledge of the network structure; however, this premise may be unrealistic, as regulators often lack the capacity to observe the relationships and characteristics of the communities in which they intervene.

Second, there are two extensions of this study that warrant further investigation. The first concerns the behavioral responses of agents to interventions: when an intervention is carried out and social pressure arises, some agents may reduce their own effort, relying on the intervention and becoming complacent. This generates imperfect substitution and leads to lower-than-expected levels of cooperation, producing adverse social effects. In the literature, this phenomenon is known as the displacement effect. The second extension involves incorporating the agents' intrinsic motivation to cooperate, which is determined by individual moral considerations. This agent-specific parameter can generate polarization within the network. Both extensions are based on behavioral economics and can significantly influence the effectiveness of regulatory interventions.

4.7. Conclusion

This paper highlights that the effectiveness of interventions by regulators and policymakers aimed at promoting and maximizing cooperative behavior depends not only on which nodes are targeted, but also on how cooperation is sustained within a social network characterized by trust and compliance. Beyond standard diffusion-based approaches—which emphasize targeting highly connected nodes that can generate broader reach through cascade effects—we develop a theoretical model in which agents sustain cooperation through informal mechanisms, facing additional costs when exerting pressure on defectors. We show that targeting highly connected individuals is not always optimal when monitoring and enforcement are costly and unevenly distributed across the network.

Our results emphasize a fundamental trade-off between reach and budget. While central agents can amplify the diffusion of interventions, they also face disproportionately higher enforcement costs, which may limit overall effectiveness. In contrast, when the network includes agents embedded in more cohesive and redundant local structures, these agents are better able to sustain cooperation, albeit with a more limited scope of influence but at lower cost.

Our findings are derived from analyzing marginal costs within a fixed intervention budget, evaluating different scenarios, and testing networks with varying levels of density, where each agent's utility function depends on its degree and clustering.

From a public policy perspective, our results suggest that interventions designed solely to maximize diffusion may perform poorly under budget constraints if network structure and node positioning are not considered. Instead, effective targeting strategies must balance the potential for wide diffusion with enforcement costs, while considering the multiscale nature of social interactions.

Overall, this work underscores the need to integrate network structure and enforcement considerations into the design of policy interventions, opening the door to more context-sensitive and cost-effective approaches to promoting cooperation.

Appendices

Proposition 1 (Efficiency)

For an agent i with degree $k_i \in [1, n-1]$ and local cooperation share $c_i \in [0,1]$, define the regulator´s per-agent intervention cost (fine or subsidy):

$$\theta_i \equiv \theta_i(k,c) = \pi_i(0) - \pi_i(1) - w_i(c_i) + \alpha(1-c_i)k^f.$$

With $\pi_i(0) - \pi_i(1) > 0$, $\alpha > 0, f > 0$. Let $s_i(k_i) > 0$ denote the marginal social impact of targeting a degree-k agent. Assume that s_i is continuously differentiable. The regulator ranks candidates by:

$$R(k,c) = \frac{s(k)}{\theta(k,c)}.$$

For the baseline, we consider $\frac{dc}{dk} = 0$ (c is treated as fixed) and $w(c)$ can be any function.

Define the impact elasticity as $\eta_s^k \equiv \frac{d\ln(s(k))}{d\ln(k)}$ and the partial (holding c fixed) cost elasticity

$$\varepsilon_\theta^k(k \mid c) = \frac{\partial \ln\theta(k,c)}{\partial \ln(k)}.$$

Because $\frac{\partial\theta}{\partial k} = \alpha(1-c)fk^{f-1}$, we set that

$$\varepsilon_\theta^k(k \mid c) = \frac{k}{\theta(k,c)}\alpha(1-c)fk^{f-1} = \frac{\alpha(1-c)fk^f}{\theta(k,c)}.$$

Differentiating $\ln(R) = \ln(s) - \ln(\theta)$ with c fixed yields the generalized baseline condition

$$\frac{\partial \ln(R)}{\partial \ln(k)} = \eta_s^k(k) - \varepsilon_\theta^k(k \mid c).$$

If this difference is positive, then targeting hubs is preferred. Otherwise, targeting periphery is preferred.

Now, as an extension of the baseline use, consider $c = c(k)$. When c depends on k, we can use the total derivate:

$$\frac{d\theta}{dk} = -w_c(c)\frac{dc}{dk} + \alpha\left[-\frac{dc}{dk}k^f + (1-c)fk^{f-1}\right],$$

Where $w_c(c) \equiv \frac{dw}{dc}$. Hence, total elasticity of θ over k is $\overset{k}{\varepsilon_\theta} = \frac{k}{\theta}\frac{d\theta}{dk}$, equivalently, $\frac{d\ln(R)}{d\ln(k)} = \eta_s^k - \overset{k}{\varepsilon_\theta}$. We can identify two cases.

Case 1. When cooperation increases with degree, $\frac{dc}{dk} > 0$. Because $\omega_c \geq 0$ (pressure increases with c) and $\frac{dc}{dk} > 0$, the terms $-\omega_c\frac{dc}{dk}$ and $-\alpha\frac{dc}{dk}k^f$ are negative. Therefore $\overset{k}{\varepsilon_\theta} < \varepsilon_\theta^k(k \mid c)$. This means that hubs are more attractive because the threshold condition $\eta_s^k(k) > \overset{k}{\varepsilon_\theta}$ become easier to satisfy. As such, the planner should exert more often than under the baseline case. This assumption, $\frac{dc}{dk} > 0$ is plausible when hubs face stronger reputational incentives, more peer monitoring or greater exposure to social norms. Hubs are too visible to defect because deviations are more likely to be noticed and sanctioned. In contrast, peripheral agents are less exposed, so they cooperate less. In summary, the planner should expect $\frac{dc}{dk} > 0$ when sanctions and peer pressure are (i) strongly linked to visibility, (ii) social norms are enforced locally and observed by many peers and (iii) hubs are hold to high standards. If instead cooperation depends mainly on private characteristics rather than network exposure, the planner should expect $\frac{dc}{dk} = 0$.

Case 2. When cooperation decreases with degree, $\frac{dc}{dk} < 0$. In this case $-\omega_c\frac{dc}{dk}$ and $-\alpha\frac{dc}{dk}k^f$ are positive. Hence,

$$\overset{k}{\varepsilon_\theta} > \varepsilon_\theta^k(k \mid c).$$

This means that hubs are less likely to be optimal since the inequality $\eta_s^k > \overset{k}{\varepsilon_\theta}$ becomes harder to satisfy. Consequently, the planner will be more often favor peripheral agents. This assumption, $\frac{dc}{dk} < 0$, is plausible when hubs connect a lot of weak ties, dilating monitoring, or have degree-dependent private incentives. In such cases, hubs face weaker peer pressure and have more incentives to act in their own interest.

Corollary: Regime shifts

Assume $S(k)=\alpha k^{s}$ with $0\leq s\leq 1$, $\omega=\omega(c)$ and $f>0$. Then the function

$$\phi(k)=\eta_{s}^{k}(k)-\varepsilon_{\theta}^{k}=s-\frac{k}{\theta}\left(-\omega_{c}\frac{dc}{dk}-\alpha\frac{dc}{dk}k^{f}+\alpha(1-c)fk^{f-1}\right),$$

is generally strictly decreasing in k. Consequently, $\phi(k)$ crosses at most once and there exist at most one cutoff k^{*} such that $\phi(k^{*})=0$. If $\frac{dc}{dk}>0$, the cutoff shifts upward, favoring hubs. Otherwise, the cutoff downward, favoring periphery. The implication of this result is the following. For any $f>0$, the cost of inefficiency noncooperators grows with k, but whether hubs or periphery are more attractive for targeting depending on whether local cooperation increases or decreases with connectivity. The single-crossing property ensures that there is one optimal threshold degree for intervention.

Proposition 2: Redundancy

We model redundancy (clustering coefficient, τ_i) as an overlapping factor $h(\tau_i)$ affecting θ_i such that

$$\theta_i(k_i,\tau_i,c_i)=\theta_i=\pi_i(0)-\pi_i(1)-\omega_i(c_i)+\alpha(1-c_i)h(\tau_i)k_i^{f},$$

where $h'(\tau_i)\equiv\frac{\partial h}{\partial\tau_i}<0$, $h(0)=1$, $h:[0,1]\rightarrow(0,1]$ allow local impact to weakly fall in redundancy

$$S_i=S_i(k_i,\tau_i)\,,\ \frac{\partial S_i}{\partial\tau_i}\leq 0\,,\ \frac{\partial S_i}{\partial k_i}\geq 0.$$

Define $R_i(\tau_i)\equiv\frac{S(k_i,\tau_i)}{\theta(k_i,\tau_i,c_i)}$. Holding k_i and c_i fixed.

If $f > 1$ and $\frac{\partial S_i}{\partial \tau_i} \le 0$, then R_i is increasing in τ_i, which implies that targeting higher-redundant agent is preferred. If $f < 1$ and $\frac{\partial S_i}{\partial \tau_i} \le 0$, then R_i is decreasing in τ_i, which implies that targeting lower-redundant agent is preferred.

Proof:

$$\frac{\partial R}{\partial \tau_i} = \underbrace{\frac{1}{\theta_i}\frac{\partial S_i}{\partial \tau_i}}_{\le 0} - \underbrace{\frac{S}{\theta_i^2}\frac{\partial \theta}{\partial \tau_i}}_{<0};$$

With $\frac{\partial \theta_i}{\partial \tau_i} = \alpha\left(1-c_i\right)h'(\tau_i)k_i^f$. Note that $\frac{\partial R_i}{\partial \tau_i} > 0$ if $\frac{1}{S_i}\frac{\partial S_i}{\partial \tau_i} > \frac{1}{\theta_i}\frac{\partial \theta_i}{\partial \tau_i}$, which is more likely if $f > 1$.

Δ sufficient condition is:

$$\frac{\partial \ln R_i}{\partial \ln \tau_i} = \eta_s^\tau - \varepsilon_\theta^k \eta_h.$$

Where $\eta_s^\tau \equiv \frac{\partial \ln S}{\partial \tau} \le 0$ and $\eta_h \equiv -\frac{\partial \ln h}{\partial \tau} > 0$. Thus, $\frac{\partial \ln R_i}{\partial \tau_i} > 0$ iff $\varepsilon_\theta^k > -\frac{\eta_S^\tau}{\eta_h}$. With $f > 1$, ε_θ^k increases and does the probability for $\frac{\partial \ln R_i}{\partial \ln \tau_i} > 0$.

Proposition 3: Budget allocation

We study now optimal budget allocation under concave marginal social impact and spillovers.

Consider a connected networks of n agents. Each agent i has degree $k_i \in [1, n-1]$ and clustering coefficient $\tau_i \in [0,1]$. The planner has a divisible budget $B \in \mathbb{R}_+$ to allocate across agents, denoted by $s = (s_1, ..., s_n)^T$, such that $\sum_{i=1}^{n} s_i = B$. The social impact of allocations is

$$S(s) = \sum_{i=1}^{n} f_i(s_i)\left(\alpha k_i - \beta \tau_i\right) + \frac{1}{2} s^T W_s,$$

where $f_i(s_i)$ is strictly increasing and concave, $f_i^{''}(s_i) < 0$ and W is a symmetric spillover matrix. Linearizing $f_i(s_i)$ around small s_i, $f_i(s_i) \simeq f_i^{'}(0)s_i \simeq f^{'}(0)$, the optimal allocation s^* is the solution to the earlier system

$$(I + W)s^* = \lambda \cdot 1 + f^{'}(0)(\alpha k - \beta\tau).$$

Where 1 is the $n \times 1$ vector of ones, $k = (k_1, ..., k_n)^T$, $\tau = (\tau_1, ..., \tau_n)^T$ and λ is chosen to satisfy $\sum_{i=1}^{n} s_i^* = B$ Therefore,

$$s^* = \left(I + w\right)^{-1} \left(f^{'}(0)(\alpha k - \beta\tau) + \lambda \cdot 1\right).$$

Under concave marginal returns, $s^* > 0$ for all agents, spreading the budget across hubs and peripherical agents depending on both network structure and spillovers.

Approximation method:

We now propose and approximation method that approximates well when budget allocations are small relative to concavity of f_i and W are small. It is particularly useful for initial design, pilot studies or settings with limited non linearities. Otherwise, full numerical optimization is recommended.

When W is small, we obtain that $(I + W)^{-1} \simeq I - W \simeq I$.

Then,

$$s^* = f^{'}(0)(\alpha k - \beta\tau) + \lambda \cdot 1.$$

Subject to budget constraints $\sum_{i=1}^{n} s_i = B$, define $\psi_i = \alpha k_i - \beta\tau_i$. Then, $s_i^* = f^{'}(0)\psi_i + \lambda$. Now sum over i.

$$\sum_{i=1}^{n} s_i^* = f^{'}(0)\sum_{i=1}^{n} \psi_i + n\lambda = B,$$

$$\lambda = \frac{B - f^{'}(0)\sum_{i=1}^{n}\psi_i}{n}\text{, so, } s_i^* = f^{'}(0)\psi_i + \frac{B}{n} - f^{'}(0)\frac{\sum\psi_i}{n} = \frac{B}{n} + f^{'}(0)\left(\psi_i - \overline{\psi}\right),$$

For simplicity $f^{'}(0) = 1$, then $s_i^* = \frac{B}{n} + \psi_i - \overline{\psi}$, which leads to

$$s_i^* = \frac{B}{n} + \alpha\left(k_i - \overline{k}\right) - \beta\left(\tau_i - \overline{\tau}\right),$$

Where $\overline{k}$ and $\overline{\tau}$ denote average degree and clustering coefficient respectively.

Proposition 4: Network effects on total interventions

In our economic model, we have the following functions

$$\begin{aligned} U_i^C &= \pi_i(1) - v_i^C + \theta_i \\ U_i^D &= \pi_i(0) - w_i^C. \end{aligned}$$

Where the social dilemma implies that $\pi_i(0) - \pi_i(1) > 0$. We define $w_i^C \in \mathbb{R}_+$ as the peer pressure cooperators exert to noncooperators, being $v_i^C \in \mathbb{R}_+$ the individual cost of exerting peer pressure. Finally, $\theta_i \in \mathbb{R}_+$ denotes the intervention (fine or subsidy) to cooperators or noncooperators. Hence, the functions w_i^C and v_i^C represent informal enforcement already present in the social network, while θ_i the formal enforcement that has to be designed by the planner.

The decision whether to cooperate or not to cooperate for each agent is probabilistic, capturing bounded rationality and uncertainty in adaptive games. It is modeled according to a softmax rule, similarly to a smoothed best response function, as follows,

$$p_i = \frac{1}{1 + e_i^{U_i^D - U_i^C}}.$$

We focus on the problem the planner faces when defining which θ_i apply to each agent i. The objective is to promote efficient cooperation within the social network.

As a baseline case, without loss of generality, we focus on reaching the individual tipping point $p_i = \frac{1}{2}$ for each agent. At this point, we have that $U_i^C = U_i^D$. Reorganizing previous expression, we obtain that

$$\theta_i = \pi_i(0) - \pi_i(1) - w_i^C + v_i^C.$$

Recall that $w_i^{'} \equiv \frac{\partial w_i^C}{\partial c_i} > 0$ and $w_i^{"} < 0$, where c_i is local cooperator share in the neighborhood of each agent, that is, the share of compliers in the neighborhood of each agent i. It means, whether the number of compliers grows, then social pressure grows. On the other hand, let $v_i^C = v(d_i, c_i) = \alpha d_i^{\beta} \cdot (1 - c_i)$. If degree d_i increases, i's costs increase (because there are more peers to monitor), it means, $\frac{\partial v_i^C}{\partial d_i} \equiv (v_i^C)' > 0$ and $(v_i^C)'' < 0$, that is v_i^C is a concave function in k_i.

At the network level, defining $\theta_i \equiv f(k_i)$ and knowing that the function is concave in k_i, we can apply Jensen's inequality. It says that

$$E[f(k)] \leq f(E[k]).$$

Which implies that, given a fixed average degree $\bar{k} = E[k]$ a more disperse degree distribution (higher variance) related to scale-free distribution, reduces the expected value of the intervention. We can approximate the expected value of the intervention throughout the Taylor expansion as follows

$$f(k) \approx f(\bar{k}) + f^{'}(\bar{k})(k - \bar{k}) + \frac{1}{2} f^{"}(\bar{k})(k - \bar{k})^2.$$

Taking the expected value, it gives

$$E[f(k)] \approx f(\bar{k}) + f^{'}(\bar{k}) E[k - \bar{k}] + \frac{1}{2} f^{"}(\bar{k}) E[k - \bar{k}]^2.$$

Which leads to

$$E[f(k)] \approx f(\bar{k}) - \frac{1}{2}\left|f^{"}(\bar{k})\right| \mathrm{var}(k).$$

From the planner's perspective it reads as

$$E[\theta] \approx f(\bar{k}) - \frac{1}{2}\left|f^{"}(\bar{k})\right| \mathrm{var}(k).$$

Note that, for a complete network where $k_i = n-1\ \forall i$ or very regular networks where $\bar{k} \simeq k_i$, then $E[\theta] = f(\bar{k})$ given that $\mathrm{var}(k) = 0$. We compare networks with identical $\bar{k}$ but different $\mathrm{var}(k)$ to capture the network effect on the intervention.

Extension n agents

Case 1

n	10			100			1000		
C/Density	**0**	**0.5**	**1**	**0**	**0.5**	**1**	**0**	**0.5**	**1**
0	1000	1000	1000	10000	10000	10000	100000	100000	100000
0.1	904	723,754175	732,024691	9092	7573,06877	7070,20569	90016	75365,9461	69898,6938
0.2	800	521,206281	407,135802	8116	5258,83509	4101,32456	80158	52191,5889	40930,7424
0.3	699	309,646181	216,246914	6991	3021,15743	1280,82094	70029	31311,3319	13486,8237
0.4	556	161,942942	121,037037	5953	1219,88992	59,8718498	60128	11506,3198	0
0.5	488	95,8018913	33,3580247	4879	164,230323	0	50203	0	0
0.6	369	37,7638099	10,0493827	3918	0,98806309	0	40322	0	0
0.7	285	4,0015	0	3039	0	0	29854	0	0
0.8	218	0	0	2057	0	0	20088	0	0
0.9	118	0,07685185	0	1001	0	0	10038	0	0
1.0	0	0	0	0	0	0	0	0	0

Case 2

n	10			100			1000		
C/Density	**0**	**0.5**	**1**	**0**	**0.5**	**1**	**0**	**0.5**	**1**
0	1000	1000	1000	10000	10000	10000	100000	100000	100000
0.1	816	657,546032	670,666667	7934	6136,07327	6118,74747	79758	61958,9125	61981,6136
0.2	626	359,750794	362	5978	2722,2661	2903,75758	60058	27601,739	28130,3704
0.3	428	178,348413	173,555556	4074	473,713984	443,030303	39862	743,040104	902,762763
0.4	260	49,502381	28	2184	12,9165549	0,4040404	19712	0	0
0.5	120	22,2761905	8,44444444	330	0	0	880	0	0
0.6	54	1,86190476	0	8	0	0	0	0	0
0.7	12	0	0	0	0	0	0	0	0
0.8	2	0	0	0	0	0	0	0	0
0.9	0	0	0	0	0	0	0	0	0
1.0	0	0	0	0	0	0	0	0	0

Case3

n	10			100			1000		
C/Density	**0**	**0.5**	**1**	**0**	**0.5**	**1**	**0**	**0.5**	**1**
0	1000	1133,704	1486	10000	158686,948	598060	100000	149927077	598900600
0.1	897	902,33596	1107,13126	9022	127800,22	482412,949	89770	121497515	486737803
0.2	791	592,980473	731,794123	7998	101035,776	379904,521	79986	95421801,4	383594479
0.3	713	327,307405	385,540593	7059	75976,5873	287882,164	69875	73564928,2	295043528
0.4	620	276,121307	190,932	5971	55473,0538	215209,694	59942	53695199,5	215009218
0.5	485	101,652225	75,295358	5013	36382,5034	146439,015	50030	37306154,5	149564056
0.6	372	43,1795827	20,0160988	3980	21994,0347	94626,0853	39907	23946475,7	95278200
0.7	300	9,9958301	6,31377778	3063	10896,3611	46806,8587	29836	13564911,4	54278262
0.8	196	0	0	1986	1799,14178	15059,9555	20008	5951338,52	23900556,3
0.9	100	0,19225	0	1007	1,20561011	630,50703	10040	1445212,49	6087146,23
1.0	0	0	0	0	0	0	0	0	0

5. Conclusions

This work analyzes and deepens the understanding of conflicts, environmental crimes, and organized crime. These different phenomena can be examined separately, as is done in the present study; however, they are closely interconnected. Understanding each of them, as well as their interrelations, is highly valuable, as it helps reduce the uncertainty arising from their illegality and opacity. This, in turn, leads to a better understanding of how they operate and enables more informed decisions and actions for control and prevention, given their significant environmental, social, and economic impacts. To conduct this study, I draw on complexity theory through different approaches, including network theory and agent-based models. Likewise, computational mathematical modeling and economic analysis play a central role.

Conflicts over natural resources account for a large share of conflicts worldwide, particularly in resource-rich countries that often exhibit weak institutions. Environmental conflicts may serve both as the initial cause of conflict and as a driving force behind its persistence and escalation. While there are different ways to study them, for example, by analyzing the scarcity–abundance–violence relationship or measuring intensity through forms of violence (e.g., deaths, damages), the analysis presented in this work measures conflict intensity through economic losses associated with the natural resource under dispute, capturing how rents are dissipated. This is done by considering key characteristics defined by the model's parameters, including those of armed groups, their appropriation effort (e.g., number of fighters), and the positive and negative relationships among them (modeled through a signed network), as well as resource-specific features such as abundance and price. The analytical and numerical results show that power asymmetries among agents (i.e., when one-armed group is significantly more powerful than others) are among the main drivers of economic losses. Moreover, in scenarios of resource abundance, network structure plays a fundamental role, and resource prices can reduce rent dissipation.

The armed groups involved in these conflicts are often part of organized crime supply chains or make use of their services to trade resources. This connection opens the door to further exploring how organized crime operates through one of its main channels: illegal markets. This study examines, through the implementation of an agent-based model, how organized crime traffics cocaine from South America to Europe, emphasizing the role of maritime transport and legal trade as a means of concealment. Ports emerge as key actors for traffickers, not only as points of loading and unloading, but also as spaces where violence, corruption, and bribery take place. The results show that corruption undermines the effectiveness of port authorities' inspection capacity. Additionally, findings confirm that traffickers adapt by updating routes in response to increased inspection efforts.

On the other hand, this study highlights the importance of the diffusion of cooperation norms, interpreted as compliance with rules and norms. Individuals are embedded in social and professional networks where monitoring, reporting, and sanctions often rely on informal mechanisms such as peer pressure. Through a theoretical model and its analytical and numerical development, we identify how regulators should intervene to propagate cooperation, depending on key characteristics such as density, the presence of central nodes, and redundancy. The results reveal a trade-off between the scope of an intervention and its associated costs. Therefore, interventions should not focus solely on central nodes but should also consider the characteristics of the network. This theoretical model aims to be extended to anti-corruption interventions, recognizing that corruption is one of the main mechanisms through which organized crime operates, penetrating governments and institutions and generating substantial economic and social damage.

Overall, this work contributes to the literature across its different chapters by providing a deeper understanding of environmental conflicts and organized crime, with the aim of improving or designing policies to control and reduce their economic, social, and environmental impacts, based on the results of the models developed.

References

1. Achim Wennmann (2009) Grasping the Financing and Mobilization Cost of Armed Groups: A New Perspective on Conflict Dynamics, Contemporary Security Policy, 30:2, 265-280, DOI: 10.1080/13523260903059864
2. Abel, D. L. (2007). Complexity, self-organization, and emergence at the edge of chaos in life origin models. *Journal of the Washington Academy of Sciences*, 1-19.
3. Ambika, G., & Kurths, J. (2021). *Tipping in complex systems: Theory, methods and applications*. *The European Physical Journal Special Topics, 230*(16-17), 3177-3179. https://doi.org/10.1140/epjs/s11734-021-00281-z
4. Anderton, C. H., & Carter, J. R. (2009). Principles of Conflict Economics: A Primer for Social Scientists. Cambridge University Press. https://doi.org/10.1017/CBO9780511813474
5. Anderson, S., Baland, J. M., & Moene, K. O. (2009). Enforcement in informal saving groups. Journal of Development Economics, 90(1), 14–23. https://doi.org/10.1016/j.jdeveco.2008.09.003.
6. Antonopoulos, G. A. (2008). The Balkans as a 'laboratory (for the study) of transnational criminality'. European Journal of Criminology, 5(4), 337–353. https://doi.org/10.1177/1477370808090830
7. Armada de Colombia. Centro Nacional de Investigación y Análisis contra Narcotráfico Marítimo. (2021). *Informe anual 2021 sobre narcotráfico marítimo*. https://www.armada.mil.co
8. Armstrong, R. A., Eperjesi, F., & Gilmartin, B. (2002). The application of analysis of variance (ANOVA) to different experimental designs in optometry. *Ophthalmic and Physiological Optics, 22*, 1–9.
9. Artaza, E., & Guillaumont, P. (2022). Economic vulnerability and the risk of civil war. World Development, 158, 105971. https://doi.org/10.1016/j.worlddev.2022.105971

10. Azrieli, Y., & Chambers, C. P. (2024). Success functions in large contests. arXiv. https://doi.org/10.48550/arXiv.2403.07152

11. Badeeb, R. A., Lean, H. H., & Clark, J. (2017). The evolution of the natural resource curse thesis: A critical literature survey. Resources Policy, 51, 123–134. https://doi.org/10.1016/j.resourpol.2016.10.015

12. Baker, M. J. (2003). An equilibrium conflict model of land tenure in hunter-gatherer societies. Journal of Political Economy, 111(1), 124–173. https://doi.org/10.1086/344800
13. Ballester, C., Calvó-Armengol, A., & Zenou, Y. (2006). Who's who in networks. Wanted: The key player. Econometrica, 74(5), 1403–1417. https://www.jstor.org/stable/3805930.
14. Banerjee, A., Chandrasekhar, A., Duflo, E., & Jackson, M. O. (2013). The diffusion of microfinance. Science, 341(6144), 1236498. https://doi.org/10.1126/science.1236498.
15. Banfield, Edward. 1958. The Moral Basis of a Backward Society. New York: Free Press.
16. Beaman, L., BenYishay, A., Magruder, J., & Mobarak, A. M. (2018). Can network theory-based targeting increase technology adoption? American Economic Review, 108(6), 1913–1947. https://doi.org/10.1257/aer.20200295.
17. Besley, T., & Coate, S. (1995). Group lending, repayment incentives and social collateral. Journal of Development Economics, 46(1), 1–18. https://doi.org/10.1016/0304-3878(94)00045-E.

18. Bernard, B. (2009). Container security and the global drug trade: The case of cocaine. *Maritime Policy & Management, 36*(3), 247–260. https://doi.org/10.1016/j.marpol.2009.03.002

19. Bhat, I. H. (2024). Eco-Crimes in Armed Conflicts: Legal Approaches to Environmental Violations Under International Criminal Law. *IUP Law Review*, *14*(3).

20. Bicchieri, C. and R. Muldoon (2014). Social Norms The Stanford Encyclopedia of Philosophy. E. Zalta. Stanford.
21. Bier, V., Oliveros, S., & Samuelson, L. (2007). Choosing what to protect: Strategic defensive allocation against an unknown attacker. Journal of Public Economic Theory, 9(4), 563–587. https://doi.org/10.1111/j.1467-9779.2007.00320.x

22. Blume, L. E. (1993). The Statistical Mechanics of Strategic Interaction. Games and Economic Behavior 5(3): 387–424.
23. Bonacich, P. (1987). Power and centrality: A family of measures. American Journal of Sociology, 92(5), 1170–1182. https://www.jstor.org/stable/2780000.
24. Bramoullé, Y., & Kranton, R. (2007). Public goods in networks. Journal of Economic Theory, 135(1), 478–494. https://doi.org/10.1016/j.jet.2006.06.006.
25. Breza, E., Chandrasekhar, A. G., & Tahbaz-Salehi, A. (2018). Seeing the forest for the trees? An investigation of network knowledge. National Bureau of Economic Research. Working Paper Series, 24359. http://www.nber.org/papers/w24359.
26. Brock, W. A. and C. H. Hommes (1997). A Rational Route to Randomness. Econometrica 65(5): 1059–1095.
27. Bueger, C., & Edmunds, T. (2020). Blue crimes: Conceptualising transnational organised crime at sea. *Marine Policy, 119*, 104067. https://doi.org/10.1016/j.marpol.2020.104067
28. Butler, C. K., & Gates, S. (2012). African range wars: Climate, conflict, and property rights. Journal of Peace Research, 49(1), 23–34. https://doi.org/10.1177/0022343311426166
29. Calvó-Armengol, A. & Jackson, M. O. (2007). Networks in labor markets: Wage and employment dynamics and inequality. Journal of Economic Theory, 132 (1), 27-46. https://doi.org/10.1016/j.jet.2005.07.007.
30. Canh, N. P., Schinckus, C., & Thanh, S. D. (2020). The natural resources rents: Is economic complexity a solution for resource curse? Resources Policy, 69, 101800. https://doi.org/10.1016/j.resourpol.2020.101800
31. Chandrasekhar, A. G., Larreguy, H. A., & Xandri, J. P. (2020). Testing models of social learning on networks: Evidence from two experiments. Econometrica, 88(1), 1-32. https://doi.org/10.3982/ECTA14407.
32. Cisneros-Velarde, P., & Bullo, F. (2020). Signed network formation games and clustering balance. Dynamic Games and Applications, 10(4), 783–797. https://doi.org/10.1007/s13235-019-00346-8
33. Choi, S. G., & Storr, V. H. (2018). A culture of rent seeking. Public Choice, 181(1–2), 101–126. https://doi.org/10.1007/s11127-018-0557-x

34. Collier, P., & Hoeffler, A. (2004). Greed and grievance in civil war. Oxford Economic Papers, 56(4), 563–595. https://doi.org/10.1093/oep/gpf064
35. Collins, P. (1999). Strategic management and the planning of foreign aid: Introduction. Oxford Economic Papers, 51(1), 161–167. https://doi.org/10.1093/oep/51.1.161
36. Cornes, R., & Hartley, R. (2005). Asymmetric contests with general technologies. Economic Theory, 26(4), 923–946. https://doi.org/10.1007/s00199-004-0566-5
37. Crooks, A., Malleson, N., Manley, E., & Heppenstall, A. (2018). *Agent-based modelling and geographical information systems: A practical primer*. SAGE Publications. https://doi.org/10.4135/9781529793543
38. Davies, S., Pettersson, T., & Öberg, M. (2024). Organized violence 1989–2023, and the prevalence of organized crime groups. *Journal of Peace Research*, *61*(4), 673–688. https://doi.org/10.1177/00223433241262912
39. Dickson, A., MacKenzie, I. A., & Sekeris, P. G. (2022). The role of markets on resource conflicts. Scandinavian Journal of Economics, 124(3), 677–708. https://doi.org/10.1111/sjoe.12471
40. Duffles Teixeira Aranega, A. (2025). Transnational Organized Crime, Environmental Crimes, and Climate Change: Investigating Criminogenic Effects, Categories, Dynamics, and Consequences. In: Kaunert, C., Léonard, S., Masys, A.J. (eds) Transnational Unconventional Organized Crime: A National and Global Security Concern. Advanced Sciences and Technologies for Security Applications. Springer, Cham. https://doi.org/10.1007/978-3-031-96432-9_3
41. Dohmen, Thomas, Armin Falk, D. Huffman, and Uwe Sunde. 2009. “Homo Reciprocans: Survey Evidence on BehaviouralOutcomes.” Economic Journal 119(536): 592–612.
42. Duernecker, G. and F. Vega-Redondo (2017). Social Networks and the Process of Globalization. The Review of Economic Studies 85(3): 1716–1751.
43. Edward R. Kleemans, E. R., & Christianne J. de Poot, C. J. (2008). Criminal careers in organized crime and social opportunity structure. European Journal of Criminology, 5(1), 69–98. https://doi.org/10.1177/1477370807084225

44. Epstein, J. M. (1999). Agent-based computational models and generative social science. *Complexity, 4*(5), 41–60. https://doi.org/10.1002/(SICI)1099-0526(199905/06)4:5<41::AID-CPLX9>3.0.CO;2-F

45. Eski, Y. (2019). Policing, port security and crime control. In A. Densley & R. C. White (Eds.), *The Handbook of Transnational Crime and Justice* (pp. 239–254). Routledge.

46. Eski, Y., & Buijt, J. (2016). The 'invisible' security of the Port of Rotterdam. *Trends in Organized Crime, 19*(2), 196–214. https://doi.org/10.1007/s12117-016-9280-5

47. European Union Agency for Asylum. (2025, February). *Country of origin information report: Sudan – Security situation*. https://euaa.europa.eu/sites/default/files/publications/2025-02/2025_02_EUAA_COI_Report_Sudan_Security_Situation.pdf

48. FeldmanHall, O., J.-Y. Son and J. Heffner (2018). Norms and the Flexibility of Moral Action. Personality Neuroscience 1: e15.
49. Fehr, E., & Gächter, S. (2000). Cooperation and punishment in public goods experiments. American Economic Review, 90(4), 980–994. http://www.jstor.org/stable/117319.
50. Fehr, Ernst, and Herbert Gintis. 2007. Human Motivation and Social Cooperation: Experimental and Analytical Foundations. Annual Review of Sociology 33(1): 43–64.
51. Franke, J., & Öztürk, T. (2015). Conflict networks. Journal of Public Economics, 126, 104–113. https://doi.org/10.1016/j.jpubeco.2015.03.004
52. Frick, M., Iijima, R., & Ishii, Y. (2020). Misinterpreting Others and the Fragility of Social Learning. Econometrica, 88(6), 2281-2328. https://doi.org/10.3982/ECTA16981.
53. Fudenberg, D. and D. Levine (1998). The Theory of Learning in Games. Cambridge, MA, MIT Press.
54. Galeotti, A., Golub, B., & Goyal, S. (2020). Targeting interventions in networks. Econometrica, 88(6), 2445–2471. https://doi.org/10.3982/ECTA16173.
55. Gelb, A. H. (1988). Oil windfalls: Blessing or curse? Oxford University Press.

56. Gilbert, N., & Troitzsch, K. G. (2005). *Simulation for the social scientist* (2nd ed.). Open University Press.

57. Goetz, R., Marco, J. (2025). Social networks, norm-enforcing ties and cooperation. J Econ Interact Coord 20, 371–412. https://doi.org/10.1007/s11403-024-00435-x.
58. Golub, B., & Sadler, E. (2017). Learning in social networks. Available at SSRN: https://ssrn.com/abstract=2919146 or http://dx.doi.org/10.2139/ssrn.2919146.
59. Gries, T., & Haake, C.-J. (2016). An economic theory of 'destabilization war' - Compromise for peace versus conventional, guerilla, or terrorist warfare. Verein für Socialpolitik.
60. Groff, E. R., Weisburd, D., & Yang, S.-M. (2019). The role of agent-based modeling in crime prevention and policing. *Crime Science, 8*, Article 1. https://doi.org/10.1186/s40163-019-0100-1
61. Han, J., & Feng, F. (2023). Testing the theory, blessing or resource curse? The effect of natural resources on political violence in Africa. Journal of Strategic Studies & International Affairs, 3(1), 35–55. https://doi.org/10.17576/sinergi.0301.2023.04
62. Heider, F. (1946). Attitudes and cognitive organization. The Journal of Psychology, 21(1), 107–112. https://doi.org/10.1080/00223980.1946.9917275
63. Hiller, T. (2017). Friends and enemies: A model of signed network formation. Bristol Economics Discussion Papers, 12(629). https://doi.org/10.3982/TE1937
64. HIIK. (2021). Conflict Barometer 2020. Heidelberg Institute for International Conflict Research.
65. Hirshleifer, J. (1989). Conflict and rent-seeking success functions: Ratio vs. difference models of relative success. Public Choice, 63(2), 101–112. https://doi.org/10.1007/BF00153384
66. Ho, E., Rajagopalan, A., Skvortsov, A., Arulampalam, S., & Piraveenan, M. (2022). Game theory in defence applications: A review. Sensors, 22(3), 1032. https://doi.org/10.3390/s22031032
67. Holland, J.H. Emergence: From Chaos to Order. Addison-Wesley, Redwood City, CA, 1998.
68. Hoover Green, A. (2016). The commander’s dilemma: Creating and controlling armed group violence: Creating and controlling armed group violence. Journal of Peace Research, 53(5), 619-632.

69. Islam, S., & Clarke, M. (2002). The relationship between economic development and social welfare: A new adjusted GDP measure of welfare. Social Indicators Research, 57(2), 201–229. https://doi.org/10.1023/A:1015704817445
70. Jackson, M. O. (2020). A typology of social capital and associated network measures. Social Choice and Welfare, 54(2), 311–336. https://doi.org/10.1007/s00355-019-01189
71. Jackson, M. O. (2008). Social and economic networks. Princeton University Press. https://doi.org/10.2307/j.ctvcm4gh1.
72. Jackson, M. O., Rodriguez-Barraquer, T., & Xu Tan. (2012). Social Capital and Social Quilts: Network Patterns of Favor Exchange. American Economic Review 102 (5): 1857–97. https://doi.org/10.1257/aer.102.5.1857.

73. Jenner, M. S. (2013). International drug trafficking: A global problem with a domestic solution. *Indiana Journal of Global Legal Studies, 20*(2), 535–561. https://doi.org/10.2979/indjglolegstu.20.2.0535

74. Kalimeris, P., Bithas, K., Richardson, C., & Nijkamp, P. (2020). Hidden linkages between resources and economy: A "Beyond-GDP" approach using alternative welfare indicators. Ecological Economics, 169, 106508. https://doi.org/10.1016/j.ecolecon.2019.106508
75. Kim, D. A., Hwong, A. R., Stafford, D., Hughes, D. A., O'Malley, A. J., Fowler, J. H., & Christakis, N. A. (2015). Social network targeting to maximise population behaviour change: a cluster randomised controlled trial. The Lancet, 386(9989), 145–153. https://doi.org/10.1016/S0140-6736(15)60095-2.

76. Kleijnen, J. P. (2005). An overview of the design and analysis of simulation experiments for sensitivity analysis. *European Journal of Operational Research, 164*(2), 287–300.

77. König, M. D., Rohner, D., Thoenig, M., & Zilibotti, F. (2017). Networks in conflict: Theory and evidence from the Great War of Africa. Econometrica, 85(4), 1093–1132. https://doi.org/10.3982/ECTA14122
78. Kostakos, P. A., & Antonopoulos, G. A. (2010). The 'good', the 'bad' and the 'Charlie': The business of cocaine smuggling in Greece. *Global Crime, 11*(1), 34–57. https://doi.org/10.1080/17440570903559143

79. Lahkar, R., & Sultana, R. (2023). Rent dissipation in large population Tullock contests. Public Choice, 197(1–2), 253–282. https://doi.org/10.1007/s11127-023-01103-7

80. Le Billon, P (2005) Resources and armed conflicts, The Adelphi Papers, 45:373, 29-49, DOI: 10.1080/05679320500129045

81. Leff, J., & LeBrun, E. (2014). Following the thread: Arms and ammunition tracing in Sudan and South Sudan (HSBA Working Paper 32). Geneva, Switzerland: Small Arms Survey, Graduate Institute of International and Development Studies. Retrieved from https://www.smallarmssurvey.org/sites/default/files/resources/HSBA-WP32-Arms-Tracing.pdf

82. Levinson, M. (2016). *The box: How the shipping container made the world smaller and the world economy bigger* (2nd ed.). Princeton University Press.

83. Levi, Mike, & Soudijn, Melvin. (2020). Understanding the Laundering of Organized Crime Money. *Crime and Justice: Review of Research, 49,* 579-632.

84. Lewin, R. (1999). Complexity: Life at the edge of chaos. University of Chicago Press.

85. Liu, M., Toyoda, Y., Nabaa, M., & Yamada, T. (2018). Port choice by major shipping lines in South East Asia: A discrete choice model. *Asian Journal of Shipping and Logistics, 34*(2), 117–124. https://doi.org/10.1016/j.ajsl.2018.06.001

86. Little, R. (2007). The balance of power in international relations. Cambridge University Press.

87. Löhr, K., Aruqaj, B., Baumert, D., Bonatti, M., Brüntrup, M., Bunn, C., ... & Weinhardt, M. (2021). Social cohesion as the missing link between natural resource management and peacebuilding: Lessons from cocoa production in Côte d'Ivoire and Colombia. Sustainability, 13(23), 13002. https://doi.org/10.3390/su132313002

88. Lynch, M. J., & Pires, S. F. (2019). Quantitative studies in green and conservation criminology. *Quantitative studies in green and conservation criminology: The measurement of environmental harm and crime. New York: Routledge*.

89. Macário, R. (2014). The complexity of port systems: Understanding value creation. In H. Meersman, E. Van de Voorde, & T. Vanelslander (Eds.), *Port infrastructure finance* (pp. 77–92). Informa Law.

90. Magliocca, N. R., McSweeney, K., Sesnie, S. E., Tellman, B., Devine, J., & Wrathall, D. J. (2022). Modeling cocaine trafficking networks across the Americas. *PNAS Nexus, 1*(2), pgac028. https://doi.org/10.1093/pnasnexus/pgac028

91. Malleson, N., Heppenstall, A., See, L., & Evans, A. (n.d.). *Agent-based modelling of crime: A review*. [Manuscript submitted for publication].

92. Mani, A., I. Rahwan and A. Pentland (2013). Inducing Peer Pressure to Promote Cooperation. Scientific Reports 3: 1735.

93. Manzi, M., & Calderoni, F. (2024). Modeling organized crime networks with agent-based simulations. *Crime Science, 13*, Article 2. https://doi.org/10.1186/s40163-024-00195-y

94. Manski, C. F. (1993). Identification of Endogenous Social Effects: The Reflection Problem. The Review of Economic Studies 60(3): 531–542.

95. Marco, J., & Goetz, R. (2023). Public policy design and common property resources: A social network approach. American Journal of Agricultural Economics, 106(1), 252–285. https://doi.org/10.1111/ajae.12372

96. McKelvey, R. D. and T. R. Palfrey (1995). Quantal Response Equilibria for Normal Form Games. Games and Economic Behavior 10(1): 6–38.

97. Mehlum, H., Moene, K. O., & Torvik, R. (2002). Institutions and the resource curse. University Library of Munich, Germany.

98. Mertens, J.-F. (2002). Chapter 47 Stochastic games. Handbook of Game Theory with Economic Applications, Elsevier. 3: 1809–1832.

99. Middleton, D., & Levi, M. (2015). *Let sleeping lawyers lie: Organized crime, lawyers and the regulation of legal services*. *British Journal of Criminology*, 55(4), 647–665. https://doi.org/10.1093/bjc/azv001

100. Moffatt, P. (2020). Experimetrics: Econometrics for experimental economics, Bloomsbury Publishing.

101. Morris, M. D. (1991). Factorial sampling plans for preliminary computational experiments. Technometrics, 33(2), 161–174. https://doi.org/10.1080/00401706.1991.10484804

102. Nillesen, E., & Bulte, E. (2014). Natural resources and violent conflict. Annual Review of Resource Economics, 6(1), 69–83. https://doi.org/10.1146/annurev-resource-100913-012521

103. Nitzan, S. (1994). Modelling rent-seeking contests. European Journal of Political Economy, 10(1), 41–60. https://doi.org/10.1016/0176-2680(94)90061-2

104. Nordstrom, C. (2007). *Global outlaws: Crime, money, and power in the contemporary world*. University of California Press.

105. Nyborg, K. (2018). Social Norms and the Environment. Annual Review of Resource Economics 10(1): 405–423.

106. Nyborg, K. and M. Rege (2003). On social norms: the evolution of considerate smoking behavior. Journal of Economic Behavior & Organization 52(3): 323–340.

107. Olsson, O., & Congdon Fors, H. (2004). Congo: The prize of predation. Journal of Peace Research, 41(3), 321–336. https://doi.org/10.1177/0022343304043773

108. Ostrom, E. (1990). Governing the commons: The evolution of institutions for collective action. Cambridge University Press. https://doi.org/10.1017/CBO9780511807763.

109. Parise, F., & Ozdaglar, A. (2023). Graphon games: A statistical framework for network games and interventions. Econometrica, 91(1), 191–225. https://doi.org/10.3982/ECTA17564.

110. Pettit, S. J., & Beresford, A. K. C. (2009). Port development: From gateways to logistics hubs. *Maritime Policy & Management, 36*(3), 253–267. https://doi.org/10.1080/03088830902861148

111. Platteu, Jean P. 2000. Institutions, Social Norms and Economic Development. Amsterdam: Hardwood Academic Publishers and Routledge.

112. Polishchuk, L., & Tonis, A. (2013). Funciones de éxito de concurso endógeno: Un enfoque de diseño de mecanismos. Economic Theory, 52(1), 271–297. https://doi.org/10.1007/s00199-012-0701-7

113. Ravichandran, C., & Padmanaban, G. (2023). A numerical simulation-based method to predict floor-wise distribution of cooling loads in Indian residences using Tukey honest significant difference test. *Advances in Building Energy Research, 17*(1), 1–29.

114. Reksulak, M., Razzolini, L., & Shughart, W. F. (Eds.). (2013). The Elgar Companion to Public Choice (2nd ed.). Edward Elgar Publishing.

115. Rettberg, A., & Ortiz-Riomalo, J. F. (2016). Golden opportunity, or a new twist on the resource–conflict relationship: Links between the drug trade and illegal gold mining in Colombia. World Development, 84, 82–96.

116. Ross, M. L. (2004). What do we know about natural resources and civil war? Journal of Peace Research, 41(3), 337–356. https://doi.org/10.1177/0022343304043773

117. Rykiel, E. J. (1996). Testing ecological models: The meaning of validation. *Ecological Modelling, 90*(3), 229–244. https://doi.org/10.1016/0304-3800(95)00152-2

118. Sachs, J. D., & Warner, A. (1995). Natural resource abundance and economic growth. National Bureau of Economic Research.

119. Sachs, J. D., & Warner, A. M. (1999). The big push, natural resource booms and growth. Journal of Development Economics, 59(1), 43–76. https://doi.org/10.1016/S0304-3878(99)00005-X

120. Sachs, J. D., & Warner, A. M. (2001). The curse of natural resources. European Economic Review, 45(4–6), 827–838. ttps://doi.org/10.1016/S0014-2921(01)00125-8

121. Sampó, C., & Troncoso, V. (2023). Cocaine trafficking from non-traditional ports: Examining the cases of Argentina, Chile and Uruguay. *Trends in Organized Crime, 26*, 235–257. https://doi.org/10.1007/s12117-021-09441-y

122. Sen, E. 1979. Personal Utilities and Public Judgements: Or What's Wrong With Welfare Economics, The Economic Journal, Volume 89, Issue 355, 1 September 1979, Pages 537–558, https://doi.org/10.2307/2231867.

123. Sergi, A. (2020). *Ports, crime and security: Governing ports in a globalised world*. Palgrave Macmillan.

124. Sibley, M. J. N. (2016). Simulating piracy: Agent-based modelling of maritime piracy. *Journal of Simulation, 10*(1), 17–26. https://doi.org/10.1057/jos.2015.9

125. Shin, E., Jeong, D. & Lim, T. (2024). Robust Intervention in Networks Available at SSRN: https://ssrn.com/abstract=5077382 or http://dx.doi.org/10.2139/ssrn.5077382.

126. Skaperdas, S. (1996). Contest success functions. Economic Theory, 7(2), 283–290. https://doi.org/10.1007/BF01213906

127. Sthle, L., & Wold, S. (1989). Analysis of variance (ANOVA). *Chemometrics and Intelligent Laboratory Systems, 6*, 259–272. https://doi.org/10.1016/0169-7439(89)80095-2

128. Soliman, A., & Baldo, S. (2025, March 25). *Gold and the war in Sudan*. Chatham House. https://www.chathamhouse.org/sites/default/files/2025-03/2025-03-25-gold-and-the-war-in-sudan-soliman-and-baldo.pdf

129. Steven M. Manson (2001). *Simplifying complexity: A review of complexity theory*. *Geoforum, 32*(3), 405–414. https://doi.org/10.1016/S0016-7185(00)00035-X

130. Sun, Y., Zhao, W., & Zhou, J. (2021). Structural interventions in networks. International Economic Review, 64(4). https://doi.org/10.1111/iere.12639.

131. Torvik, R. (2002). Natural resources, rent seeking and welfare. Journal of Development Economics, 67(2), 455–470. https://doi.org/10.1016/S0304-3878(01)00195-X

132. Tosi Rodriguez, L & C, Stefano (2025): Exploring How Armed Groups Organize the Exploitation of Natural Resources, Studies in Conflict & Terrorism,
    a. DOI: 10.1080/1057610X.2025.2567858

133. Tullock, G. (1967). The welfare costs of tariffs, monopolies, and theft. Economic Inquiry, 5(3), 224–232. https://doi.org/10.1111/j.1465-7295.1967.tb01923.x

134. Tullock, G. (1980). Efficient rent seeking. In Toward a Theory of Rent Seeking Society (pp. 97–112). Texas A&M University Press.

135. UNCTAD (United Nations Conference on Trade and Development). (2024). *Review of Maritime Transport 2024*. https://unctad.org

136. UNEP, MONUSCO, & OSESG. (2015). Experts' background report on illegal exploitation and trade in natural resources benefitting organized criminal groups and recommendations on MONUSCO's role in fostering stability and peace in eastern DR Congo: Final report (April 15, 2015). United Nations Environment Program. https://www.unep.org

137. UNODC (United Nations Office on Drugs and Crime). (2023). *World Drug Report 2023*. https://www.unodc.org

138. United Nations Environment Programme. (2009). From conflict to peacebuilding: The role of natural resources and the environment. https://www.iisd.org/system/files/publications/conflict_peacebuilding.pdf

139. United Nations Office on Drugs and Crime. (2020). *World wildlife crime report 2020: Trafficking in protected species*. United Nations.

140. van Koppen, M. V. (2013). Involvement mechanisms for organized crime. *Crime, Law and Social Change*, *59*(4), 447-472. https://doi.org/10.1007/s10611-012-9396-8

141. https://doi.org/10.1016/j.worlddev.2016.03.020

142. Vaněk, O., Mařík, V., & Jakob, M. (2013). Modeling and simulation of maritime piracy. In *Proceedings of the 2013 Winter Simulation Conference* (pp. 2791–2802). IEEE. https://doi.org/10.1109/WSC.2013.6721655

143. Weisburd, D., Groff, E. R., & Yang, S.-M. (2017). *The criminology of place: Street segments and our understanding of the crime problem*. Oxford University Press.

144. Wick, K., & Bulte, E. H. (2006). Contesting resources – rent seeking, conflict and the natural resource curse. Public Choice, 128(3–4), 457–476. https://doi.org/10.1007/s11127-005-9010-z

145. Yandell, B. S. (1997). *Practical data analysis for designed experiments*. Chapman & Hall/CRC.

146. Young, H. P. (2004). Strategic Learning and its Limits, Oxford University Press.

147. Young, H. P. (2015). The Evolution of Social Norms. *Annual Review Economics*. 7:359-387. https://doi.org/10.1146/annurev-economics-080614-115322.

148. Zaidi, L. (2007). Ports and drugs: Towards a comprehensive model of drug trafficking via commercial shipping. *Trends in Organized Crime, 10*(4), 281–292. https://doi.org/10.1007/s12117-007-9013-9

149. Zaitch, D. (2002). *Trafficking cocaine: Colombian drug entrepreneurs in the Netherlands*. Kluwer Law International.

150. Zallé, O. (2023). Natural resource rents and regime durability: Identifying cross-country durability regimes. Resources Policy, 81, 103318. https://doi.org/10.1016/j.resourpol.2023.103318